NITRATION OF AROMATIC COMPOUNDS OVER SOLID ACID CATALYSTS

SHARDA PRABHAKAR DAGADE

NOVEMBER 2002

NITRATION OF AROMATIC COMPOUNDS OVER SOLID ACID CATALYSTS

A THESIS

SUBMITTED TO THE

UNIVERSITY OF PUNE

FOR THE DEGREE OF

DOCTOR OF PHILOSOPHY

(IN CHEMISTRY)

By

SHARDA PRABHAKAR DAGADE

CATALYSIS DIVISION

NATIONAL CHEMICAL LABORATORY

PUNE – 411 008, INDIA

NOVEMBER 2002

DEDICATED
TO
MY BELOVED PARENTS, SOU. KAMAL &
SHRI. PRABHAKAR DAGADE

CERTIFICATE

This is to certify that the work incorporated in the thesis, **"Nitration of aromatic compounds over solid acid catalysts"** submitted by **Ms. Sharda Prabhakar Dagade,** for the Degree of **Doctor of Philosophy**, was carried out by the candidate under my supervision in the Catalysis Division, National Chemical Laboratory, Pune, INDIA.

Dr. M. K. Dongare

Research Guide

ACKNOWLEDGMENTS

I express my profound gratitude to my research guide, Dr. M. K. Dongare, Scientist, NCL, Pune, for his invaluable guidance, numerous discussions and constructive suggestions through out the course of this investigation.

I am grateful to Dr. A.V. Ramaswamy, Head, Catalysis Division, NCL, for providing me all facilities required for my work.

I am also deeply indebted to Dr. S.G. Hegde, and Dr. Pradeepkumar for their stimulating discussions and constant personal help they rendered throughout the course of investigation.

I wish to express my thanks to Dr. Rode, Dr. (Mrs.) Pardhy, Dr. B. S. Rao, Dr. Sivsankar, Dr. C. Gopinath, Dr. (Mrs.) Chandwadkar, Ms. Agashe, Ms. Jacob, Dr. (Mrs.) Deshpande, Dr. (Mrs.) Degaonkar, Dr. (Mrs.) A. A. Belhekar, Dr. Soni, Dr. Mirajkar, Dr. Satyanarayana, Dr. (Mrs.) V. Ramaswamy, Dr. (Mrs.) Awate, Dr. Waghamare, Dr. A. P. Singh, Dr. Rajivkumar, Dr. Halligudi, Violet madam and all other scientific and nonscientific staff in the Catalysis Division, NCL, for their help and cooperation given to me in completing my research work successfully.

I take the opportunity to thank my friends Vandana, Kusum, Pratap, Jainy, Vrushali, Sushama, Shilpa, Karuna, Ranjeet, Sush, Pandeyji & Bhabhi, Vijay, Sabde, Laha, Chotu, Senapati, Balkishan, Suresh, Sushil, Jyoti, Venkatesan, Sachin, Chidambaram, Anand, Shiju, Thomas, Pai, Biju, Trisa, Dhanashree, Smita, Surekha and my numerous friends from whom I have received invaluable help and moral support.

It gives me great pleasure to thank my parents, Aai & Appa, in laws Aai, Bhau and my family members Aaji, Aajoba, Nana, Kaki, Uncle, Aunty, Satida, Shradha, my beloved sisters, Akka, Shobhadidi, Vaishu & Chaitu, my brother Shivaji, Vinod and my sister in

law, Swati and for their love, unfailing support, tremendous patience, trust and encouragement that they have shown to me.

I take this opportunity also to extend my heartfelt thanks to my beloved husband Rajan. This work would never have received the present shape had it not been backed by his constant encouragement and patience.

Finally, my thanks to Dr. P. Ratnasamy, Ex-Director, and S. Sivram, Director, National Chemical Laboratory, for permitting me to carry out my research work at NCL.

Sharda P. Dagade

CONTENTS

CHAPTER I

INTRODUCTION

1. INTRODUCTION

1. 1 NITRATION

Nitration of organic compounds has been a very active and rewarding area of research and is the subject of a large body of literature. Aromatic nitro compounds or their derivatives are used as solvents, analytical reagents, and are important intermediates in organic synthesis of perfumes, drugs, pesticides, and explosives [1]. Aromatic nitro compounds are convertible by reduction into primary amines, which in turn are valuable intermediates in the synthesis of dyes, pharmaceuticals, photographic developers and antioxidants [2].

The earliest nitro compounds were obtained by **MITSCHERLICH** in 1834 by treating hydrocarbons from coal tar with fuming nitric acid [2]. Later in 1845, **HOFMANN** and **MUSPRATT** reported their work on the nitration of benzene to give mono- and dinitrobenzenes by using a mixture of nitric and sulfuric acids.

PERKIN started work on the process development and scale-up of the nitration and reduction processes. The continued work by many others resulted in the trade price of aniline dropping from 50Fr/kg in 1858 to 10 Fr/kg in 1863 [3].

The number of naturally occurring nitroaromatic compounds are less; the first recognized compound was *chloramphenicol*, an important compound extracted from cultures of a soil mold *Streptomyces venezuelae* identified in 1949. This discovery stimulated investigations into the role of the nitro group in pharmacological activity, following the earlier discovery in 1943 of the antibacterial activity of nitrofuran derivatives.

Nitration, an electrophilic substitution reaction, is represented by the equation:

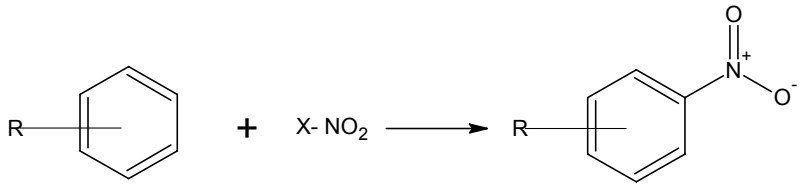

The nitration reaction is always strongly exothermic, as exemplified by the mononitration of benzene (ΔH = -117 kJ/mol) and naphthalene (ΔH = -209 kJ/mol) and is probably the most potentially hazardous industrially operated unit process. Fundamentally this is due to the heat generated, which can trigger the power of nitric acid to degrade organic materials exothermically to gaseous products with explosive violence [4].

Nitration is the dominant method for introducing the nitro group into aromatic systems. Several indirect methods also exist:

1) Oxidation of nitroso or amino compounds

2) Replacement of diazonium groups

3) Rearrangement of nitramines &

4) Nucleophilic displacement reactions.

These indirect methods have very little industrial applications. Conventionally aromatic nitro compounds are produced by liquid phase nitration reactions employing mixed acids. A sulfuric acid/nitric acid mixture is the most commonly used nitrating agent [5-6].

Many important nitro compounds are produced by applying unit processes (sulphonation, halogenation, or amination) to primary nitro starting materials, most of which are derived from the key primaries nitrobenzenes, nitrotoluenes and nitrochlorobenzenes.

Introduction of the nitro group deactivates the ring to further electrophilic substitution, therefore dinitration rarely occurs under the conditions used for mononitration. The nitration process may be carried out on either a batch (discontinuous) or a continuous basis. Continuous reaction for large tonnage intermediates (e.g. nitrobenzene and nitrotoluenes) is attractive for reasons of safety as well as the obvious economic considerations.

1. 2 REACTION MECHANISM

Heterogeneously catalyzed reactions are composed of purely chemical and physical reaction steps. For the catalytic process to take place, the starting materials must be transported to the catalyst. Thus, apart from the actual chemical reaction, diffusion, adsorption, and desorption processes are of importance for the progress of the overall reaction.

The mechanism of electrophilic aromatic nitration has been studied over the last 50 years. The foundation of the reaction mechanism was laid by Ingold and Hughes [7]. In the course of their studies they developed the concept of activating and deactivating groups in aromatic molecules.

The mechanism of nitration depends on the reactants and operating conditions [8]. Whereas NO_2^+ was suggested to be a nitrating species, as early as in 1903, its existence was substantiated only in 1946. Much experimentation has been applied to aromatic nitration since the nitronium ion NO_2^+, was confirmed as the active species by the Ingold-Hughes school in 1950 through study of Raman spectra. Evidences by Raman measurements are also given for the existence of the NO_2^+ ion in the solid phase.

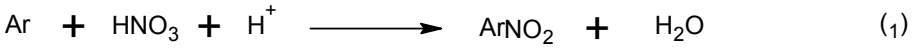

(1)

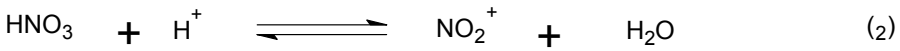

(2)

This ion, recognized as a nitrating species, is formed from nitric acid by equilibrium (2) under a suitable acidity of medium and is present in spectroscopically detectable amounts in very strong acid systems [9]. Two mechanisms for such aromatic nitrations are established: one, occurring with all of the compounds studied involving reaction through the nitronium ion and the other, limited to the more reactive aromatic compounds (amines, phenols, and alkyl substituted hydrocarbons), involving some form of nitrous acid catalysis. The reaction paths that they proposed are shown in Schemes 1 and 2. In Scheme 1, the rate-determining stage can be either reaction 2 or reaction 3 depending on the concentration and reactivity of the aromatic compound. In Scheme 2, the nitrosation stage was considered to be rate determining under all conditions. In this Scheme, the final reaction regenerates the nitrous acid and so only trace amounts of the nitrous acid are required for the catalysis to take place.

Scheme 1

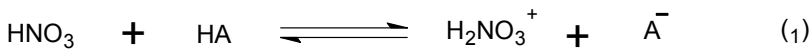

(1)

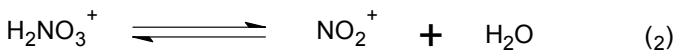

(2)

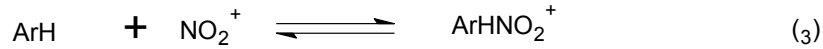

(3)

(4)

Scheme 2

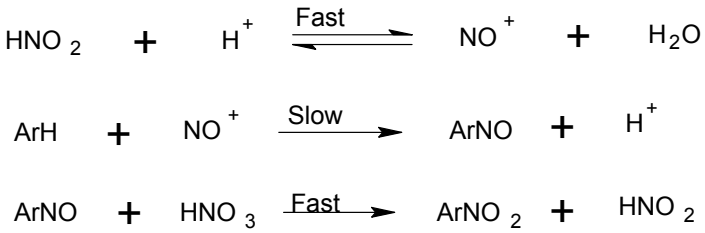

Scheme 3

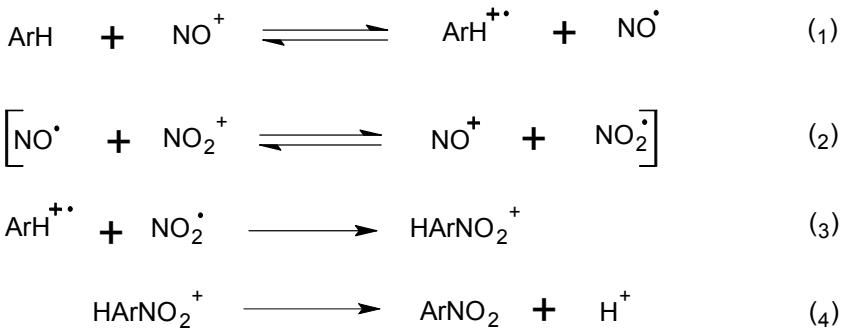

In recent years, alternative reaction paths have been supported for both the nitronium ion reaction and the reaction involving nitrous acid catalysis. The nitrous acid catalysis mechanism (Scheme 3) was later shown to be more general [10] and was supported by CIDNP effects [11], and kinetic studies [12]. Either stage 1 or stage 3 of Scheme 3 can apparently be rate determining depending on the conditions. In Scheme 3, the second stage is in brackets since the reaction shown indicates only the stoicheiometry of the process. The mechanism of this stage must be more complex since the rate of the nitrous acid catalyzed reaction frequently exceeds the rate of formation of nitronium ions in the medium.

Kenner [13] proposed that one-electron charge transfer may play an important role in the mechanism of nitronium ion nitration. In support to Kenner's suggestion, Nagakura and Tanaka [14] using molecular orbital theory proposed a mechanism

involving single-electron transfer, but no sufficient attention was paid to this at that time.

In the middle 1950s, however, stable σ-complexes was isolated. These complexes originated from the molecules with several substituents. The arenonium nature of these species was proved by NMR and the reaction mechanisms have been reviewed by Olah et al. [15-16].

In 1986 Feng et al. [17] suggested that the radical-pair recombination mechanism will be favored for nitration whenever the ionization potential of the aromatic is much less than that of NO_2. Substituents or reaction conditions that raise the ionization potential of the aromatic to a value higher than that of NO_2 prevent this radical-pair formation by preventing the one-electron transfer and force the classical electrophilic mechanism.

The rate of nitration with nitric acid in organic solvents was found to be of zero-order with respect to substrates at a more than 10-fold excess of nitric acid. The rate-limiting step becomes the formation of NO_2^+, and the nitration is zero-order in the aromatic [6]. Nitric acid heterolysis is considered to be accelerated with the increase of medium polarity provided by the increase of acid concentration [18]. Another assumption is that several molecules of nitric acid form associates, thus producing the active complex, which yields nitronium ion. Thus, the obtained experimental data required revision of the Ingold mechanism.

Another way to revise the Ingold mechanism was suggested by Schofield [15,18]. It differs from the Olah mechanism by the nature of the first intermediate complex. He proposed as first intermediate an encounter pair between a NO_2^+ ion and an aromatic molecule held in a solvent shell very closely. The two species are not interacting with each other [15a]. It is assumed to be possible for highly active aromatic

compounds. During its lifetime it can produce a σ-complex. This could explain the low substrate selectivity. The kinetic role of π-complexes of aromatic hydrocarbons in nitration has not been elucidated yet. Olah et al. pointed out that the Wheeland structure is not a transition state but a stable intermediate [15b].

In 1994 Eberson et al. [19] proposed that electrophilic aromatic nitration by nitronium ion takes place via an initial electron transfer, followed by recombination of an intermediate radical pair, and is critically examined. They proved by using recent experimental results from a model reaction, photoexcitation of ArH-tetramethane using tetranitromethane.

The mechanism of aromatic nitration continues to be a subject of active research [20] and there still exists some controversy, especially with respect to ipso attack. Ipso attack is not easily explained by the usual theory of aromatic electrophilic substitution. According to this theory the electrophilic reagent, in this case the nitronium ion, NO_2^+, should attack preferentially the position with the largest electron density. Most calculations, however, indicate that the ipso position is seldom the position with the largest electron density [21].

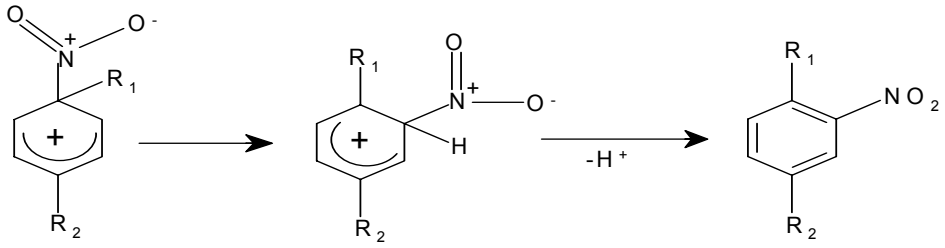

(4) (3)

Ipso-electrophilic attack at a substituent position represents another exception to the general mechanism. With di-and polyalkyl benzenes, the ipso-nitroarenium ion (4) may be formed instead of (3). Although rearrangement of (4) to the conventional Wheland intermediate does occur, it is accompanied by side reactions such as

nitrodealkylation, thus giving nitration of polyalkyl benzene potentially more variable mixture products than other nitration. Increasing understanding of the formation of ipso-Wheland intermediates has led to the exploitation in other reactions, especially with nucleophiles.

1. 3 NITRATING AGENTS

For reasons of practicability and economics, industrial-scale nitration is usually carried out with a mixture of nitric and sulfuric acids (mixed acid), and occasionally with aqueous nitric acid in acetic acid, or nitric acid in acetic anhydride and nitrogen oxides.

The strength of the nitrating agent ($X\text{-}NO_2$) decreases with decreasing electronegativity of X [22]: nitronium ion (e.g., $BF_4NO_2^+$) > nitracidium ion ($OH_2^+\text{-}NO_2$) >nitronium chloride ($Cl\text{-}NO_2$) > acetyl nitrate ($AcO\text{-}NO_2$) > nitric acid ($HO\text{-}NO_2$) > ethyl nitrate ($C_2H_5O\text{-}NO_2$).

The nitronium ion, NO_2^+, is considered to be the active species in all of these systems. The overall equation is:

$$HNO_3 + 2H_2SO_4 = NO_2^+ + H_3O^+ + 2HSO_4^-$$

A typical nitrating agent for large-scale mononitration consists of 20 % HNO_3, 60 % H_2SO_4, and 20 % water, which are referred to as 20/60/20 mixed acid. Stronger nitric acid leads to oxidative side reactions, whereas higher temperature leads to decreased NO_2^+ ion concentration.

Nitration is alternatively carried out using nitrogen dioxide/ozone mixture [23], but in this nitration selective production of mononitrated products is difficult because of powerful nature of nitrating agent.

Some of these methods using less stable acetyl nitrate requires *in situ* generation of nitric acid using metal nitrates and organic acid which requires tedious work up procedures. On the basis of the above facts, it is clear that there is a need for more regioselective control of nitration using nitric acid as a nitrating agent to obtain higher conversion and selectivity. To our understanding very little study has been done on the regioselective nitration using nitric acid as a nitrating agent over solid acid catalysts.

Catalytic nitration of aromatics with aqueous nitric acid would be an interesting alternative environmental friendly route for the production of aromatic nitro compounds provided that it is economically attractive. Replacement of sulfuric acid in "mixed acid" aromatic nitrations by inorganic solids, with accumulation or elimination of produced water results in a fundamentally different behavior of the "HNO_3 – solid" couple. If water accumulates, nitric acid becomes a selective oxidative coupling agent, whereas when water is eliminated efficiently, nitric acid alone behaves as a strong nitrating agent, with increased para selectivity as compared to the sulfo-nitric system [24].

The major drawback of the use of sulfuric acid could be overcome by the use of solid acid catalysts. Nitration using solid acids may be the answer to these problems. The use of solid acid catalysts is potentially more attractive because of the ease of removal and recycling of the catalyst and the possibility that the solid might influence the selectivity. Regeneration of solid acid would be achieved by a simple thermal treatment [25].

1. 4 SOLID ACID CATALYSTS

Solid acid catalysis is one of the most important areas of research and has assumed great relevance as an economic alternative to many homogeneously catalyzed, industrially important reactions. The solid acid catalysts can also be designed to give

higher activity, selectivity, regenerability and longer catalyst life. In the last two decades, substantial progress has been made and several industrial processes that use solid acid-base catalysts have been introduced successfully. A comparative account of the acid strengths of some typical acids used in the industry may be given in terms of Hammett acidity function, H_0 scale (Table 1) [26].

Table 1. 1 – Acid strengths of some typical acids

Acid	H_0 (Hammett acidity scale)
Sulfuric acid (100%)	- 12
Hydrogen fluoride (anhydrous)	-10
Zeolites, RE-Y/H-ZSM-5/Beta	-12 to –14
Kaolinite clay	+1.2 to –2
Acid-washed montmorillonite clay	-5 to –8
Amberlyst-15 resin	-12
Sulfated zirconia	-10 to –14

Some of the unique features of solid acids are: a) their use as Brönsted and/or Lewis acids, depending on the conditions: b) the difference in the acid strength and acid site distribution, which depends on the method of preparation c) catalytic activity at higher temperatures when they are less sensitive to water and alcohols d) shape selective characteristics in some solids e) diffusional resistance in some applications.

The use of variety of solid acids and zeolitic materials in the production of aromatics and petrochemicals such as xylene, ethylbenzene, cumene and their alkylbenzenes are well known in the recent past [27]. There is a great scope for the introduction of solid catalysts in the synthesis of fine chemicals and pharmaceutical

intermediates. Recently the superacid catalysts also have come into focus for acid catalyzed reactions. Solid acid catalysts may be classified as zeolite, clay and mixed oxides including superacid catalyst.

1. 4. 1 Classification:

Generally, a solid acid catalysts following both the Brönsted and Lewis definitions, a solid acid shows a tendency to donate a proton or to accept an electron pair [28].

1	**Natural clay minerals:** Kaolinite, bentonite, montmorillonite, Zeolites (X, Y, A, H-ZSM etc).
2	**Mounted acids:** H_2SO_4, H_3PO_4, $CH_2(COOH)_2$ mounted on silica, quartz sand, alumina or diatomaceous earth
3	**Cation exchange resins:** Amberlite.
4	***Metal oxides and sulphides:*** ZnO, CdO, Al_2O_3, CeO_2, ThO_2, TiO_2, ZrO_2, SnO_2, PbO, As_2O_3, Bi_2O_3, Sb_2O_5, V_2O_5, Cr_2O_3, MoO_3, WO_3, CdS, ZnS
5	***Metal salts:*** $MgSO_4$, $CaSO_4$, $SrSO_4$, $BaSO_4$, $CuSO_4$, $ZnSO_4$, $CdSO_4$, $Al_2(SO_4)_3$, $FeSO_4$, $Fe_2(SO_4)_3$, $CoSO_4$, Cr_2SO_4, $KHSO_4$, K_2SO_4, $(NH_4)_2SO_4$, AgCl, CuCl, $AlCl_3$, CaF_2, BaF_2, $Zr_3(PO_4)_4$, $Fe(NO_3)_3$, $AlPO_4$
6	***Mixed Oxides:*** SiO_2-Al_2O_3, SiO_2-TiO_2, SiO_2-SnO_2, SiO_2-ZrO_2, SiO_2-Y_2O_3, SiO_2-La_2O_3, Al_2O_3-B_2O_3, Al_2O_3-ZrO_2, Al_2O_3-V_2O_5, Al_2O_3- WO_3, TiO_2-V_2O_5, TiO_2-MoO_3, TiO_2-WO_3, MoO_3-NiO-Al_2O_3, MoO_3-Al_2O_3-MgO, & Heteropolyacids and Perfluorinated polymer sulphuric acid catalysts e.g. Nafion-H

1. 4. 2 Nature of Acid Sites on Solid Acid Catalysts:

There are large number of reactions, which are catalyzed by acid sites, and their importance has surpassed the interest in the fundamental chemistry. The acidity of a

material is defined relative to a base used in acid-base interaction. The amount of acid on a solid is usually expressed as the number of millimole of acid sites per unit weight or per unit surface area of the solid, and is obtained by measuring the amount of a base, which reacts with the solid acid. The following two techniques are widely used to determine the nature of acid sites and acid strength of a solid acid.

a. **Adsorption and Temperature-programmed Desorption of Base Molecules**
b. **Vibrational Spectroscopy Methods**

a. Adsorption and Temperature-programmed desorption of base molecules

This method is based on desorbing volatile amines such as NH_3, pyridine, n-butylamine, quinoline, etc., that has been allowed to adsorb on a solid catalyst, by heating it at a programmed rate. This simple method is normally used to measure the number and strength of acid sites on solid catalysts [29]. Excess of gas is added, and physically adsorbed gas is then removed by prolonged evacuation. Whatever is left on the surface, after evacuation, is considered to be chemically adsorbed and that is the measure of the total acid sites. In general it is recommended to analyze the exit gases during the TPD measurements by TCD detector as well as with spectroscopic techniques in order to determine the bonding of the probe molecules with the different type of acid sites.

b. Vibrational Spectroscopy Methods

Infrared (IR) spectroscopy has been used to determine acidity of solid catalysts by studying adsorbed probe molecules [30]. IR spectroscopic method is the most widely used method for the determination of surface acidity and structural details.

IR spectroscopic studies of ammonia and pyridine adsorbed on solid surfaces makes it possible to distinguish between Brönsted and Lewis acids and to access their

amounts independently. The original work was reported in a paper by Mapes and Eischens [31], who found that the IR spectra of ammonia adsorbed on silica-alumina show two kinds of adsorption one of which indicates NH_3 adsorbed on Lewis acid sites and the other NH_4^+ on Brönsted acid sites [32].

In Table 1. 2 the IR frequencies of the bands observed by adsorbing pyridine on solid acid are given. The characteristic bands of pyridine protonated by Brönsted acid site (pyridinium ions) observed at ~1540 and 1640 cm^{-1} while the other from pyridine coordinated to Lewis acid sites appear at ~1450 and 1620 cm^{-1}[31]. It is possible to calculate the number of Brönsted and Lewis acid sites capable of retaining pyridine at certain desorption temperatures.

Table 1. 2. Infrared bands of pyridine on acid solids in the 1400 ~1700 cm^{-1} region*

Hydrogen bonded pyridine	Coordinately bonded pyridine	Pyridinium ion
1440 ~ 1447(v.s.)	1447 ~ 1460 (v.s.)	
1485 ~ 1490 (w)	1488 ~ 1503 (v)	1485 ~ 1500 (v.s.)
		1540 (s)
1580 ~ 1600 (s)	~ 1580 (v)	
	1600 ~ 1633 (s)	~ 1620 (s)
		~ 1640 (s)

* Band intensities: v.s. – very strong; w – weak; v - variable

To measure the surface acidity of the solid acid catalysts, three more methods are also used as given below:

c. Nuclear Magnetic Resonance Methods

d. Photoelectron Spectroscopy Methods

e. Surface acidity from the Analysis of the Positron Annihilation Line Shapes

1. 5 ZEOLITES

Zeolites form an extraordinary, diverse and interesting class of inorganic macromolecules. They have continued to fascinate scientists for decades due to the immense opportunities they offer for research. They have benefited the chemical industry equally, in numerous ways. Recently, their range of application has widened considerably, more noticeably as heterogeneous catalysts, catalyzing a number of organic reactions.

Zeolites are crystalline hydrated alumino-silicates, possessing a rigid framework based on an infinitely extending three-dimensional network of SiO_4^{-4} and AlO_4^{-5} tetrahedra, linked through oxygen atoms. Within this framework are present well-defined channels and cavities of specific dimensions rendering them microporous. The excess negative charge on the AlO_4 tetrahedron is compensated by cations, resulting in an electrically neutral framework. The crystallographic unit cell of a zeolite may be represented as $M_2x/n\{(Al_2O_3)_x.(SiO_2)_4\}.zH_2O$, where `M' represents exchangeable cation of `n' valency generally from group I or II, rare earth ions or an organic species and `z' gives the number of water molecules [33].

Zeolites are classified according to their morphological characteristics [34-36], crystal structure [34-35], effective pore diameter (Table 1.3), chemical composition [37] and natural occurrence.

Table 1.3 : Classification of zeolites on the basis of the effective pore diameter [38].

Small pore (8 MR)	**Medium pore (10 MR)**	**Large pore (12 MR)**
Li-A	Dachiardite	Linde X, Y, L
MTN.	Epstilbite	Gmelinite
NU-1	Ferrierite (FER)	Mazzite
Bikitaite	Heulandite	Mordenite
Brewsterite	Laumontite	Offretite
Chabazite	ZSM-5 (MFI)	ZSM-12 (MTW)
Edingtonite	ZSM-11 (MEL)	Omega
Erionite	EU-1 (ZSM-50)	Beta (BEA)
Gismondine	ZSM-23	
ZK-5	Theta-1 (ZSM-22)	
Levynite	ZSM-48 (EU-2)	
Linde A		
Merilonite		
Natrolite		

1. 5. 1 Zeolite Synthesis

Synthetic zeolites are normally crystallized from aqueous alkaline gels containing sources of silica, alumina and cations. Crystallization may take hours or weeks and is generally carried out hydrothermally in the temperature range of ~333 to 473K under autogenous pressure and static / stirred conditions. The nature of the product is controlled by kinetic factors and small changes in the conditions can alter the product.

The first step in zeolite synthesis essentially involves the dissolution /depolymerization of aluminum and silicon species to form aluminate and silicate ions,

which then couple with the template and/or inorganic cations to form a gel by condensation/polymerization. The chemical transformations steps involved in zeolite crystallization have been summarized by Sand [39-40].

Crystallization of a zeolite generally occurs from a molecule in homogenous system i.e., the reactive gel. Based on experimental evidence, two theories have been postulated to explain the crystallization mechanism in zeolite formation: i) The solid-solid phase transformation and ii) Solution-solid phase transformation [41]. The exact nature of the mechanism depends upon the reactants, method of mixing and other synthesis conditions.

1. 5. 2 Special Features of Zeolite

1. 5. 2. 1 Generation of Acidity

When the cationic form of any zeolite is converted into its H-form or proton form, the zeolite is said to be acidic. Acidity is dependent upon the number of Al^{3+} present in the framework or in other words zeolites with low silica to alumina ratios are highly acidic and their acidity decreases with increase in silica to alumina ratio.

When hydrogen (proton) of the zeolite framework exhibits the property to act as a proton donor it is referred to as Brönsted acid [42]. When the zeolite is heated to 823 K, Si—O—Al bond breaks giving rise to Lewis acid site and water.

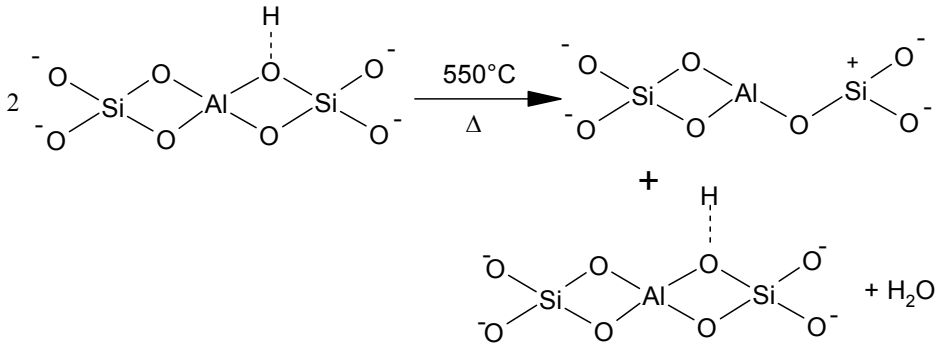

Generally, in zeolites both Bronsted and Lewis acid sites exit simultaneously.

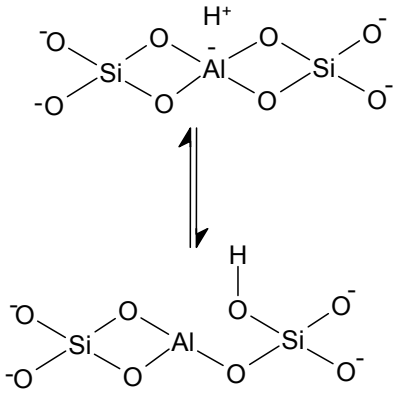

1. 5. 2. 2 Shape selectivity of zeolites

Shape selectivity plays an important role in molecular sieve catalysis. Weisz and Frilette [44] were the first to describe the shape selectivity. The pore size and shape may affect the selectivity of a reaction in four 4 ways:

Reactant shape selectivity:

This results from limited diffusivity of some of the reactants, which cannot effectively enter and diffuse inside the crystal. The zeolite pore is such that it admits only certain smaller molecules from the reactants and excludes larger molecules and hence in the reaction mixture only the smaller molecules react effectively [Fig. 1.1a].

Product shape selectivity:

When certain bulkier compounds are formed or produced within the zeolite pores during a reaction they cannot diffuse out due to large dimensions. These will either be converted to smaller products and diffuse out or they may block the pores resulting in the deactivation of the catalyst. For example in toluene methylation, p-xylene is the major product in modified zeolites as compared to bulky o- and m- isomers due to pore diameter restrictions [Fig. 1.1b].

Restricted transition state shape selectivity:

This type of shape selectivity is observed when certain reactions are prevented because of restrictions in the inner pore space for the corresponding transition state. Diffusion of reactants and products in this situation are not hindered nor are the reactions involving smaller transition state [Fig. 1.1c].

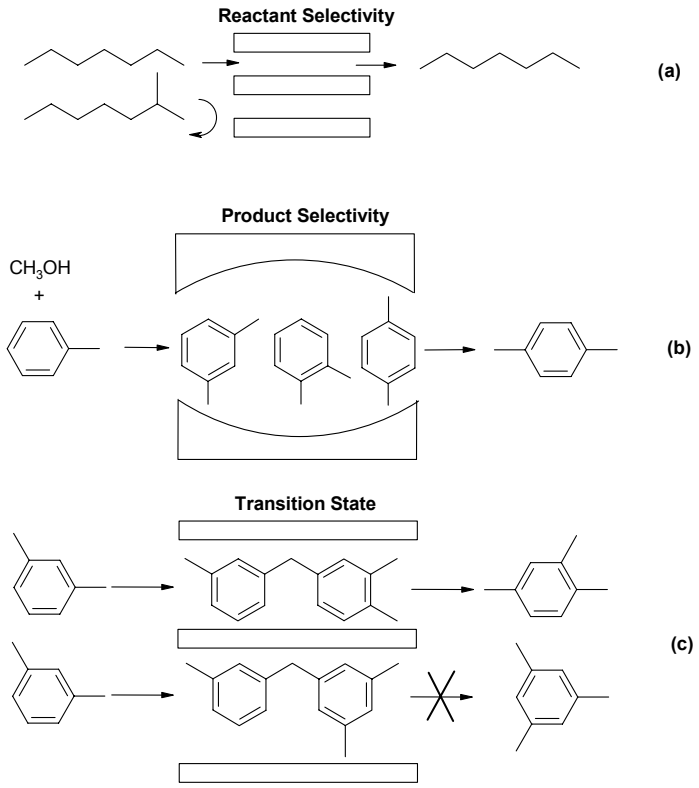

Fig. 1.1 : Shape selectivity in zeolites

1. 5. 3 Zeolite Beta :

Zeolite Beta was first synthesized in 1967, by Wadlinger et al. [44]. Its crystal structure was resolved recently [45-46]. Zeolite beta has several unique and interesting features. It is the only high silica zeolite to have fully three-dimensional, 12-membered ring pores with two different types of channel systems. It is the only large pore zeolite to possess chiral pore intersections. Unlike other zeolites, it is the only zeolite to have a near-random degree of stacking faults and adsorbs equal amounts of n-hexane and cyclohexane with a sorption capacity of about 0.23 ml. g^{-1}.

On account of its rigid three-dimensional network of large pores with high framework SiO_2/Al_2O_3 ratios, it is a potential catalyst in many hydrocarbon processes of industrial importance [47-52].

1. 6 OXIDES AND MIXED OXIDES

1. 6. 1 Mixed Oxide Catalysts

Mixed oxides, which contain two or more components, are of catalytic interest because they can be used as supports, catalysts or precursors to other materials. One interesting property that arises by mixing oxides is the generation of strong acidic sites associated with the interface or linkage between the two components [53].

According to the hypothesis proposed by Tanabe et al [54], the acidity generation is caused by an excess of a negative or positive charge in the model structure of a binary oxide. A model structure is pictured according to the two postulates:

- The coordination number of a positive element of a metal oxide, C_1 and that of a second metal oxide, C_2 are maintained even when mixed.
- The Coordination number of a negative element (oxygen) of a major component oxide is retained for all the oxygen in a binary oxide.

For example, TiO_2-SiO_2, where TiO_2 is the major component oxide, and in SiO_2-TiO_2 the SiO_2 is the major component oxide as shown in Fig.1.2. When the single component oxides of positive elements are mixed their coordination number remains 4 for Si and 6 for Ti and according to postulates for negative elements coordination number should be 3 and 2 respectively. In case of Fig.1.2a, the four positive charges of the silicon atom are distributed to four bonds, while the two negative charges of oxygen are distributed to three bonds, i.e. –2/3 distributed to each bond. Therefore for one bond the charge difference is +1-2/3 = +1/3 so for four bonds it is +1/3 x 4 = +4/3, which is excess positive charge and Lewis acidity, is assumed to appear upon the excess of positive charge.

In Fig. 1.2b, four positive charges of titanium atom are distributed to six atoms, i.e. +4/6 to each bond while two negative charges of the oxygen atom are distributed to two bonds. The charge difference for each bond is +4/6-1 = -1/3, and for all the bonds -1/3 x 6 = -2 is excess charge and in this case Brönsted acidity is assumed to appear. TiO_2-SiO_2 system is showing acidity because of the excess of a positive or negative charge [55].

(a)

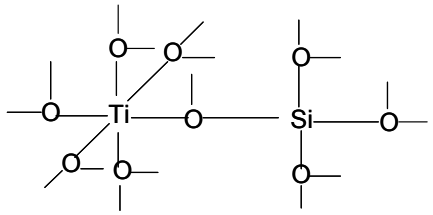

Charge difference: (+4/3 –2/3) x 4 = +4/3

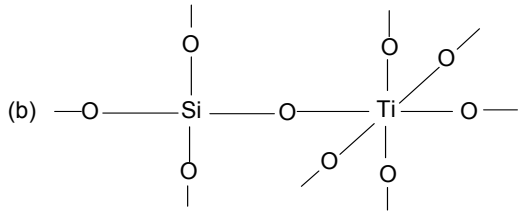

Charge difference: (+4/6 – 2/2) x 6 = -2

Fig. 1.2 Model structures of $TiO_2 – SiO_2$ pictures according to postulates (a) when TiO_2 is major oxide; (b) when SiO_2 is major oxide

In order to maximize the number of these sites, it is desirable to prepare samples that are homogeneously mixed at a molecular level.

Mixed metal oxide catalyst is prepared by two methods; dry method and wet method. In dry method the mixed-oxide catalysts is prepared by grinding or ball-milling them together, either dry or in a wet slurry; followed by calcination to temperatures of 900-1300K giving the solid with a low surface area. Mixed-oxide catalysts are prepared mostly by wet method, such as precipitation, co-precipitation, and sol-gel method. Among these methods the sol-gel method is most useful because high surface area of the catalyst and homogeneous distribution on the support.

Another important consideration in preparing mixed-oxide catalysts is the spontaneous monolayer dispersion of oxides and salts onto surfaces of support substrates on calcination. Both temperature and duration of calcination are important here [56].

1. 6. 1. 1 Sol- Gel Method for the Preparation of Catalysts:

The sol-gel process involves first the formation of a sol followed by that of a gel. A sol, which is a liquid suspension of solid particles ranging in size from 1 nm to 1 micron, can be obtained by the hydrolysis and partial condensation of a precursor such as an inorganic salt or a metal alkoxide. The further condensation of sol particles into a

three-dimensional network produces a gel, which is a diphasic material with a solid encapsulating a solvent.

The gel is dried and calcined. Based on the mode of drying, four types of dried gels are formed [57-58]:

a) conventional evaporative drying such as heating a gel in an oven gives the *xerogel.* It has relatively low surface area and pore volume.

b) in the supercritical drying, the deleterious effects of conventional method are minimized due to differential capillary pressure, giving *aerogel.* They have high pore volumes, surface areas and low bulk densities

c) freeze drying of the solvents at low temperature under reduced pressure & the product is called *cryogel.*

d) subjecting the gel to ultrasonic vibration at room temperature to remove the solvent, resulting in the formation of *sonogel.*

The sol-gel technology is used in order to synthesize materials with good homogeneity and high purity. With this method the materials can be processed at low temperatures and during short periods; it is possible to control the size and, in most of the cases, also the shape of the particles. It has been proved that the sol-gel technology is able to control particle size by calcining samples at different temperatures. For $T \leq 600$ ºC particle size ranges 20-40 nm, increasing close to 1 micron with the calcination temperature. However, three-dimensional gel network comes from the condensation of partially hydrolyzed species.

Following Fig. 1.3 shows the key steps in taking a precursor to a particular product form via sol-gel preparation: formation of a gel, aging of a gel, removal of solvent, and heat treatment.

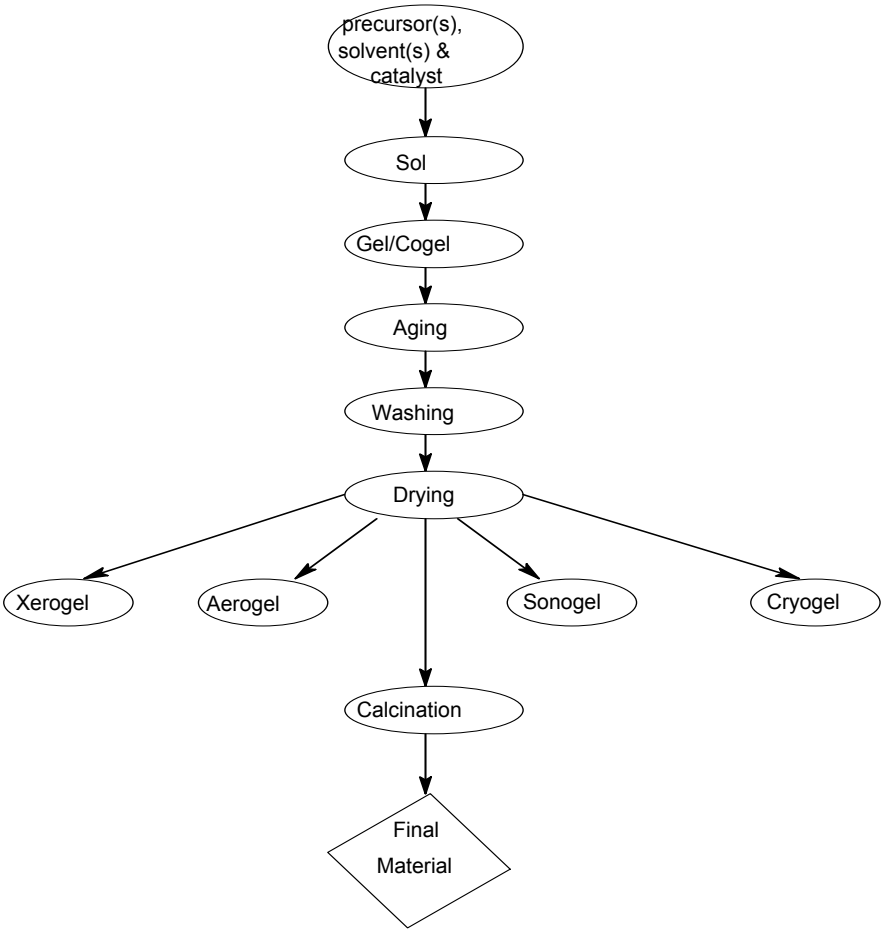

Fig.1 3. Shows the steps involved in the sol-gel process.

1. 7 SOLID SUPERACIDS

A solid superacid is defined as a solid material which shows an acid strength higher than the acid strength (H_0 = -11.9) of 100 % sulfuric acid which have opened new perspectives in the use of solid catalysts for carrying out, reactions involving very strong acid sites under mild conditions [59]. Recently, various kinds of solid superacids have been developed. The first group is metal oxides and mixed oxides containing a small amount of sulfate ion, and those modified with platinum. The second group is metal oxides, mixed oxides, metal salts, etc. treated or combined with antimony fluoride

or aluminum chloride. The third group is perfluorinated polymer sulphonic acid (Nafion-H). The fourth and fifth groups are H-ZSM-5 and a type of heteropolyacids, respectively. The last group is simply mixed oxides.

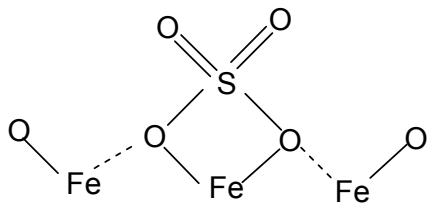

Fig.1. 4 Model structure of a superacid

In Fig 1.4 shows that Fe ion acts as a Lewis acid site, whose acid strength can be strongly enhanced by the inductive effect of S=O in the sulfur complex.

Superacidity can be measured by utilizing the temperature-programmed desorption (TPD) method using ammonia or pyridine, provided that the relative value in TPD is related to the absolute value (Ho) and the interaction of ammonia or pyridine with basic sites on solid surfaces is confirmed to be negligible.

IR spectroscopy study shows that the SO_4^{2-}/ZrO_2, SO_4^{2-}/TiO_2 gave a common strong absorption band at 1375-1390cm^{-1} which indicates high double bond nature of S=O [60].

Some mixed oxides are solid superacids according to measurement by the indicator method. B_2O_3/ZrO_2 calcined at 773 K shows an acid strength of H_0 = -13 and is active for the reactions such as decomposition of ethanol [61].

This type of oxide will offer new opportunities in catalysis, especially for reactions, which require highly thermally stable catalysts. However, their performance has to be improved in order to avoid undesired parallel reactions and catalyst deactivation.

1. 8 CHARACTERIZATION OF SOLID ACID CATALYSTS

1. 8. 1 X-ray diffraction:

X-ray powder diffraction is the single most important technique used to characterize zeolites. It furnishes vital information regarding phase purity, structure type, isomorphous substitution, degree of crystallinity and also makes possible the estimation of unit cell parameters [62-63]. Modern methods have used ab initio calculations and Reitveld analyses to solve zeolite structure using powder X-ray patterns [64-68].

1. 8. 2 Thermal analysis:

This technique provides information regarding the thermal behavior of the catalysts. It is used extensively in the study of kinetics and dehydration of zeolites and also for studying the oxidative combustion of occluded organics in zeolites [69]. Differential thermal analysis (DTA) curves provide qualitative and quantitative information about the energy of activation and enthalpy of the zeolite systems.

1. 8. 3 Adsorption measurements:

The ability of the catalysts to adsorb only selected molecules inside the channels and cavities enables adsorption measurements to be a useful tool in providing information about their void volume, crystal size, degree of crystallinity, acidity, diffusion limitations and pore blockages if any. Besides, sorption studies also help in determining specific interactions between the sorbate and sorbents as well as the strength of such interactions [70]. Various thermodynamic parameters such as entropy, heat and free energy of sorption can also be estimated with the help of sorption measurements.

1. 8. 4 Temperature programmed desorption (TPD) of ammonia:

The estimation of acid strength distribution in solid acid catalysts is carried out by this technique. It is used to characterize weak, medium and strong acid sites. The amount of ammonia released above 753K is normally considered to represent very strong acid sites. The presence of different types of acid sites have been reported by several workers using TPD method [71-72].

1. 8. 5 Fourier-Transform Infrared spectroscopy:

This is one of the most sensitive tool for the investigation of the structural features of zeolites, the isomorphous substitution in them, their acidity, and the nature of zeolite-adsorbate interactions [73-75]. Zeolites may be characterized by infrared spectroscopy yielding valuable information in the vibrational mode region (400-1300 cm^{-1}). IR spectroscopy can also distinguish large pore zeolites from small and medium pore ones on the basis of OH stretching vibrations [76]. This technique is also used to estimate the acid sites of solid acid catalysts by the adsorption of various basic probe molecules like ammonia, pyridine and benzene and to measure the acidity qualitatively as well as quantitatively.

1. 8. 6 Surface area measurement:

The Braunauer-Emmett-Teller (BET) volumetric gas adsorption technique using nitrogen, argon, etc. is a standard method for the determination of the surface areas and pore size distribution of finely divided porous samples [77]. The surface area of the sample is calculated using the Brunauer-Emmet-Teller (BET) method. The general form of the BET equation can be written as

$$1/V_{ads}\,(P_0\text{-}P) = 1/V_mC + [C\text{-}1/V_m\,C]\;P/P_0$$

where, V_{ads} = Volume of gas adsorbed at pressure P,

P_0 = Standard vapor pressure,

V_m = Volume of the gas adsorbed for monolayer coverage

C = BET constant.

By plotting the left hand side of the equation against P/P_0, a straight line is obtained with a slope $(C-1)/V_m C$ and an intercept $1/V_m C$. The BET surface area was calculated using the formula

$$S_{BET} = X_m N. A_m.$$

Where N is the Avagadro's number, A_m is the surface area of the adsorbate molecule [For N_2, $A_m = 0.162$ nm^2] and X_m is the moles of nitrogen adsorbed.

1. 8. 7 Scanning Electron Microscopy (SEM):

The crystallite size and morphology of the samples were analyzed by a scanning electron microscope equipped with energy dispersive X-ray analysis. Cathode rays are bombarded on the sample and the scattered Secondary Electrons are used to form image. A thin layer (~ 0.1 mm) of the sample was mounted on a carrier made from alumina and was coated with a film of Gold to prevent surface charging and to protect the zeolite material from thermal damage by the electron beam [78]. The major advantage of the SEM is that bulk samples can be studied by this technique. To analyze the specimen composition, EDX analysis was done.

1. 8. 9 Nuclear magnetic resonance spectroscopy :

High-resolution solid-state NMR spectroscopy using Magic angle spinning (MAS) has become a powerful method to characterize zeolite materials [79-82]. Till now about twenty different NMR active nuclei have been studied. Much attention has been focused towards ^{29}Si and ^{27}Al MAS NMR in order to investigate the nature of Si

and Al ordering in the zeolite framework [83], as well as the crystallographically equivalent and nonequivalent Si [84] and Al [85] ions in various sites.

^{1}H MAS NMR has been used to study zeolite acidity [86-87], arising out of the various types of protons.

1. 9 SCOPE OF THE THESIS

The literature review on nitration of aromatic compounds clearly indicates that there is a scope for using solid acid catalysts to replace conventional sulfuric acid in nitrating mixture to have an environment friendly process. The well known advantage of heterogeneous catalysts such as ease of separation of catalysts, its recycle as well as selective formation of desired products needs to be evaluated for developing a suitable catalyst for nitration aromatic compounds. Various zeolites and metal oxide catalysts have been studied before and among the zeolite catalysts beta zeolite has shown better catalytic activity for aromatic nitration. Among the metal oxide catalysts sulphated zirconia, binary metal oxides reportedly showing superacidity were found to be active in aromatic nitration. However, the deactivation of such catalysts was observed in previous studies probably due to the use of strong nitric acid used for nitration. Under this condition aromatics form oxidized side products leading to the deactivation of the catalysts. The presence of water from nitric acid as well as formed during the reaction was believed to be detrimental in deactivating the catalysts. Attempts were made to remove or reduce water by azeotropic distillation in order to improve the catalyst life.

Considering the literature reports and the observations as mentioned above the objective of the present work was to study the nitration of aromatic compounds such as benzene, toluene, phenol and xylenes using zeolite catalysts with emphasis on beta zeolite as well as sulfated zirconia and other metal oxide superacid catalysts. The

another objective of this work was to study the nitration of aromatics using nitric acid of various dilution to find out effect of water in the reaction medium on catalyst activity and its stability for aromatic nitration in liquid and vapor phase.

With these objectives the work was carried out as follows.

1) Commercial zeolites catalysts were used for nitration so that further optimization and scale up work becomes easier.
2) Sulfated zirconia and supported sulfuric acid catalysts were prepared and tested for its activity for aromatic nitrations.
3) Molybdenum oxide on silica support with iron oxide as promoter catalyst was prepared by sol-gel technique using ethyl silicate-40 as a new silica source and it was used for aromatic nitration reactions.
4) Borated zirconia catalyst was also prepared and tested for aromatic nitration.
5) Characterization of these solid acid catalysts, fresh and after use in nitration was done by physicochemical and spectroscopic methods such as XRD, surface area measurement, TPD of ammonia, FTIR spectroscopy and thermal analysis.
6) The study of deactivation of catalysts, which is a main problem in the nitration.
7) To study nitration of various aromatic compounds such as benzene, toluene, phenol, o-and m-xylenes over solid acid catalysts using dilute nitric acid as a nitrating agent. The studies were directed for developing a process as an attractive alternative to the conventional process from environmental as well as technological point of view.

1. 10 REFERENCES

1. K. Winnacker, L. Kuchler, in *Chemische Technologie*, Band 6, Organische Technologie II (4th edition), Edited by H. Harnisch, R. Steiner, K. Winnacker (Carl Hanser Verlag, Munchen, 1982) p. 169.
2. *Ullmann's Encyclopedia of Industrial Chemistry*, VCH, Weinheim, Vol.**A17**, 411 (1991).
3. T. Travis: "*Early Intermediates for the Synthetic Dyestuffs Industry*". Chem. Ind. London 508-514 (1988).
4. L. Bretherick: *Handbook of reactive Chemical Hazards*, 3rd ed., Butterworths, London (1985).
5. C. K. Ingold, *Structure and Mechanism in Organic Chemistry*, Cornell University Press, Ithaca, NY, (1969).
6. G.A. Olah, R. Malhotra, and S. C. Narang, *Nitration: Methods and Mechanisms*, VCH Publishers, (1989).
7. a) C. K. Ingold, D. J. Millen, and H. G. Poole, *J. Chem. Soc*., 2576 (1950); & b) R. J. Gillespie, E. D. Hughes, C. K. Ingold, and E. R. A. Peeling, *J. Chem. Soc*., 2504 (1950); & c) E.D. Hughes, C. K. Ingold, and R. I. Reed, *J. Chem. Soc*., 2400 (1950).
8. a) G.A. Olah, *Acc. Chem. Res*., **4**, 240 (1971). & b) J. H. Ridd, *Acc. Chem. Res*., **4**, 248 (1971). & c) L. M. Stock and H. C. Brown, *Adv. Phys. Org. Chem*., **1**, 35 (1963).
9. a) N.C. Marziano, A. Tomasin, C. Tortato, J.M. Zaldivar, *J. Chem. Soc. Perkin Trans. 2*, 1973 (1998).
   b) M. Sampoli, A. DeSantis, N. C. Marziano, F. Pinna, A. Zingales, *J. Phys. Chem.* **89**, 2864 (1985).
   c) N.C. Marziano, A. Tomasin, M. Sampoli, *J. Chem. Soc. Perkin Trans. 2* 1995 (1991).
10. L. Main, R. B. Moodieand, K. Schofield, *J. Chem. Soc., Chem. Commun*., 48 (1982).
11. J.H. Ridd and J. P. B. Sandall, *J. Chem. Soc., Chem. Commun*. 402 (1981).
12. a) M. Ali and J.H. Ridd, *J. Chem Soc., Perkin Trans. 2*, 327 (1986). & b) U. Al-obaidi and R.B. Moodie, *J. Chem. So., Perkin Trans.2*, 467 (1985).

13. J. Kenner, *Nature* (London), **156**, 369 (1945).

14. S. Nagakura, J. Tanaka, *J. Chem. Phys*. **22**, 563 (1954).

15. a) C. Yang and Q. Xu, *Zeolites*, **19**, 404 (1997).
b) G. A. Olah, S. J. Kuhn and S. H. Flood, *J. Am. Chem. Soc*., **83**, 4571 (1961).

16. V. A. Koptjug, *Arenonium Ions: Structure and Reaction Ability*, Nauka, Novosibirsk, (1983).

17. J. Feng, X. Zheng and M. Zerner, *J. Org. Chem*. **51**, 4531-4536 (1986).

18. K. Schofield, *Aromatic Nitration*, Cambridge University Press, London, (1980).

19. L. Eberson, M. Hartshorn and F. Radner, *Acta Chemica Scandinavica*, **48**, 937-950 (1994).

20. a) M. P. Hartshorn, R. J. Martyn, K. H. Sutton, J. M. White, *Aust J. Chem*. **38**, 1613 (1985).
b) G. S. Bapat, A. Fischer, G. N. Henderson, S. Raymahasay, *J. Chem. Soc., Chem. Commun.*, 119 (1983).
c) A. K. Manglik, R. B. Moodie, K. Schofield, A. Dutly, P. Rys, *J. Chem. Soc., Perkins Trans.* **2**, 1358 (1981).

21. P. Politzer, K. Jayaswriya, P. R. Laurence, *J. Am. Chem. Soc.*, **107**, 1174 (1985).

22. R.J. Gillespie, D. J. Millen, *Rev. Chem. Soc.* 2, 277-306 (1948).

23. Suzuki et. al., *J. Chem. Soc. Commun*., 1049-1050, (1991).

24. M. H. Gubelmann, C. Doussain, P.J. Tirel and J. M. Popa, *Stud. Surf. Sci. Catal*., **59**, 471-8, (1991).

25. L.V. Malysheva, E.A. Paukshtis, K.G. Ione, *Catal. Rev. Sci. & Eng*., **37**, 179 (1995).

26. A. V. Ramaswamy, *Chim. Ind*. (Milan), **82(6)**, E/1-E/9 (Italian) (2000).

27. K. Tanabe, W. F. Holderich, *Appl. Catal. A: General*, **181**, 399 (1999).

28. G. Ertl, H. Knozinger, J. Weitkamp, *Handbook of Heterogeneous Catalysis*, Vol. **2**.

29. J. Klinowshi, *Chem. Rev*. 91, 1459, (1991)

30. a) W. N. Delgass, G. L. Haller, R. Kellerman, *Spectroscopy in Heterogeneous Catalysis*; Academic Press, New York, (1979) & b) Ward, J. W. *J. Catal*., **17**, 355 (1970); & **18**, 248 (1970).

31. J. E. Mapes and R. R. Eischens, *J. Phys. Chem*., **58**, 809 (1954).

32. J. Turkevich, *Catal. Rev*.**1**, 1 (1968).
33. D. W. Breck, in *"Zeolite Molecular Sieves"*, Wiley Pub. New York, (1974).
34. E. P. Parry, *J. Catal*. **2**, 371 (1963).
35. Barrer, R.M., in *"Hydrothermal Chemistry of Zeolites"*, Acad. Press, New York, (1982).
36. T. R. Hughes and H.M. White, *J. Phys. Chem*., 71, 2192 (1967).
37. W. M. Meier, and D. H. Olson, in "*Atlas of Zeolite Structure Types"*, 2nd Edn. Butterworths, London, (1987).
38. E. M. Flanigen, in "*Proceedings of the fifth international zeolite conference"*, Ed. L.V.C. Rees, Heydon, London, 760 (1980).
39. L. B. Sand, *Econ. Geol.* 161 (1967).
40. L. B. Sand, *Pure and Applied chemistry*, **52**, 125 (1980).
41. a) G. T. Kerr, *J. Phys. Chem.*, **70**, 104 (1966) & b) G. T. Kerr, *J. Phys. Chem*, **72**, 1385 (1968).
42. J. W. Ward, *"Zeolite Chemistry and Catalysis",* [C. Rabo, J.A. Eds.], ACS mongraph. Chp. 2, **171**, 118 (1976). & D. W. Breck, *"Zeolite Molecular Sieves",* John Wiley and Sons, New York, 449 (1974).
43. P. B. Weisz, and V. S. Frilette, *J. Phys. Chem.* **64**, 382 (1960).
44. R. L. Wadlinger, G. T. Kerr, and E. J. Rosinki, U.S. Pat. 3, 308, 069 (1967).
45. J. M. Newsam, M. M. J. Treacy, W. T. Koetsier, and C. B. De Gruyter, "*Proc. Royal. Soc. Lond.*" **A420**, 375- 405 (1988).
46. J. B. Higgins, R. B. La Pierre, J. L. Schlenker, A. C. Rohrman, J. D. Wood, G. T. Kerr, and W. J. Rohrbaugh, *Zeolites*, **8**, 446 (1988).
47. L. B. Young, *Eur. Pat. Appl*., 30, 084 (1981).
48. M. A. Tobias, *U.S. Pat* 3, 728, 408 (1973).
49. R. B. La Pierre, and R. D. Patridge, *Eur. Pat. Appl*. **94**, 827 (1983).
50. R. B. La Pierre, R. D. Patridge, N. Y. Chen, and S. S. Wong, *US. Patent* 4,501,926 (1986).
51. J. A. Martens, J. Perez-Pariente, E. Sastre, A. Corma, and P. A. Jacobs, *Appl. Catal.* **45**, 85 (1988).
52. L. J. Leu, L. Y. Hou, B. C. Kang, C. C. Li, S. T. Wu, and J. C. Wu, *Appl. Catal*, **69**, 49 (1991).
53. K. Tanabe in *Catalysis: Science and Technology*, Springer-Verlag, Berlin, (2),

231-271 (1981).

54. Kozo Tanabe, M. Misono, Y. Ono, H. Hattori; *New Solid Acids & Bases-Their catalytic properties (Stud. in Sur. Sci. and Catal.* **51**) (1989).
55. M. Ithoh, H. Hattori and K. Tanabe, *J. Catal*., **35**, 225 (1974).
56. Y.C. Xie, Y.Q. Tang, *Adv. Catal*, **37**, 1-43 (1991). & b) H. Knozinger, E. Taglauer, *Catalysis*, The Royal Society of Chemistry, Cambridge, (1993).
57. T. Lopez, F. Tsompantzi, J. Navarrete, R. Gomez, J.L. Boldu, E. Munoz, and O. Novaro, *J. Catal.* **181**, 285-293 (1999).
58. A. Keshavaraja; *Bulletin of the Catalysis Society of India,* **6 (1)**, (1996).
59. G. A. Olah, G.K.S. Prakash, J. Sommer, *superacids*, Wiley, New York, (1985).
60. T. Jin, T. Yamaguchi, K. Tanabe, *J. Phys. Chem*. **90**, 4794 (1986).
61. K. Arata, *Appl. Catal. A: General*, **146**, 3-32 (1996).
62. Van R. Balmoos. in *"Collection of Stimulated XRD Powder Patterns of Zeolites*", Butterworths, London, (1984).
63. W. M. Meier, in *"Molecular Sieves"*, Soc. Chem. Ind, London, 283 (1968).
64. J. J. Pluth, J. V. Smith, and J. M. Bennett, *Acta. Crystallogr.* **C42**, 283 (1986).
65. J. F. Charnell, *J. Cryst. Growth*, **8**, 271 (1971).
66. H. M. Rietveld, *J. Appl. Crystallogr*. **2**, 2 (1969).
67. E. G. Derouane, S. Detremmerie, Z. Gabelica, and N. Blom, *Appl. Catal,* **1**, 20 (1981).
68. R. M. Barrer, and D. A. Langloy, *J. Chem. Soc,* 3804 (1958).
69. Ligia Siena de Saldarriga, C. Saldarrage, and M. E. Davies, *J. Am. Chem. Soc*., **109**, 109 (1987).
70. R. J. Naddenriep, *Colloid Interface Science*, **28**, 293 (1968).
71. N. Topsoe, R. K. Penderson, and E. G. Derouane, *J. Catal*, **70**, 41 (1981).
72. R. B. Borade, S. G. Hegde, S. B. Kulkarni, and P. Ratnaswamy, *Appl. Catal*, **13**, 27 (1984).
73. E. M. Flanigen, and H. Khatami, in "*Molecular Sieve Zeolites - 1*", ACS Monograph, Eds. Szymanski, H. A., **101**, 201 (1971).
74. E. M. Flanigen, in *Zeolite Chemistry and Catalysis*, ACS Monograph, (Eds. Rabo, J. A., et.al.), **171**, 180 (1976).
75. N. Kutz, in "*Heterogeneous Catalysis -II"*, Eds. Shrpiro, B. L., 121 (1984).
76. J. W. Ward, "*Zeolite Chemistry and Catalysis"*, Ed. Rabo, J. A., et.al., ACS

Monograph, **171**, 80 (1976).

77. S. A. Bradley, M. J. Gattuso, *Characterization and Catalyst Development*. ACS Symp. Ser. **411**, 2 (1989).

78. H. Knozinger, *Adv. Catal*, **25**, 184 (1976).

79. P. A. Jacobs, and Von Ballmoos, *J. Phys. Chem.*, **86**, 3050 (1982).

80. C. T-W. Chu, and C. D. Chang, *J. Phys. Chem*. **89**, 1569 (1985).

81. N. Y. Topsoe, K. Pederson, and E. G. Derouane, *J. Catal*, **70**, 41 (1981).

82. M. W. Anderson, J. Klinowski, *Zeolites*, **6**, 455 (1986).

83. E. Lippmaa, M. Magi, A. Samason, G. Engelhardt, and A. R. Grimmer, *J. Am. Chem. Soc.***, 102**, 4889 (1983). b) E. Lippmaa, M. Magi, A. Samason, M. Tarmak, and G. Engelhardt, *J. Am. Chem. Soc.*, **103**, 4992 (1981).

84. C. A. Fyfe, G. C. Gobbi, J. Klinowski, J. M. Thomas, and S. Ramdas, *Nature*, (London), **296**, 530 (1982).

85. C. A. Fyfe, G. C. Gobbi, J. K. Hartman, J. Klinowski, and J. M. Thomas, *J. Phys. Chem"*, **86**, 1247 (1982).

86. D. Freude, M. Hunger, and H. Pfeifer, *Z. Phys. Chemie* (Neue Folge), **152**, 429 (1987).

87. K. F. M. G. J. Scholle, W. S. Veeman, J. G. Post, and Van Hoof, *Zeolites*, **3**, 214 (1983).

CHAPTER II

VAPOR PHASE NITRATION OF BENZENE

2. 1 INTRODUCTION

Nitrobenzene is one of the important aromatic nitro compound used as a solvent and as an intermediate for the manufacture of variety of organic compounds. Most (95 % or more) nitrobenzene produced is converted to aniline, which has many downstream products. The nitration of benzene for commercial production of nitrobenzene (NB) is a well-established process, which has been used since about 1860 [1]. In the basic process a mixture of nitric and sulfuric acid is used as nitrating agent and strongly exothermic reaction is conducted in batch- or continuous reactors. Typically the nitrating agent is a mixture of 56-60 % (w/w) H_2SO_4, 27-32 % (w/w) HNO_3, and 8-17 % (w/w) H_2O at a reaction temperature of 50-90 °C. The reaction mixture forms two phases and the rate of reaction is accordingly dependant on the kinetics and on the mixing efficiency. Sulfuric acid is gradually deactivated by water generated during the reaction and has to be replaced after deactivation. Chemical engineering research into nitration processes has yielded many valuable improvements and results related to improve mixing of the reactants, better energy management of modern nitration plants [2].

Other conventional methods with several variations have also been proposed to produce mononitration of benzene. Single-phase nitration of benzene is carried out with a 2-4-fold excess of 98 % nitric acid at a reaction temperature of 20-60 °C and ambient pressure and total conversion is claimed to be high. Other azeotropic nitration of benzene conducted at 120 °C – 160 °C with excess amount of benzene. Water generated during the reaction is removed as a water-benzene azeotrope and may be separated from the benzene, which is recycled to the reactor. The sulfuric acid remains dry and can be used for longer periods between regeneration.

Acidic solids have been used for selective nitration reactions, in particular the

mononitration of aromatic compounds. The solid acid catalysts can also be designed to give higher activity, selectivity, regenerability and longer catalyst life. In the last two decades, substantial progress has been made and several industrial processes that use solid acid catalysts have been introduced successfully.

Benzene being a less reactive molecule its nitration using concentrated nitric acid over solid acid catalyst in liquid phase results in very low conversion because of slow reaction.

Vapor phase nitration of benzene to nitrobenzene over solid acid catalysts is expected to be a clean process without sulfuric acid waste, in contrast to the conventional liquid phase process which uses a mixed acid (concentrated nitric and sulfuric acid) as a nitrating agent and is accompanied with a large amount of dilute sulfuric acid waste. Many efforts devoted to developing a vapor phase process have been unsuccessful, because either the activity or life of catalysts was not satisfactory [3].

Suzuki et al [4] investigated the vapor phase nitration of benzene with NO_2 using polyorganosiloxanes bearing sulfonic acid groups and silica-supported benzenesulfonic acid catalysts. Sulphated catalysts are not stable catalyst and are faced with several technical problems such as moisture sensitivity, and sulphate leaching.

R. Prins et al. [5-6] have reported modified H-Y zeolite and a modified mordenite catalysts for the vapor phase nitration of benzene by dilute nitric acid [7]. The modified mordenite kept high yield of nitrobenzene at a high space time yields.

Vapor phase nitration of benzene with 56 % nitric acid over H-ZSM-5 at 140-170 °C was studied by Kuznetsova et al. [8] and they observed that the catalysts were rapidly deactivated because of strongly adsorbed species which decomposed when the catalyst was heated in nitrogen at 220-250 °C.

Sato et al. [9-10] studied the vapor phase nitration of benzene over solid acid catalysts such as montmorillonite ion-exchanged with a multivalent metal ion, mixed oxides (e.g., $TiO_2 - MoO_3$), the same oxides treated with sulfuric acid at 500°C and heteropolyacids partially neutralized. Among various solid acid catalysts examined the supported sulfuric acid catalyst was the most active and long-lived catalyst. Although supported sulfuric acid showed good results for the vapor phase nitration of benzene, catalyst activity dropped rapidly after 144h on-stream because of leaching of sulphuric acid [11]. This was related to the slow motion of the catalytically active zone through the catalyst bed.

Vapor phase nitration of aromatic compounds, benzene and toluene at temperature ranging from about 275 °C to about 310 °C using silica gel was reported by McKee and Wilhelm [12]. Bauxite and alumina were reported to be ineffective as catalyst in the vapor phase nitration of benzene.

These reported processes for the vapor phase nitration of benzene have the limitations of low conversions, low space-time yield, low yield, short catalyst life, contamination of the products by undesirable by-products and the complicated nature of catalysts. These processes use concentrated nitric acid as nitrating agent, which leads to the oxidation products deactivating the catalyst.

Subsequently zeolite beta has shown better catalytic activity for vapor phase nitration of aromatics, particularly in nitration of toluene [13]. However this promising catalyst has not been studied in detail for the vapor phase nitration benzene.

Jin S. Yoo et al. reported the metal oxides as catalysts for hydroxylation of benzene to phenol using nitric acid. $Fe/Mo/SiO_2$ catalyst showed good activity for hydroxylation of benzene to phenol via gas phase nitric acid oxidation because of its dual functions: Nitrobenzene was selectively formed below 370°C and selective phenol

formation above 400°C [14].

Considering the potential of beta zeolite and Fe/Mo/SiO_2 for vapor phase nitration of benzene we investigated these two catalysts in detail for its activity for nitration of benzene.

The advantage of using vapor phase conditions is the continuous thermal removal of water and the simple implementation of a continuous nitration process based on a downflow fixed-bed of the solid acid. Elevated reaction temperatures, however, lead to problems of safety, catalyst stability, by-product formation, and therefore the optimization of the reaction parameters is highly desired.

2. 2 EXPERIMENTAL

2. 2. 1 Catalyst Preparation

2. 2. 1. 1 Fe/Mo/SiO_2:

Fe/Mo/SiO_2 catalyst was prepared by sol-gel process to obtain the catalyst with high surface area as well as for uniform distribution of Fe/Mo on silica support. Ethylsilicate-40 (CAS Registry No. 18954-71-7) was used as a silica source for the first time because of its higher silica content as well as low cost as compared to tetraethyl orthosilicate, which is generally preferred silica source for sol-gel synthesis of silica support in catalysis [15]. 250 g of ethylsilicate-40 was mixed with 250 ml of dry isopropyl alcohol under constant stirring. 5.225 g of ferric nitrate was dissolved in 100 ml of isopropyl alcohol and was added to ethyl silicate solution under vigorous stirring. 20.31 g of ammonium heptamolybdate was dissolved in 100 ml of water and was added to the above solution under constant stirring.

A viscous gel was obtained which was further stirred for another two hours and

was kept overnight. A transparent solid product was obtained which was air dried and heated in an oven at 110°C for 12 hours. The product was further calcined at 450°C for 12 hours. The product was ground to fine powder, pressed in the form of pellet and granulated by crushing the pellet to –10 + 20 mesh size for use as a catalyst for reaction. The catalyst had the following composition.

$$0.2\ MoO_3: 0.01Fe_2O_3: 0.79SiO_2$$

2. 2. 1. 2 Mo/SiO_2 & Fe/SiO_2:

The Mo/SiO_2 and Fe/SiO_2 catalysts were similarly prepared by using ammonium molybdate and ferric nitrate respectively with ethyl silicate-40 as a silica source in the catalyst.

2. 2. 1. 3 Zeolite H-beta:

Commercially available pure H-beta zeolite (Si/Al=30) in the powder form was procured from United Catalyst India Ltd. The pure form of H-beta catalyst was compacted without binder in the form of pellets and further granulated to 20-mesh size for use in nitration reactions.

2. 2. 2 Catalysts Characterization

The catalysts were characterized by using XRD (Rigaku MiniFlex), SEM (Model JEOL JSM 5200), FT-IR (Nicolet 60, SX B), Thermal analysis (METTLER TA 4000 System), EDX (Kevex system), TPD of NH_3 (Micrometrics, Autochem-2910) and surface area (Omnisorb 100 CX, COULTIER corp., USA). The detailed information about these techniques is given in Chapter I.

2. 2. 3 Reaction Procedure

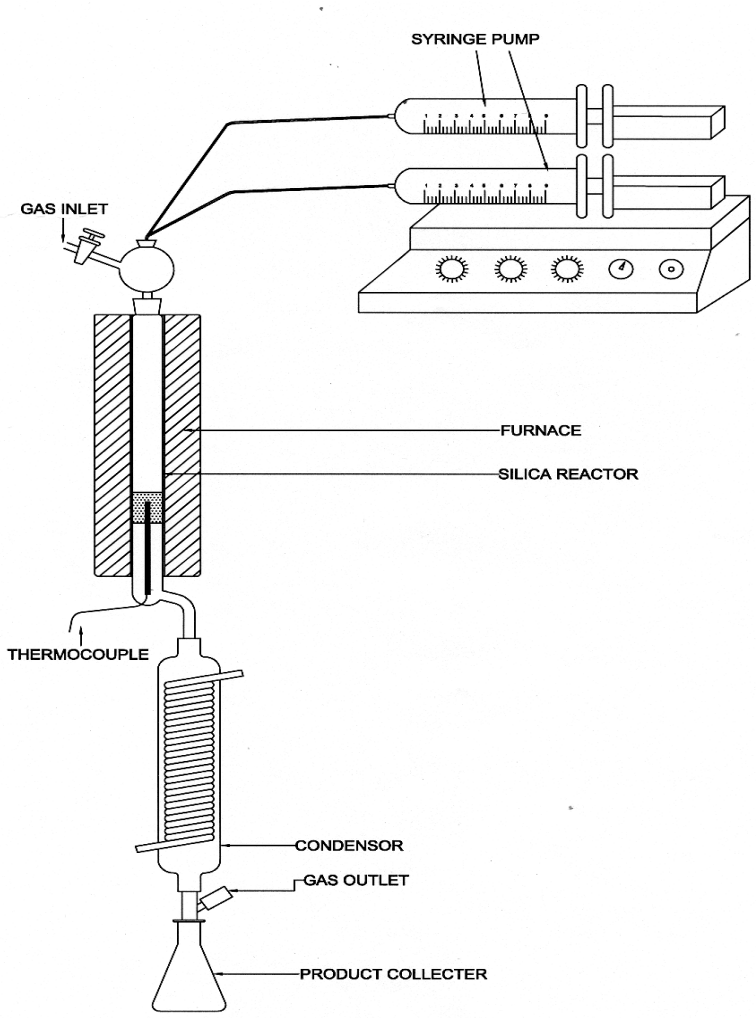

Fig. 2. 1: Schematic diagram of down-flow glass reactor with setup.

Vapor phase nitration was carried out by using a down-flow glass reactor with a fixed catalyst bed at an atmospheric pressure [Fig.2.1]. 10 g of granulated catalyst was loaded in tubular glass reactor of 15 mm diameter and 25 mm length. The upper part of the reactor was packed with inert ceramic beads as preheating zone. The glass reactor was fixed inside the heater and reaction temperature was controlled by the thermocouple inserted in the catalyst bed.

Diluted nitric acid (30 %) and benzene were introduced into the flow reactor (Sage feed pumps) with nitrogen as a carrier gas. The product was condensed at 5°C and collected in a receiver. The reaction product was extracted with diethyl ether, which was analyzed by gas chromatography using GC (HP 6890, column: HP-1, 30m, 0.25mm ID), GC/MS (SHIMADZU, column, DB-I).

2. 3 RESULTS AND DISCUSSION

2. 3. 1 Catalyst Characterization

2. 3. 1. 1 X-ray Diffraction:

The X-ray diffraction (XRD) patterns of the sample were recorded to ascertain the phase purity of the sample. The XRD pattern of H-beta (Fig. 2.2) matched well with the reported pattern showing the phase purity of the material. The XRD pattern of $Fe/Mo/SiO_2$ matched well with the reported MoO_3 pattern without any reflections of silica species indicating the dispersion of MoO_3 on amorphous silica (Fig. 2.3). In case of Mo/SiO_2 with Mo content of 5-15 mol %, the catalysts were found to be amorphous showing high dispersion of MoO_3 on amorphous silica support and above 20 % MoO_3, the highly dispersed MoO_3 forms crystalline clusters visible in XRD pattern as reported earlier [16-17].

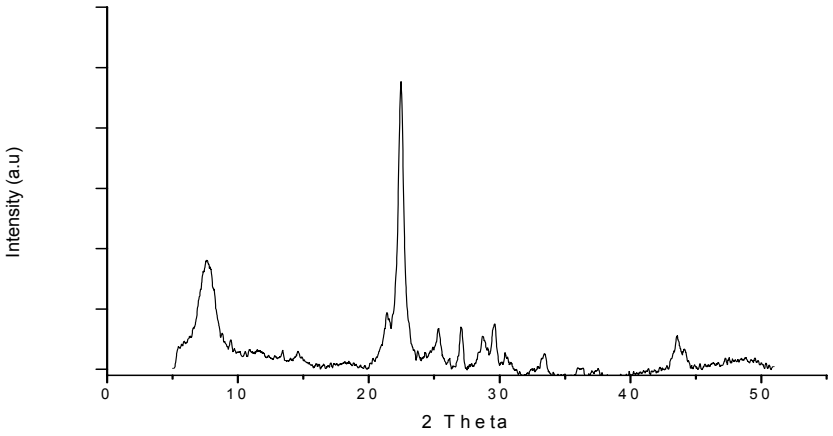

Fig. 2.2: XRD of zeolite H-Beta

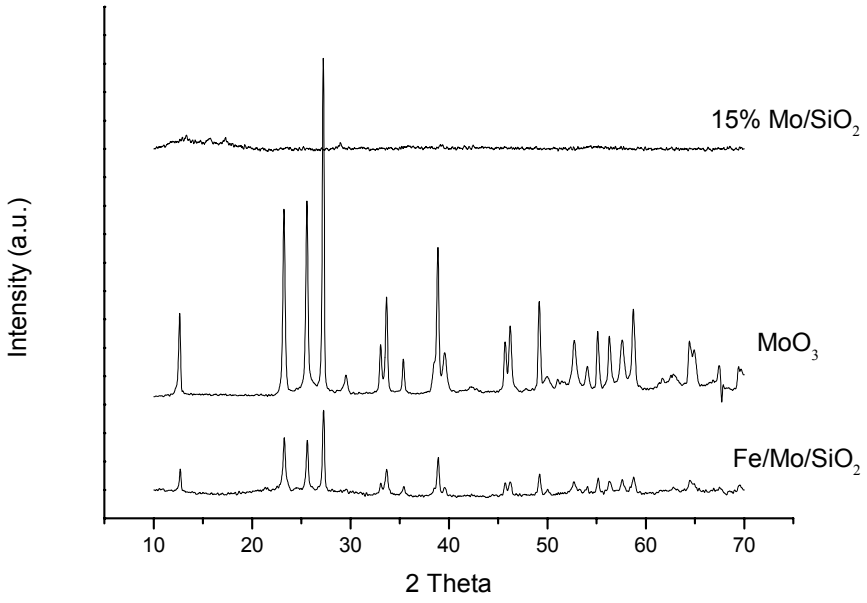

Fig. 2.3: XRD of $Fe/Mo/SiO_2$ and MoO_3

2. 3. 1. 2 Thermal Analysis:

The thermal stability of catalyst $Fe/Mo/SiO_2$ was tested using TG/DTA/DTG analysis. It showed that thermal stability of the catalyst upto 700 °C.

2. 3. 1. 3 FTIR spectra of chemisorbed pyridine:

FTIR spectra of chemisorbed pyridine at temperature 100 and 200 °C are showed in Fig 2.4. In spectra observed with two bands at 1450 and 1610 cm^{-1} were observed which are due to co-ordinatively bonded pyridine to the surface, i.e. due to Lewis acid sites [18]. The bands observed at 1630 and 1540 cm^{-1} is due to pyridinium ion formed on Brönsted acid sites (which is very weak and negligible). The intensity of band due to Lewis acidity was measured at 100 °C was very high, almost six times that observed at 200 °C. It shows that Lewis acidity in $Fe/Mo/SiO_2$ is also weak in nature.

The FTIR spectra of chemisorbed pyridine at 100, 200, 300 and 400 °C on the fresh zeolite beta is shown in Fig.2.5 (a-d). The bands observed at 1636, 1490 and 1543 cm^{-1} are assigned to pyridine molecules bound to Brönsted acid sites and those at 1612, 1490, and 1448 cm^{-1} are assigned to pyridine molecules bound to Lewis acid sites. The intensity of bands due to Brönsted acid sites started decreasing from 100 °C to 400 °C. It indicates that Brönsted acid sites of H-beta are stronger at 100 °C compared to spectra at 400 °C.

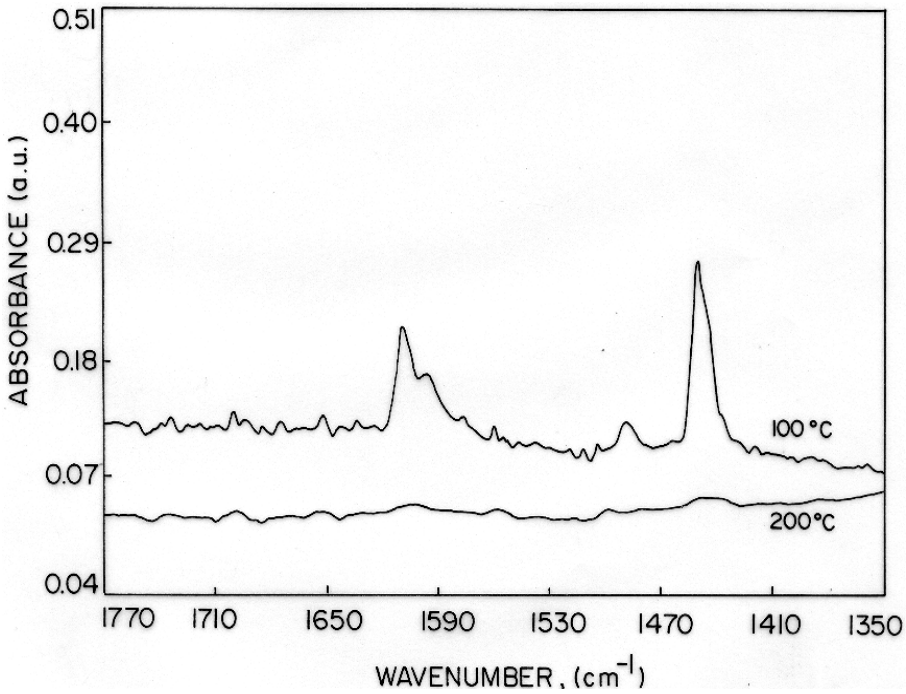

Fig. 2.4: IR of chemisorbed pyridine of $Fe/Mi/SiO_2$.

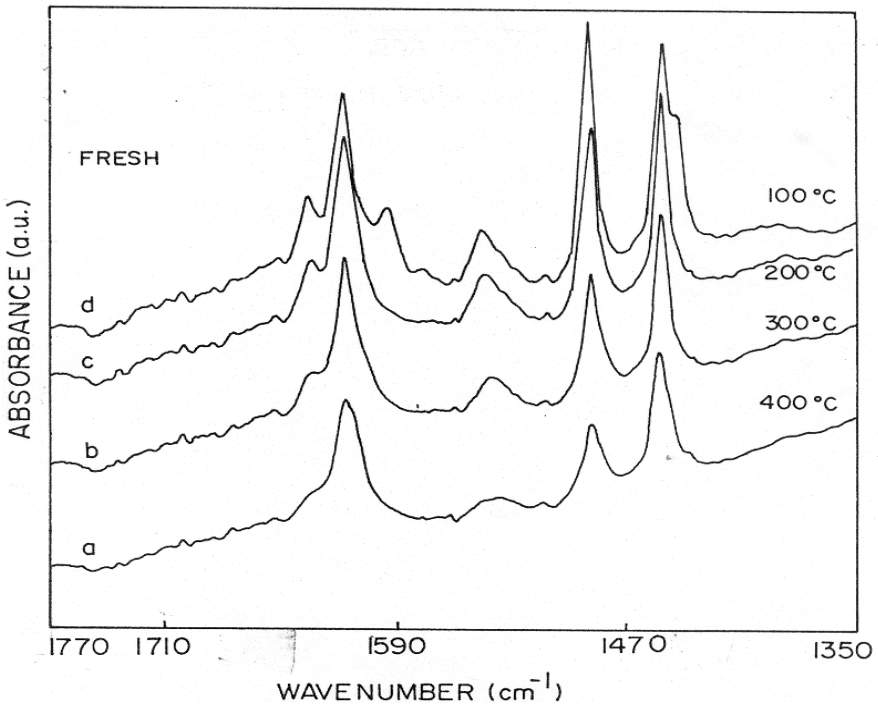

Fig. 2.5: IR of chemisorbed pyridine of H-beta catalyst.

2. 3. 1. 5 SEM Analysis:

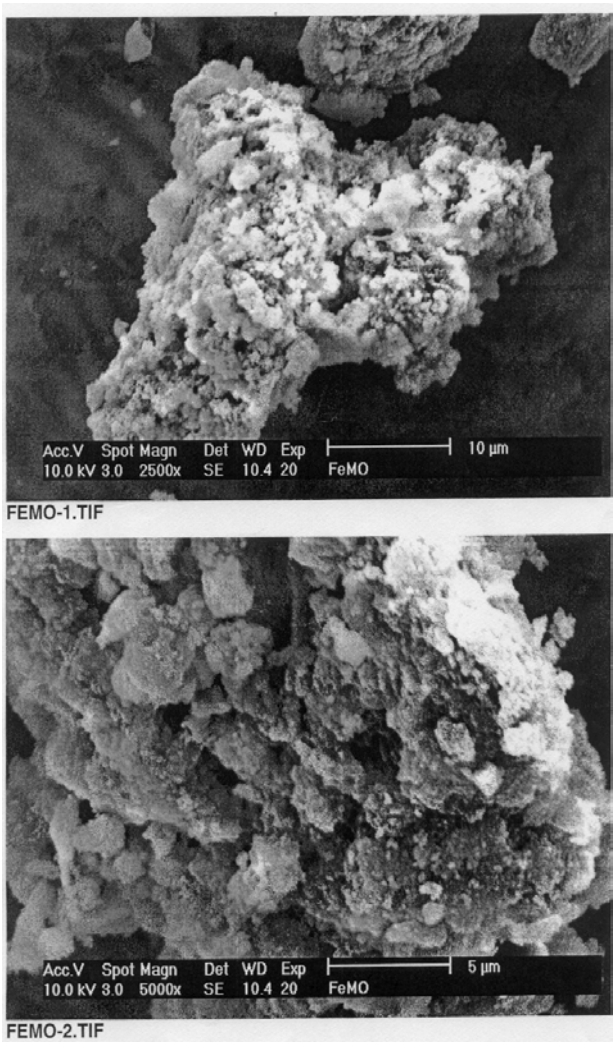

Fig. 2.6: Scanning electron micrograph of $Fe/Mo/SiO_2$.

Scanning electron micrograph of $Fe/Mo/SiO_2$ is presented in the Fig.2.6. The micrograph reveals agglomerates of small particles in the range of 0.1-0.3 µm.

2. 3. 1. 6 Surface Area measurement:

The surface area of the sample was calculated by the BET method [19], is given in the Table 2.1.

Table 2.1: Surface area of the catalysts

	Surface area, m^2/g
H-Beta	640
$Fe/Mo/SiO_2$	490.7
Mo/SiO_2	496

The values show that H-beta is free from occluded impurities. The high surface area of supported Fe/Mo catalyst indicates that fine dispersion of Fe and Mo on silica support.

2. 3. 1. 6 Temperature-programmed desorption (TPD) of ammonia:

Temperature-programmed desorption (TPD) of ammonia is a common method for investigating both the strength and the number of acid sites present on the surface of a solid acid catalysts [20]. TPD of $Fe/Mo/SiO_2$, H-beta and Mo/SiO_2 are given below in Fig. 2.7. In $Fe/Mo/SiO_2$ catalyst ammonia desorption was about $1.22 mmol g^{-1}$. TPD curve shows that mostly adsorbed NH_3 is desorbed below 300°C.

In case of H-Beta, ammonia desorption was about $0.78 mmol\ g^{-1}$, which is desorbed at higher temperature, indicating that it is having stronger acid sites than $Fe/Mo/SiO_2$. TPD of Mo/SiO_2 showed about $1.10 mmol g^{-1}$ was desorbed. The temperature of desorption is identical to $Fe/Mo/SiO_2$. The addition of Fe to Mo/SiO_2 catalyst does not seem to have changed the nature of acidity significantly. Comparison of acidity of H-beta, Mo/SiO_2 and $Fe/Mo/SiO_2$ showed that the $Fe/Mo/SiO_2$ is having more acidity compared to others.

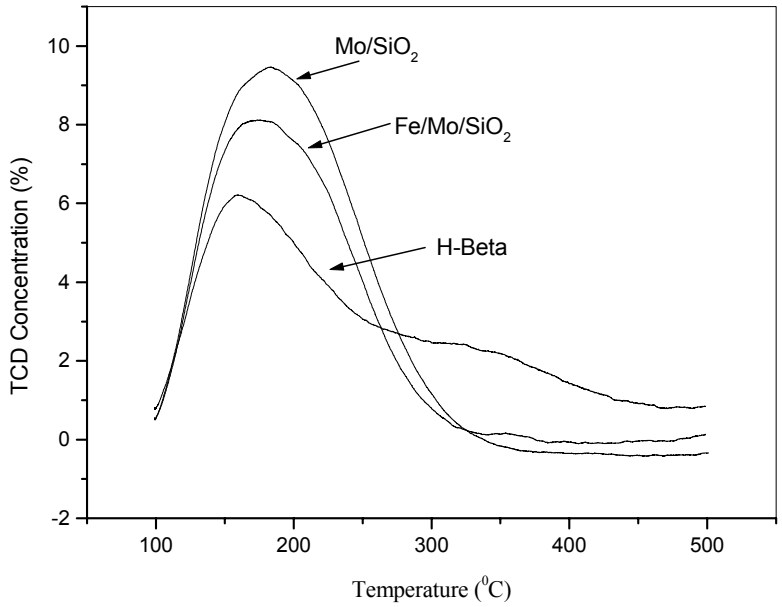

Fig. 2.7: TPD of ammonia of H-beta, $Fe/Mo/SiO_2$ and Mo/SiO_2 catalysts.

2. 4. 1 Reaction Study

2. 4. 1. 1 Investigation of active catalysts for nitration of benzene:

Nitrobenzene is the main product in the nitration of benzene by nitric acid. It is produced according to the equation (1):

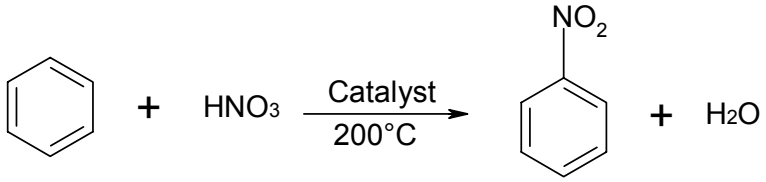

The nitration of benzene is an exothermic reaction (ΔH = -117 kJ/mol), therefore the heat of reaction during vapor phase nitration needs to be removed to maintain the reaction temperature in the range of 100 to 200 °C. Use of dilute nitric acid would be an advantageous because heat is removed by steam generated from dilute nitric acid. It is also useful for generation of NO_2^+ ion where as concentrated nitric acid produces nitrous oxide leading to low conversion of benzene to

nitrobenzene. Considering these aspect benzene nitration was carried out using dilute nitric acid.

Table 2.2: Vapor phase nitration of benzene over zeolite H-beta catalyst

TOS,	%, Conv.	%, Product distribution			%, Selectivity
(h)	Benz	NB	DNB	Others	NB
5	40.05	40.05	0	0	100
10	35.96	35.87	0	0.10	99.8
21	47.77	47.58	0	0.17	99.6
24	46.26	45.75	0.20	0.23	98.9
44	42.64	42.29	0.14	0.20	99.2
53	43.98	43.5	0.18	0.26	99.1
72	46.65	46.2	0.18	0.24	99.1

Conditions: Benz: HNO_3 ratio = 1.34:1; WHSV = 0.17 h^{-1}; HNO_3 = 30%; Temp=200°C
NB = Nitrobenzene; DNB= dinitrobenzene; others = unidentified byproducts

The results of vapor phase nitration of benzene with dilute nitric acid (30 %) over zeolite H-beta catalyst are summarized in the Table 2.2. H-beta catalyst is quite active catalyst showing almost 100 % selectivity with conversion of 46.8 % (Theoretical = 69.3 %). It also shows constant conversion upto 72 hours. Afterwards it slowly decreases due to deactivation of the catalyst, presumably because of strongly adsorbed species such as dinitro and other unidentified byproducts. It was also observed that dinitro formation increased by increasing time on stream.

For comparison nitration of benzene was also carried out over various other solid acid catalysts using dilute nitric acid (30 %) at temperature 200 °C shown in Fig. 2.8. Nitrobenzene was the major product in vapor phase nitration of benzene. Among

these catalysts investigated, the mixed oxide catalyst comprising $Fe/Mo/SiO_2$ (I, Fe=0.72 & Mo=20 mol %) showed good yield of nitrobenzene with almost no decay of activity for 300h. Other solid acid catalysts such as zeolite H-beta (Si/Al=30), Mo/SiO_2 (Mo= 20 mol %), MoO_3, and various compositions of $Fe/Mo/SiO_2$ (Fe/Mo = 12/8 mol %, 10/10 mol %) showed less conversion and activity of the catalysts and conversion was decreased with time on stream. $Fe/Mo/SiO_2$ (I) was found to be active and having longer catalyst life. This may be due to the promotional effect of iron on the catalyst $Fe/Mo/SiO_2$ (I) [14, 16]. Comparison of activity of $Fe/Mo/SiO_2$ (I) catalyst with that of other compositions of $Fe/Mo/SiO_2$ catalysts shows that by increasing the amount of iron the conversion decreased as shown in Fig. 2.9. It indicates that small percentage of iron in $Fe/Mo/SiO_2$ catalyst is significantly effective for the benzene nitration.

Reaction Mechanism:

The higher catalytic activity of $Fe/Mo/SiO_2$ compared to H-beta zeolite in benzene nitration may be attributable to redox mechanism with $Fe/Mo/SiO_2$ catalyst. H-beta zeolite with Brönsted acid sites are responsible for generation of NO_2^+ where as in case of $Fe/Mo/SiO_2$ the Lewis acid sites and redox nature of Mo seems to be more effective in benzene nitration [14].

$$2\ HNO_3 + 2\ Mo^{6+} \longrightarrow 2\ NO_2^+ + H_2O + 2\ Mo^{5+}$$

And

$$2\ HNO_3 + H^+ \longrightarrow [H_2NO_3]^+ \longrightarrow NO_2^+ + H_2O$$

(Brönsted acid site)

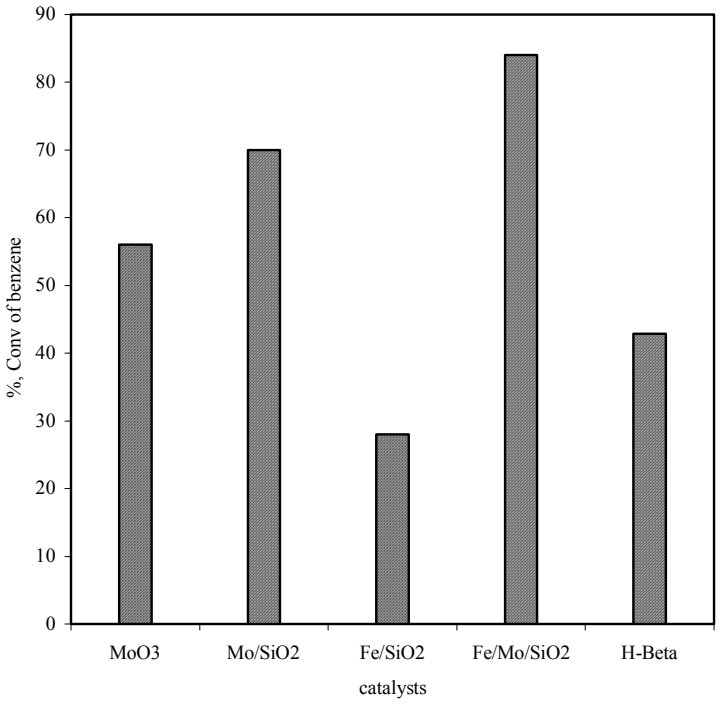

Fig. 2.8: Influence of various solid acid catalysts.

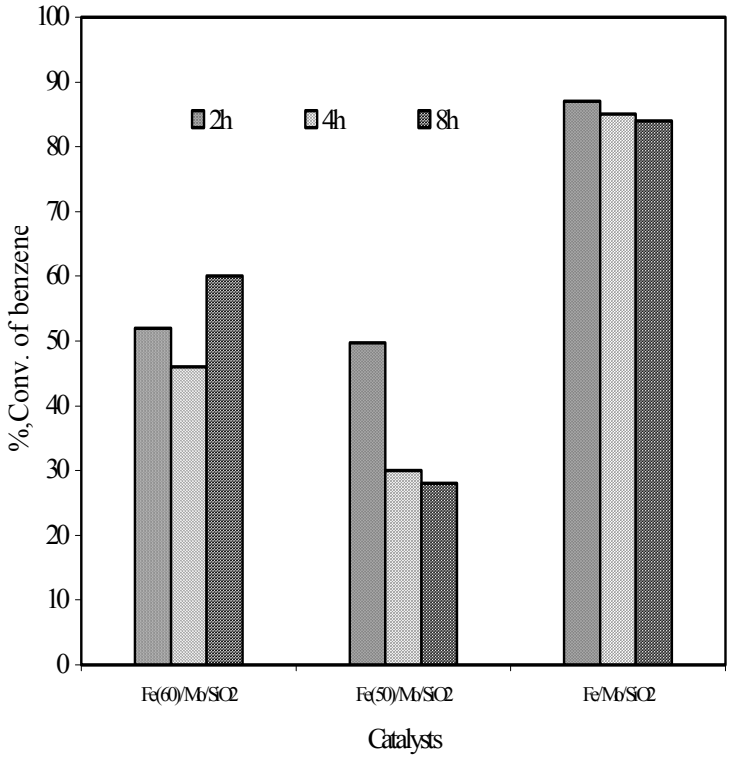

Fe (60)/Mo/SiO_2 = Fe/Mo=12/8; Fe (50)/Mo/SiO_2= Fe/Mo=10/10;
Fe/Mo/SiO_2= Fe/Mo= 0.72/20

Fig. 2.9: Comparison of Fe/Mo/SiO_2 catalyst with different composition.

2. 4. 1. 2 Effect of Temperature:

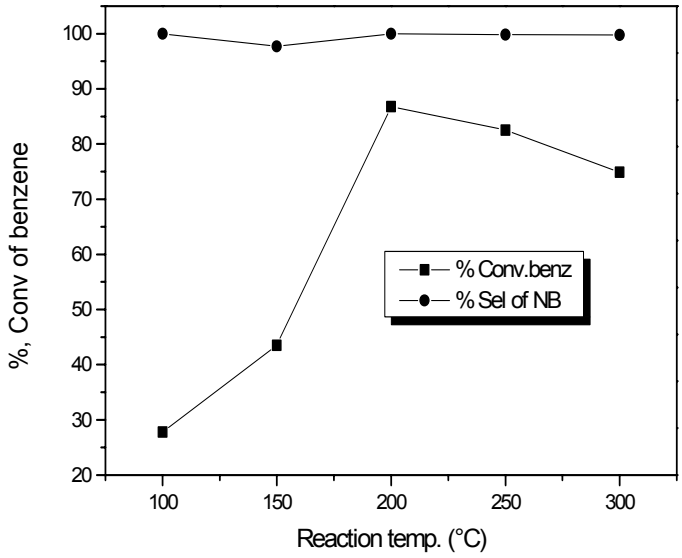

Fig. 2. 10: Effect of temperature over $Fe/Mo/SiO_2$ catalyst.

As the temperature increased from 100 °C to 300 °C, the conversion increases and after temperature 200 °C it start decreasing with formation of dinitro and other unidentified products in traces. The results of nitration of benzene over $Fe/Mo/SiO_2$ using dilute nitric acid (30 %) as a nitrating agent at weight hourly space velocity (WHSV) $0.087h^{-1}$ at nitric acid to benzene molar ratio 1.2 were shown in Fig.2.10. It showed that at 200 °C the conversion and selectivity were higher with no other byproducts, but at 250 °C it showed low conversion for nitrobenzene and formation of dinitrobenzene in traces. As temperature increased there may be less formation of nitronium ion and more formation of nitrous oxide decreasing the formation of nitrobenzene [21]. The catalyst $Fe/Mo/SiO_2$ exhibits dual function i.e. the formation of

nitro product below 370 °C and other is the formation of oxidation product above 400 °C [14].

2. 4. 1. 3 Influence of Nitric acid to Benzene Molar Ratio:

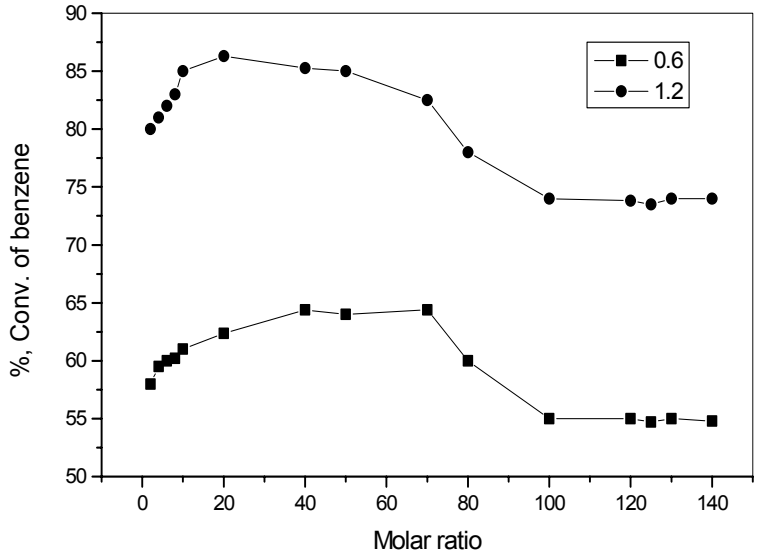

Fig. 2. 11: Influence of molar ratio.

The influence of the HNO_3/benzene molar ratio at temperature 200 °C was examined over Fe/Mo/SiO_2 (I) catalyst with time on stream. In the Fig. 2.11 variation of conversion of benzene with time on stream of reaction for nitric acid to benzene ratio of 0.6 and 1.2 are presented. After initial increasing conversion, it decreases further on time on stream and later it remains almost constant as can be seen in the Fig. 2.11. As nitric acid/ benzene ratio decreased the conversion also decreased. In the case of higher nitric acid to benzene molar ratio, as the available nitric acid was more, the conversion was also comparatively more. Dinitro formation was not observed below 200°C when HNO_3/Benzene ratio was 0.6 because of lower than stoichiometric

amount of HNO_3 available. However at higher temperature and higher mole ratio of HNO_3, dinitro product was also obtained in traces.

2. 4. 1. 4 Effect of WHSV on Nitration of Benzene:

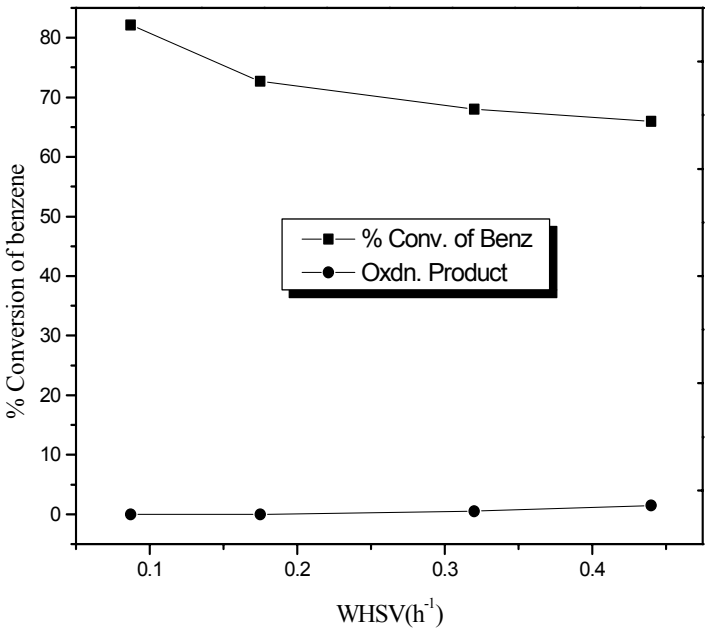

Fig. 2. 12 Effect of WHSV.

The influence of WHSV on nitration of benzene at 200°C over catalyst $Fe/Mo/SiO_2$ (I) using dilute nitric acid at nitric acid to benzene molar ratio 1.2 is presented in Fig.2.12. An increase in WHSV decreases conversion, product yield and increases the oxidation and dinitro products. It showed that at lower WHSV ($0.087h^{-1}$) the conversion was higher (86 %) indicating that an optimum residence of reactants is required for maximum conversion.

2. 5 CONCLUSIONS

Nitration of benzene (BZ) using dilute nitric acid (30 %) is promoted by solid acid catalysts zeolite H-Beta, $Fe/Mo/SiO_2$ and related catalysts. Nitrobenzene was the major product and small amount of oxidation and dinitro products were formed. Among all catalysts studied, the $Fe/Mo/SiO_2$ (I) catalyst gives higher conversion and selectivity for longer period of time (> 300 hrs).

One of the major advantage of this reaction was the use of dilute nitric acid as a nitrating agent, resulting in high selectivity and longer catalyst life. The use of sulfuric acid is avoided, which is essential in the conventional process. This process is avoiding hazardous waste disposal, which makes the process environmentally friendly.

2. 6 REFERENCES

1. Adkins, R.L., Nitrobenzene and Nitrotoluenes in "*Encyclopedia of Chemical Technology*" 4th ed., Vol. **17**, Wiley-Interscience, New York, p133 (1996).
2. *Ullmann's Encyclopedia of Industrial Chemistry*, VCH, Weinheim, Vol.**A17**, 411 (1991).
3. a) S. Suzuki, K. Tohmori, Y. Ono. *Chem. Lett*., 747 (1986) b) *U.S. Patent* 4660702 (1986).
4. S. Suzuki, K. Tohmori, and Y. Ono, *J. Mol. Catal.* **43**, 41 (1987).
5. b) L. E. Bertea, H. W. Kouwenhoven, and R. Prins, *Stud. Surf. Sci. Catal.* **84**,1973 (1994).
6. L.E. Bertea, H. W. Kouwenhoven, R. Prins, *Stud. Surf. Sci. Catal.* **78**, 607 (1993).
7. L.E. Bertea, H. W. Kouwenhoven, R. Prins, *Appl. Catal. A* **129**, 229 (1994).
8. T. G. Kusnetzova, K. G. Ione, and L. V. Malysheva, *React. Kinet. Catal. Lett.* **63**, 61 (1998).
9. H. Sato, K. Hirose, *Appl. Catal. A: General*, **174**, 77 (1998).
10. H. Sato, K. Hirose et al., *Appl. Catal. A: General*, **175**, 201 (1998).
11. Sato, H., Nagai, K., Yoshioka, H., *Appl. Catal. A: General* **180**, 359 (1999).

12. McKee and Wilhelm, *Industrial and Engineering Chemistry*, **28(6)**, 662-667 (1936) and *U.S. Pat*. 2,109,873.
13. D. Vassena, D. Malossa, A. Kogelbauer, R. Prins, (Ed: M.M.J. Treacy, B.K. Markus, M.E. Bisher, J.B. Higgins), *Proceedings of 12th International Zeolite Conference*, Materials Research Society Warrendale, Pennsylvania, USA, p. 1909 (1999).
14. Jin S. Yoo, A. R. Sohail, S. S. Grimmer and J. Z. Shyu, *Appl Catal. A: General*, **117**, 1-16 (1994).
15. D. P. Sabde, S.G. Hegde and M. K. Dongare, *J. Mater. Chem*. **10(6)**, 1365 (2000).
16. L. Lietti, G. Ramis, G. Busca, F. Bregani and P. Forzatti, *Catal. Today*, **61**, 187–195 (2000).
17. J. J. P. Biermann, F. J. J. G. Janssen, *J. Mol. Catal.*, **60**, 229-238 (1990).
18. C. Jia, P. Massiani, D. Barthomeuf, *J. Chem. Soc., Faraday Trans*. **89 (19)**, 3659–3665 (1993).
19. B.C. Lippens and J.H. de Boer, *J. Catal*. **4**, 319 (1965).
20. K. Parida, V. Quaschning, E. Lieske and E. Kemnitz, *J. Mater. Chem*., **11**, 1903-1911 (2001).
21. L. V. Malysheva. E.A. Paukshtis, K.G. Ione, *Catal. Rev. Sci. Eng*., **37**,179 (1995).

CHAPTER III

NITRATION OF TOLUENE

3. 1 INTRODUCTION

Nitro-toluenes are important intermediates in the chemical industry, industrially produced by liquid phase nitration of toluene using a mixture of nitric and sulfuric acid as a nitrating agent having several downstream products shown in Fig. 3.1 [1]. The typical product distribution of *ortho*, *meta* and *para* isomers in the conventional nitration is about 58:4:38, whereas the thermodynamic equilibrium concentration is 29:33:38 respectively [2]. The para isomer has better commercial value as the pharmaceutical intermediate and is sold at about three times the cost of the *o*-isomer [3]. A large quantity of dilute sulfuric acid is generated as waste in the conventional process and its disposal or recycle is very expensive; this makes the toluene nitration one of the most environmentally harmful processes. The replacement of sulfuric acid with solid acid catalysts with high selectivity for *para* isomer would be an attractive environmentally benign route for the production of nitro-toluenes.

Several solid acid catalysts have been investigated for the liquid and vapor phase nitration process. McKee and Wilhelm [4] used silica gel as a solid acid catalyst for the vapor phase nitration of benzene and toluene. Other solid acid catalysts studied for nitration are sulfonated polyorganosiloxanes [5], acidic resins [6], modified clays [7], zeolites [8-9], sulfated zirconia [10], and supported sulfonic acid [11].

Kogelbauer et al. [12] studied the liquid phase nitration of toluene using supported sulfuric acid catalysts such as silica-supported heteropolyacid, sulfated zirconia and sulfated silica the performance in terms of selectivity was somewhat lower compared with conventional results. The impregnated acid was only half active on weight basis compared to liquid sulfuric acid because of weight of inert carrier support.

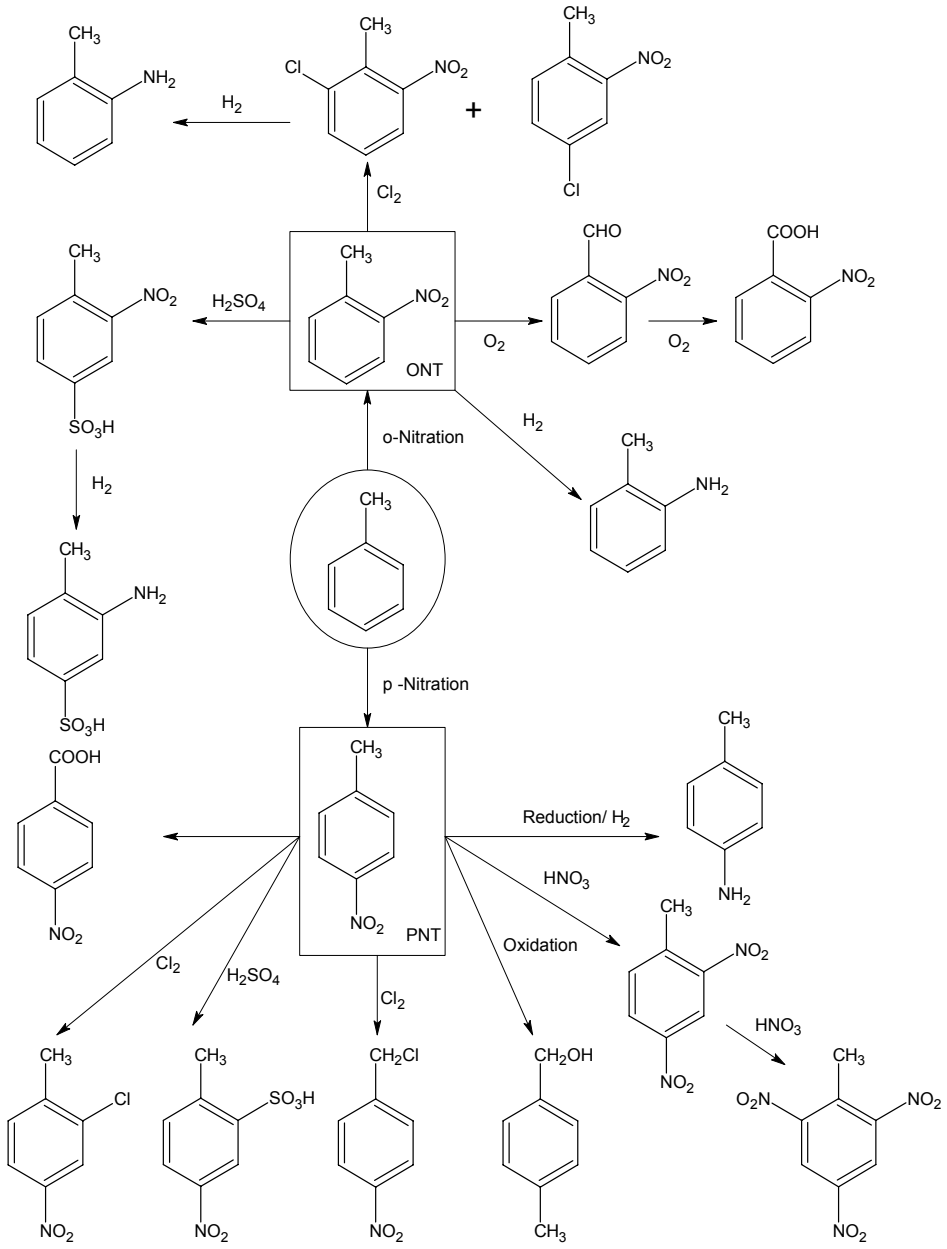

Fig. 3.1: *Ortho*-and *para*-nitrotoluene derivatives.

The advantage of using vapor phase conditions is the continuous thermal removal of water and the simple implementation of a continuous nitration process based on a fixed-bed of the solid acid. Optimization of reaction conditions are required

because of elevated reaction temperatures, which lead to problems of safety, catalyst stability, and byproduct formation.

Nitration of aromatics with solid acids in the vapor phase was attempted as early as 1936 [13]. Although H-beta performed well with several aromatic compounds, with toluene complete deactivation was observed within 30 min on-stream at 140°C accompanied by the formation of numerous by-products.

Among acidic zeolite catalysts such as H-mordenite, H-beta, H-ZSM-5 and H-Y, zeolite H-beta has shown higher conversion and remarkable selectivity for *para* isomer in vapor phase nitration of toluene. Choudary et al. [14] carried out the nitration of toluene in liquid phase employing nitric acid of 60-90 % concentration over solid acid catalysts and by azeotropic removal of water. Zeolite beta proved to be the best catalyst among the zeolites, in terms of space-time yield (STY), *para* selectivity and consistent activity and selectivity even after five cycles without dealumination of the catalyst. R. Prins et al. [15] investigated the nitration of toluene in the gas phase at 158 °C with 65 % nitric acid over zeolite catalyst; among the catalysts studied, zeolite H-beta showed promising results. The activity and selectivity decreased over a period of about 5 h on stream, due to pore filling/blockage by strongly adsorbed products /byproducts. Nitration of toluene using H-beta zeolite catalyst to replace the sulfuric acid in the conventional process could not be commercialized because of deactivation of catalyst, leading to low space time yields.

Jeffrey M. Smith et al. [16] have investigated deactivation and shape selectivity effects in toluene nitration in vapor phase with NO_2 as nitrating agent, as well as in liquid phase using n-propyl nitrate over zeolite, MCM-41 and sulfated zirconia

catalysts. Almost all the catalysts exhibited deactivation over a period of about 5 h on stream due to pore filling/blockage by strongly adsorbed products and byproducts.

However, the deactivated catalysts and the byproducts formed after deactivating the catalyst were not enough characterized to understand the deactivation process. The concentrated nitric acid (65–70 wt %) and higher temperature (160 °C) used in the earlier studies led to the oxidative side reactions, resulting in faster deactivation of the catalyst. Liquid phase nitration of toluene was carried with various impregnated catalysts such as ZrO_2/H_2SO_4, $Y_2O_3/ZrO_2/H_2SO_4$, $ZrO_2/SiO_2/H_2SO_4$, SiO_2/H_2SO_4, $Fe/Mo/SiO_2$ and H-beta zeolite catalyst and also studied the vapor phase nitration of toluene using beta zeolite catalyst with dilute nitric acid of different concentrations at various temperatures and the deactivated catalyst was analyzed using various analytical techniques to understand the deactivation process. We have also carried out molecular modeling and fitting studies for nitration of toluene over beta and MFI zeolites to highlight that this simple theoretical approach is suitable to answer the fundamentally important question of the nature of interaction of the guest molecule with zeolite lattice.

3. 2 EXPERIMENTAL

3. 2. 1 Catalyst preparation

3. 2. 1. 1 Sulfated Zirconia:

Commercially available $ZrOCl_2$ was hydrolyzed with 28 % aqueous ammonia. A white precipitate of zirconium hydroxide was obtained. The pH of the solution was maintained between 9 and 10. After complete precipitation, it was allowed to digest for 4h. The precipitate was then washed and filtered through a buchner funnel and tested

for chloride ions using silver nitrate [17]. The precipitate was dried at 373K overnight to obtain Zr $(OH)_4$. The hydroxide was then immersed in 2N H_2SO_4 and the suspended solution was evaporated to dryness followed by calcination in air at 500-650 °C to obtain sulfated zirconia catalyst.

3. 2. 1. 2 Sulfated Y_2O_3/ZrO_2:

The catalyst was prepared by treating a mixture of aqueous solutions of yttrium nitrate and zirconyl nitrate (molar ratio 16:84) with aqueous ammonia (28 %). The mixture was stirred vigorously until a pH value of 8-9 was achieved. The precipitate formed was washed with deionized water, dried at 110 °C, treated with 2N H_2SO_4, dried again at 120 °C for 24h and subsequently was heated to 500 °C and then calcined for 3h [18].

3. 2. 1. 3 Sulfated Silica:

Sulfated silica is used to carry out industrially important reactions. For its preparation, commercially available column grade silica gel 60-120 mesh was used. The silica supports were calcined in static air at 400 °C for 18h and cooled in a desiccator. 50-98 % H_2SO_4 was then added to silica gel (1.5g H_2SO_4/g silica). This mixture was vigorously shaken for 5 minutes and allowed to rest for 1-10 days in a stoppered conical flask without maintaining incipient wetness. The resulting catalyst was dried at 120 °C in static air for 18h. Subsequently, the catalyst was stored in a desiccator under vacuum and recalcined at 120°C prior to reaction [19].

3. 2. 1. 4 Fe/Mo/SiO_2:

The catalyst was prepared by sol-gel method. The catalyst had the following composition.

0.2 MoO_3: 0.01Fe_2O_3: 0.79SiO_2.

Preparation method of the catalyst is given in chapter II in detail.

3. 2. 1. 5 Zeolite H-beta:

Commercially available H-beta zeolite (Si/Al=30) in the powder form (non-formulated) and in the extrudate form (formulated, Si/Al=30, zeolite/alumina binder = 80:20) were procured from United Catalyst India Ltd. The non-formulated H-beta catalyst was compacted in the form of pellets and further granulated to 20-mesh size for use in nitration reactions.

3. 2. 2 Liquid phase nitration

3. 2. 2. 1 Reaction procedure:

The nitration reaction was carried out in a 100ml two-neck glass reactor. Weighed quantity of toluene and catalyst was added to the flask and stirred using a magnetic stirrer in an oil bath at the required temperature. Aqueous nitric acid (70 %) was added to the flask dropwise using an addition funnel in a time period of about 25 minutes. The reaction was carried out for 24 hours. Samples were taken out periodically and analyzed using GC. The unreacted nitric acid was neutralized to pH 6-7 using $NaHCO_3$.

The product was extracted with diethyl ether, and analyzed off-line by gas chromatography (HP5890, column SPB-1, 30m, 0.53mm ID), GC/MS (SHIMADZU, column, DB-I) and FTIR (Nicolet-60, SXB). The catalyst was characterized for its physical and chemical properties using various techniques such as XRD (Regaku, Miniflex), surface area (Omnisorb CX-100), TG/DTA (SETARAM TG_DTA 92), EDX (KEVEX 7000 system), ^1H NMR (Bruker AC 200 NMR Spectrometer 200MHz) and FTIR (Nicolet, 60 SXB spectrometer).

3. 2. 3 Vapor phase nitration

3. 2. 3. 1 Reaction procedure:

Vapor phase nitration experiments were performed in a fixed-bed continuous down flow glass reactor at atmospheric pressure. 10 g of the catalyst was loaded in a tubular glass reactor of 15 mm diameter and 25 mm length. The upper part of the reactor was packed with inert ceramic beads as the preheating zone. Before the reaction, the catalyst sample was preheated at 450 °C for 12 h in a 10 ml /min flow of air. Then the reactions were carried out by passing aqueous dilute nitric acid and toluene using syringe pumps (Sage feed pump), in the temperature range of 120 °C to 200 °C with nitrogen as carrier gas at the rate of 10 ml/min. The weight hourly space velocity (WHSV) was varied from 0.1 to 1 h^{-1}.

The reaction product was collected in a receiver maintained at 5 °C. This product was extracted with diethyl ether, and the extracted product was analyzed by same methods as given in above liquid phase nitration. The deactivated catalyst was washed with acetone/carbon tetrachloride and the washing was analyzed using GC, GC-MS, and GC-IR for the identification of products/byproducts deactivating the catalyst.

3. 3 METHODS AND MODELS

Several zeolites have been tried experimentally for this reaction. Much attention has been focused on beta zeolite due to its high activity and predominant shape selectivity. The unique twelve-member (12-M) channel system in beta zeolite has been believed to be the cause of shape selectivity. However, medium pore zeolites with a 10 member (10-M) channel system, particularly ZSM-5 [20], have not shown considerable shape selectivity in nitration of toluene to para nitrotoluene. Although the

zeolites are broadly classified as small, medium and large pore zeolites, each one of the structurally distinct 105 zeolites known to date [21], has different architecture, and hence the diffusion characteristics of molecules inside their pores cannot be generalized. The catalytic behavior of most of the zeolites arises from the catalytically active Brönsted acid sites. These active sites are located inside the intriguing pore structures. In such cases molecular modeling and graphics can provide better understanding of the active sites.

The computational studies reported here were carried out using software programs – InsightII and Discover, supplied by Molecular Simulations Inc., USA. The force field energy minimization calculations were done with the Discover program, using consistent valence force field (CVFF) of Hagler et al. [22] and the parameters were obtained from the reports of Dauber-Osguthorpe et al. [23]. The actual values used in these calculations have been listed in our earlier work [24]. The interaction energy of the molecule with the zeolite framework is calculated using the force field expression [22] that contains the terms corresponding to deformation of bond lengths, bond angles, torsion angles, etc. of the molecule. The non-bonding interactions of the molecule with the zeolite framework are calculated by determining the long and short-range forces in terms of electrostatic interaction and Lennard-Jones potentials. Molecular graphics displays were obtained from InsightII molecular modeling system using Silicon Graphics workstation. Energy minimization is carried out in a sequence with steepest-descent, conjugate gradient and Newton-Raphson algorithms.

The extents of the molecule in space were calculated for the energetically favorable conformation and their sizes and shapes were analyzed. The dimensions of molecules in three-dimensional space are measured according to the procedure detailed elsewhere [25]. The three largest dimensions (a X b X c) of the nitronium ion

(**1**), toluene (**2**), o-nitrotolune (**3**), m- nitrotolune (**4**), p- nitrotolune (**5**), and dinitrotoluene (**6**) molecules in mutually perpendicular directions are given in Table 3.1.

Table 3.1: Dimensions of different molecules in their minimum energy configuration.

Molecules	Dimensions		
	a (Å)	b (Å)	c (Å)
Nitronium ion (**1**)	4.6	3.0	2.7
Toluene (**2**)	6.9	5.3	2.8
ONT (**3**)	8.0	6.9	2.9
MNT (**4**)	8.3	7.0	2.9
PNT (**5**)	8.8	5.3	2.8
DNT (**6**)	9.9	7.1	3.0

Qualitative structural fitting of the molecules inside the zeolites was studied by molecular graphics (MG) as well as by comparing the dimensions of the molecules with the pore diameters of the zeolites. Three zeolite lattices were generated from the X-ray crystal structures reported for MFI [26] and beta [27]. Further, the chemical interaction between the zeolite host and guest molecules was studied using energy minimization calculations to understand the adsorption sites and diffusion characteristics of the molecules **1** to **6**. The simulation box contained the zeolite generated from its crystal structure and the actual dimensions of the simulation box for each zeolite are given in Table 3.2. The size of the simulation boxes are chosen in such a way that the symmetry along the channel direction is taken care of and the box

is just large enough in the other two directions to take care of the non-bonded interactions, whose cut-off distance was taken as 8.5 Å. The diffusion energy profiles symmetrically repeat themselves in each unit-cell, indicating the validity of the simulation box size, potential parameters and energy minimization calculation procedures.

The calculations were performed following the well established forced diffusion procedure. This procedure has been widely used to study the diffusion of methanol [28], toluene nitration [14], aromatic hydrocarbons [29], isomers of alkylated naphthalene [30], n-butane and isobutane [31], isomers of isobutylethylbenzene [24,32-34], isomers of acylated 2-methoxynaphthalene [35a], acylated 4-hydroxyphenol [35b], isomers of butene [36,37] and isomers of xylenes [24]. Here, we investigated the shape-selective production of **5** over two zeolites. The sorbate molecule was forced to diffuse in regular steps of 0.2 Å along the diffusion path defined by the initial and final positions within the channel. At each point, a strong harmonic potential constrains the molecule to lie at a fixed distance from the initial position while the energetically favorable conformation and orientation of the molecule are derived by varying the internal degrees of freedom as well as non-bonding interaction of the molecule with the zeolite framework. The interaction energy at each point is calculated using equation 1:

$$\text{Interaction energy} = E_{\text{zeolite: molecule complex}} - (E_{\text{zeolite}} + E_{\text{molecule}}) \quad \text{..... (1)}$$

Thus, the diffusion energy profile is a graph showing the variation of interaction energy between a single molecule and the zeolite framework as the molecule diffuses

within the channel of the zeolite. The diffusion energy profiles are useful to identify the most favorable (minimum energy) and unfavorable (maximum energy) adsorption sites for the molecules inside the zeolite channels. The difference in energy between the most favorable and most unfavorable sites in the diffusion energy profile gives the diffusion energy barrier for self-diffusivity. Since our interest is to study the influence of the pore architecture and dimensions on the diffusion characteristics of the molecules, we considered a fully siliceous zeolite lattice. The influence of the presence of more molecules on the diffusivity (mutual effect) and the influence of temperature are not considered here. In view of these approximations, suitable care was taken to interpret the results.

The mean energy is the numerical average of the interaction energy of the molecules at all locations in the diffusion path. The ratio of mean energy to minimum energy (the most favorable site) is a diffusivity index parameter. If the mean energy is close to minimum energy, the situation represents the presence of several minima and the mean/minimum energy ratio will be closer to 1. On the contrary, if the mean energy is much higher than the minimum energy, the situation represents the presence of several maxima and the mean/minimum energy ratio will be closer to 0. Thus the ratio is an indicator of the diffusivity of the molecule; the higher the value, the greater is the diffusivity.

3. 4 RESULTS AND DISCUSSION

3. 4. 1 Liquid phase nitration

A typical reaction of nitration of toluene over solid acid catalysts using dilute nitric acid as a nitrating agent is shown in scheme below:

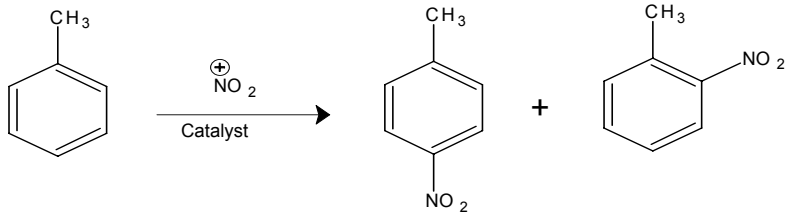

3. 4. 1. 1 Nitration using sulfated catalysts:

Liquid phase nitration of toluene was carried with sulphated silica (sulphated with 98%, 70%, 50% H_2SO_4), sulphated zirconia (sulphated with 2N H_2SO_4), sulphated zirconia/ silica (2N H_2SO_4) at room temperature and the results are summarized in the Table 3.3.

Table 3. 3: Liquid phase nitration of toluene over sulfated catalysts

Catalyst	%, Conv. of toluene	%, Selectivity			*p/o* ratio
		ONT	MNT	PNT	
ZrO_2/H_2SO_4	10.62	57.72	4.52	36.16	0.63
$Y_2O_3/ZrO_2/H_2SO_4$	20.53	61.86	5.36	31.56	0.51
$ZrO_2/SiO_2/H_2SO_4$	11.44	62.94	2.62	40.21	0.64
SiO_2/H_2SO_4	10.1	50.5	5.0	37.92	0.75

Conditions: Tol/HNO_3= 2:1; Temp = RT; HNO_3=70%; Reaction Time= 4h; Catalyst = 10 wt %; ONT = *o*-nitrotoluene; MNT = *m*-nitrotoluene; PNT = *p*-nitrotoluene.

The *p/o* ratio obtained with all these catalysts were found to vary between 0.5 and 0.75. With conventional mixed acid catalyst, the reported *p/o* ratio is 0.6. All the catalysts used were sulphated catalysts. Sulfated catalysts faced with several technical problems such as

a. Moisture sensitivity (handling of the catalyst is difficult)

b. Sulfate leaching (again disposal is a problem)

c. Deactivation of the catalyst (reuse is not feasible)

The conversion was found to be maximum for the catalyst $Y_2O_3/ZrO_2/H_2SO_4$, that is 20.53 % with minimum selectivity (*p/o*=0.51). The selectivity towards *para* isomer was found to be highest for sulfated silica, but with low conversion (10.1 %)

Activities of these catalysts were even lower upon the reuse of these catalysts due to the difficulties encountered during the drying, as these are very hygroscopic materials. The characterization results reported for the silica-supported sulfuric acid catalysts shows that the loading of H_2SO_4 led to a reduction in the BET surface area and a concomitant decrease of pore volume, Table 3.4.

Table 3.4: Surface area measurement

	BET (m^2/g)	Pore Volume (cm^3/g)	Average pore diameter (A^o)	H_2SO_4 loading (Wt.%)
SiO_2 (silica gel 60)	430	0.76	71	-
50 % H_2SO_4	204	0.4	78	37
70 % H_2SO_4	54	0.11	81	48

This suggested that despite the higher acid loading fewer catalytic sites may be accessible for the reactants if the reaction occurs on the liquid surface. The observed increase in the average pore diameter furthermore suggests that smaller pores are preferentially filled and that an acid film is not formed on the carrier surface.

The drawbacks associated with the sulfated catalysts can be overcome by using suitable alternative solid acid catalysts. Therefore further study has been done on the other alternative catalysts such as $Fe/Mo/SiO_2$ and zeolite beta.

3. 4. 1. 2 Nitration of toluene using $Fe/Mo/SiO_2$ and zeolite H-Beta:

Liquid phase nitration of toluene was carried out over $Fe/Mo/SiO_2$ and zeolite H-beta catalysts using nitric acid as a nitrating agent at temperature 70 ºC. Both the catalysts were found to be selective to the more desired *p*-isomer. The conventional sulfo-nitric acid mixture process gives the *p/o* ratio 0.6. In the case of $Fe/Mo/SiO_2$ catalyst *p/o* ratio obtained is ≈ 0.8. With zeolite H-beta *p/o* ratio was obtained between 1.5 and 2.2. Therefore the nitration of toluene was carried out with zeolite H-Beta catalyst with the variation in different parameters like temperature, molar ratio, and nitric acid concentration.

Analysis showed that the products obtained from toluene nitration are 2-nitrotoluene, 3-nitrotoluene, 4-nitrotoluene and others (by comparing with the authentic samples). Along with all these products, alpha nitro toluene compound was also formed quite in major fraction approximately equal to 2-NT. The formation of alpha nitrotoluene formed was identified by GC-MS and ^{1}H NMR.

3. 4. 1. 3 Effect of temperature:

The Liquid phase nitration of toluene was studied at various temperatures such as 25, 60, 70, and 95 ºC over both catalysts using 70 % nitric acid (Fig. 3.2). As the temperature increased, the conversion as well as para selectivity also increased. At room temperature, *ortho*- isomer was predominant over para-isomer at 70ºC. At 95ºC,

p/o ratio decreased from 2.2 to 1.4 and also lots of brown fumes were observed indicating the loss of nitric acid in the form of NO_x. The selectivity towards side chain nitration product was found to remain almost same.

In case of $Fe/Mo/SiO_2$ catalyst the selectivity decreases as temperature increases which may be due to less acidity compared to H-beta.

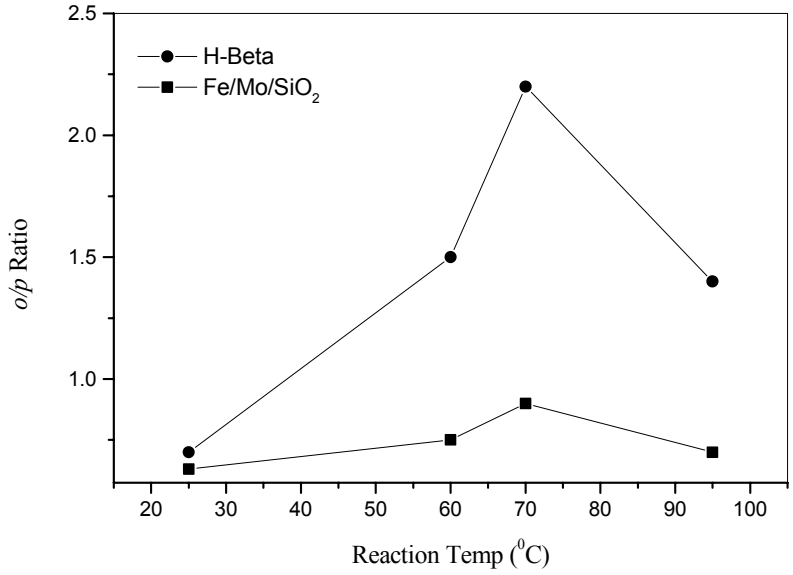

Fig. 3. 2: Effect of temperature on *o/p* ratio of $Fe/Mo/SiO_2$ and H-beta catalyst.

3. 4. 1. 4 Effect of Concentration of HNO_3:

The influence of concentration of nitric acid on the conversion of toluene was studied with 30, 50 and 70 % HNO_3 (Fig. 3.3).

In the case of zeolite H-beta, with 70 % HNO_3, the conversion of toluene was 20 % and with 50 % HNO_3, the conversion was about 16 %. The absence of inhibitory effect of water over zeolite beta can be justified in terms of the low hydrophilicity of this catalyst and high capacity for the adsorption of aromatics. But the selectivity towards alpha-nitrotoluene was greater with 50 % HNO_3 (61.5 %), than with 70 %

HNO_3 (36.1 %). The *p/o* ratio was also greater with 50 % nitric acid. 30 % HNO_3 showed low conversion (9 %) and better selectivity (1.8 %).

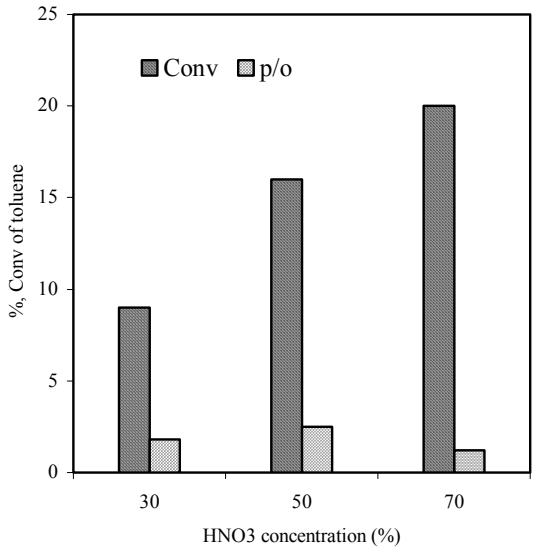

Fig. 3.3: Effect of concentration of nitric acid.

Therefore the liquid phase nitration of toluene was carried out at 70 ºC using 50 % nitric acid over H-Beta catalyst gives higher conversion and selectivity.

3. 4. 2 Vapor phase nitration

The toluene nitration reactions were performed in a downflow reactor with dilute nitric acid over H-beta as a catalyst. Nitration involves electrophilic attack on the aromatic ring by the nitronium ion (NO_2^+).

3. 4. 2. 1 Influence of temperature over nitration of toluene:

The results of toluene nitration using dilute nitric acid over beta zeolite at different temperatures are given in Table 3. 5.

Table 3.5: Effect temperature on product distribution in toluene nitration

Temperature	%, Conv.	Product Distribution, %			%, Oxidation	*p/o*
(C)	HNO_3	ONT	MNT	PNT	Products	ratio
90	8.00	2.56	0.36	1.78	0	0.70
120	83.42	12.1	2.68	33.9	0.31	2.80
140	76.96	11.3	3.38	30.6	0.45	2.71
160	70.40	10.4	2.58	27.12	1.21	2.61
180	57.60	8.6	2.4	21.6	1.36	2.51

Reaction conditions: Toluene : Nitric acid (molar ratio) =1.7:1; HNO_3 (wt.%)= 20%; catalyst = H-beta (Formulated); Oxidation products: Benzaldehyde, Benzoic acid, 4-nitrobenzoic acid & Anthraquinone; ONT= o-nitrotoluene; MNT= m-nitrotoluene; PNT= p-nitrotoluene

The conversion of toluene to mono nitro-toluene was low (4.3 %) at 90 °C and attained a maximum (55 %) at 120 °C and then decreased with increase in temperature. The maximum conversion of toluene at 120 °C was 55 % at toluene: nitric acid ratio of 1.7: 1, with a selectivity of 73 % for *para* nitrotoluene. As the temperature of the reaction is increased from 120 to 180 ^{o}C, the oxidation products, benzaldehyde, benzoic acid and 4-nitrobenzoic acid were increased from 0.31 % to 1.36 % (Fig. 3.4) and the catalyst life was decreased from 75 to 10 hours.

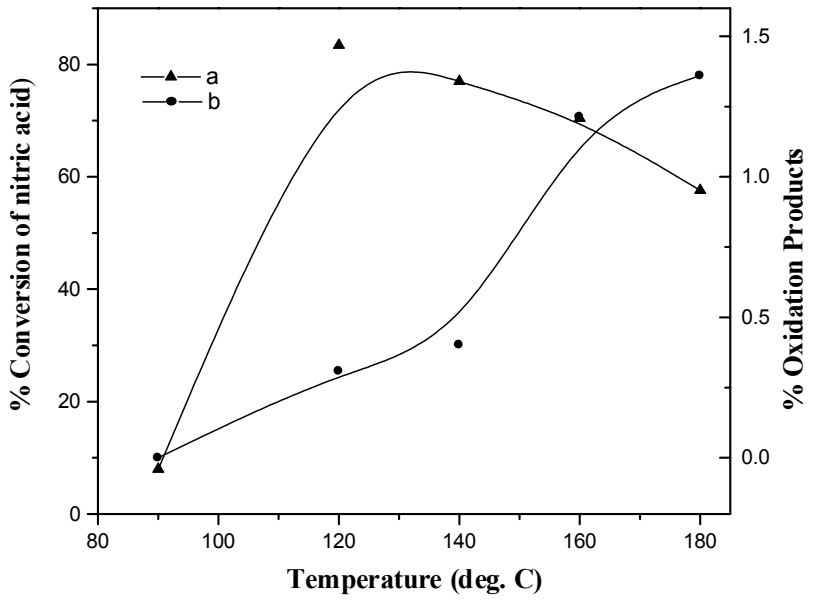

Fig. 3. 4: Effect of temperature (°C) on formation of oxidation products over beta zeolite.

3. 4. 2. 2 Influence of concentration of nitric acid:

The influence of concentration of nitric acid on toluene nitration over beta zeolite is shown in Fig.3. 5. It is seen that, as the concentration of nitric acid was increased from 20 to 40 %, the conversion of toluene decreased and the formation of oxidation products increased, leading to a decrease in catalyst life because of the deposition of oxidation products on the surface of the catalyst. From these results it is seen that, when the toluene nitration was carried out at 120 ^{o}C with 20 % nitric acid over beta zeolite, the toluene conversion and selectivity for *para* nitrotoluene was highest. Under these conditions, the catalyst remains active for up to 80 hours, which is higher than any values reported in the literature for any catalyst [14-16]. The deactivation of the catalyst at a temperature higher than 120 °C and with concentrated nitric acid higher than 20 % may be attributed to the generation of nitrous oxide (NO),

which oxidizes toluene to benzaldehyde and other side chain oxidation products causing the deactivation of the catalyst [41]. Nitration of toluene is an exothermic reaction, and the use of dilute nitric acid provides water vapors, which dissipates the heat of reaction so that the formation of oxidation side products is minimized. That the dilute nitric acid is cheaper than concentrated nitric acid provides an added advantage for the commercialization of the process.

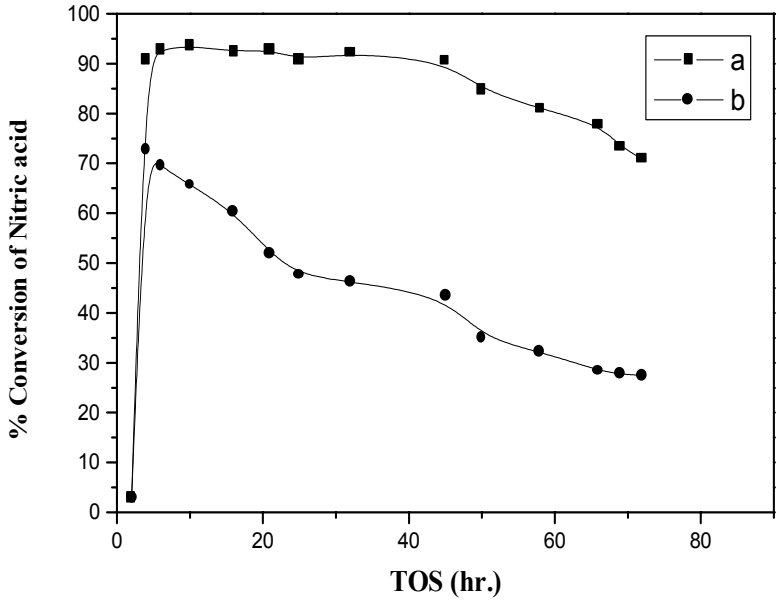

Fig. 3. 5: Effect of dilution of nitric acid on the catalyst life (a) performance of catalyst using 20 % HNO_3 and (b) performance of catalyst using 30 % HNO_3.

3. 4. 2. 3 Effect of WHSV on the catalyst deactivation:

The increase in WHSV from 0.2 to 1 lowered the toluene conversion as well as the catalyst life (Fig. 3. 6). It is interesting to note that, even though the catalyst is deactivated, lowering the conversion of toluene, the selectivity for para isomer remains

almost constant (73 %). This indicates that the oxidation products are deposited on the surface, leaving only a few pores open for the shape-selective reaction inside the pores. This may be due to the orientation of toluene molecule on the catalyst surface, causing steric hindrance for the formation of other isomers of nitrotoluene.

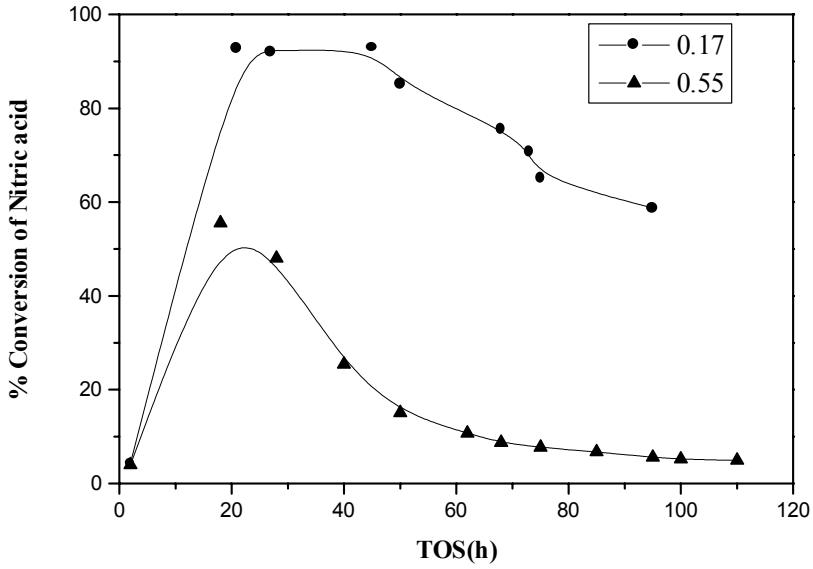

Fig. 3.6: Effect of WHSV on the catalyst deactivation over beta zeolite.

3. 4. 2. 4 Effect of binder on the activity of beta zeolite:

When the reaction is carried out using non-formulated catalyst, the conversion of toluene was less (37.6 %) compared to that using formulated catalyst (55 %) with similar selectivity for *para* isomer, as well as the life of the catalyst was also more in the case of formulated catalyst (Fig. 3. 7). The non-formulated catalyst has mainly Brönsted acid sites which generate nitronium ions from nitric acid adsorbed on the catalyst surface, whereas the formulated catalyst has both Brönsted and Lewis acid sites because of the alumina binder, which affects the acidity of the catalyst, leading to

the higher conversion compared to that with non-formulated catalyst. When the reaction was carried out over ZSM-5 (MFI) catalyst, the conversion of toluene, as well as the *para* nitrotoluene formation, were lower as compared to the values for beta zeolite.

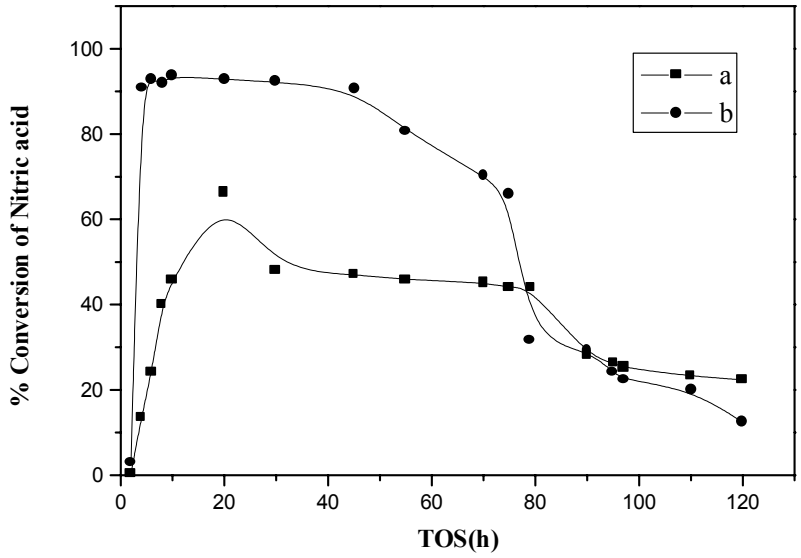

Fig. 3. 7: Effect of binder on the activity of beta zeolite; (a) indicates beta zeolite without binder and (b) indicates beta zeolite with binder (alumina).

The deactivated catalyst, after washing with acetone and methyl ethyl ketone solvents, regains about 90 % of its original activity. This indicates that the deactivation of the catalyst is partly due to fouling of the catalyst surface by the deposition of the oxidation products, which are soluble in these solvents and are washed away after washing. By washing the catalyst intermittently with these solvents, one can minimize the thermal regeneration cycle of the catalyst, increasing the space-time yield between two regeneration cycles. Such a regeneration protocol is not described in the literature.

3. 4. 3 Characterization of the deactivated H-Beta catalyst

A comparison of XRD patterns of H-beta sample before and after nitration shows no loss in crystallinity, indicating the structural stability of the catalyst in acid environment of the reaction.

EDX analysis shows leaching of the aluminum from the catalyst H-beta may be from the catalyst due to the effect of nitric acid.

Thermal analysis (TG/DTA/DTG) of the deactivated beta zeolite in flowing air is shown in Fig. 3. 8. It indicates that up to 200 °C there is an endothermic weight loss of adsorbed water/toluene from the catalyst [38] and above 200 to 400 °C the weight loss is due to evaporation of volatile oxidation products deposited on the zeolite. The final exothermic weight loss of 12.85 % below 690 °C is due to the combustion of adsorbed species, suggesting the formation of coke precursors. This shows that the adsorption of high boiler species inside the pores and on the external surface of the catalyst were responsible for the deactivation. These species may be coke precursors. For checking the reactivation of the catalyst, different treatment has been given to the catalyst such as washing of the catalyst with water and acetone and by heating the catalyst at 250 °C to 500 °C. After the treatment the thermal analysis has been done and we observed the % weight loss shown below in Table 3. 5.

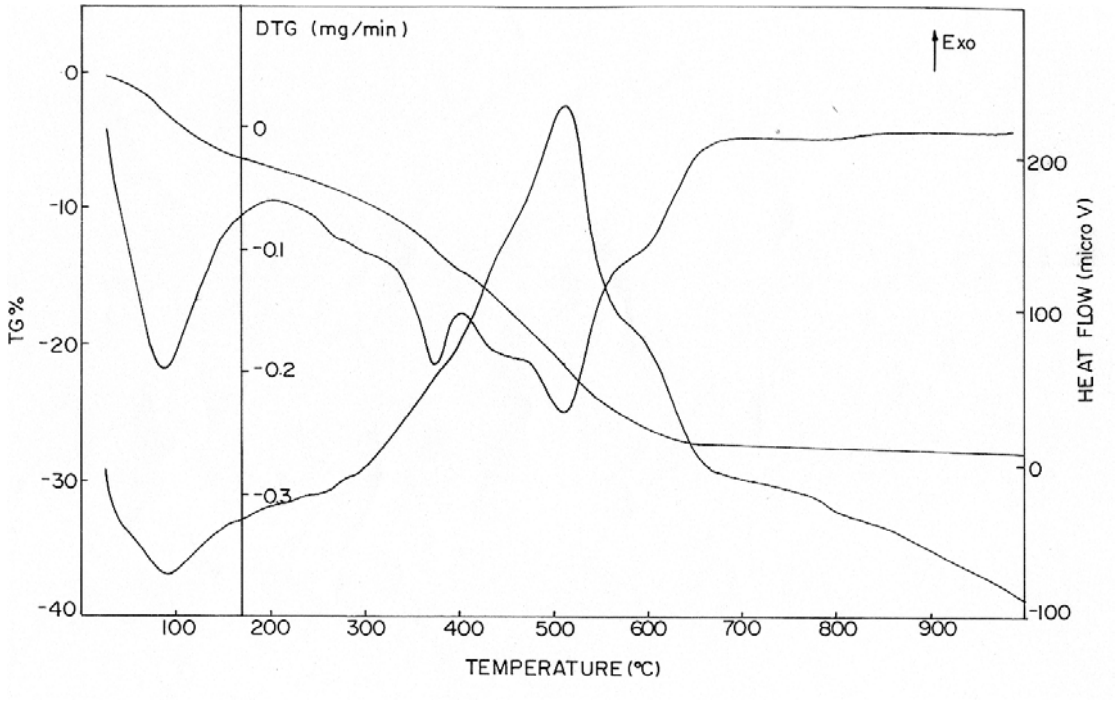

Fig. 3. 8: Thermal analysis of deactivated beta zeolite.

Table 3. 5: Thermal analysis of deactivated catalyst

	Sample	**Temperature (°C)**	**% wt. loss**
1.	Deactivated catalyst	166	5.8
		670	28.0
2.	Deactivated catalyst heated at 250°C	212	2.0
		674	24.5
3.	Deactivated catalyst with water wash	217	5.4
		679	21.1
4.	Deactivated catalyst with acetone wash	194	1.1
		665	18.8

The acetone washed catalyst was tested for its activity in toluene nitration and it showed higher conversion (40 %) as compared to its deactivated form (20 %) suggesting the reactivation of the catalyst by washing with acetone.

The FTIR spectra of deactivated formulated zeolite showed the presence of aluminum nitrate, indicating the leaching of aluminum from binder alumina, which can also block the active sites on catalyst surface.

The FTIR spectra of chemisorbed pyridine at 100, 200, 300 and 400 °C on the fresh and reactivated zeolite beta are shown in Fig.3. 9 (a-h). The bands observed at 1636 and 1543 cm^{-1} are assigned to pyridine molecules bound to Brönsted acid sites and those at 1612, 1490, 1448 cm^{-1} are assigned to pyridine molecules bound to Lewis acid sites [39]. The IR spectra of the deactivated sample obtained at 200 °C showed the deposition of high boilers on the sample. When the pyridine was chemisorbed on a

reactivated sample, the FTIR spectra revealed regeneration of both types of acid sites, which are shown in Fig. 3. 9 (e-h).

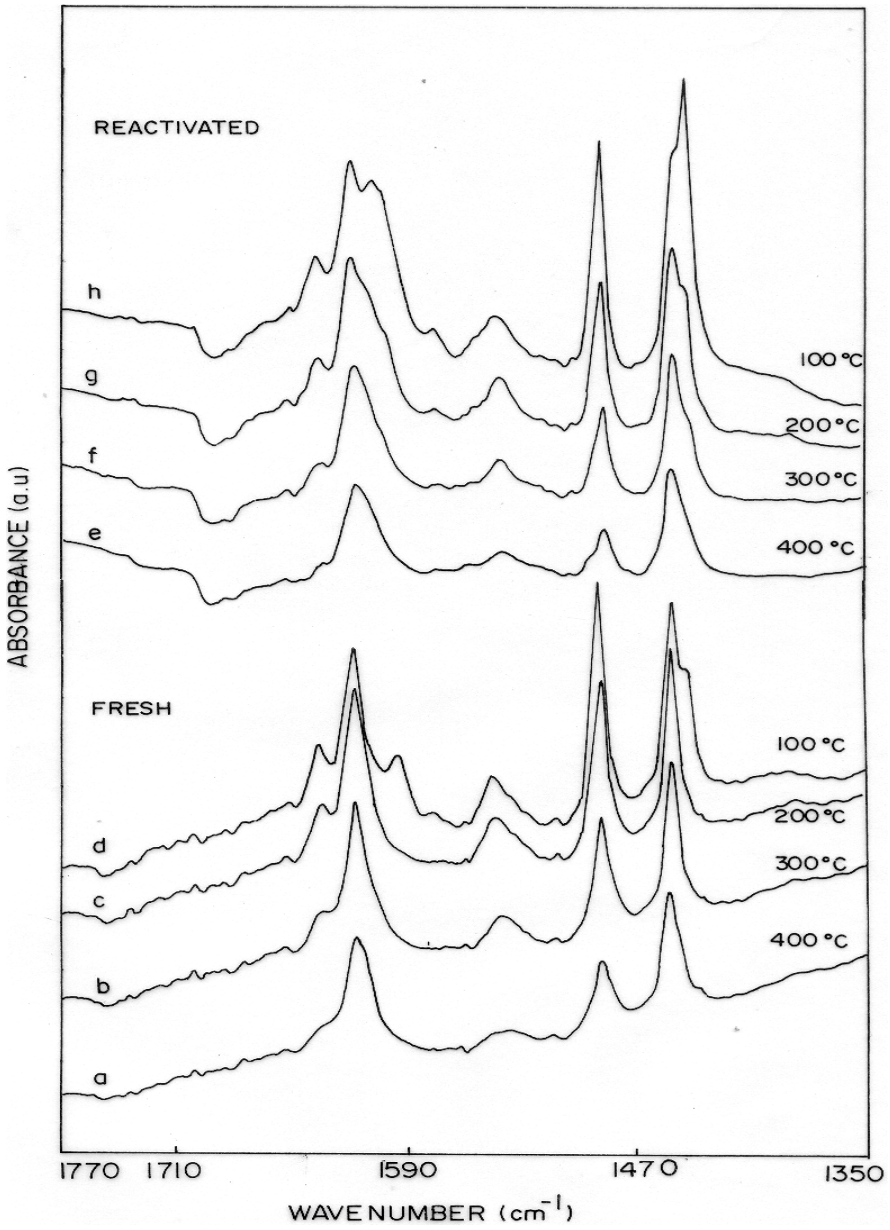

Fig. 3.9: FT-IR of chemisorbed pyridine, (a-d)- Fresh H-beta spectra; (e-h) - Reactivated H-beta catalyst spectra.

The surface area which was determined according to the t-plot method [40] of the deactivated zeolite showed a substantial loss after nitration indicating pore filling/blockage by strongly bound byproducts (Table 3. 6).

Table 3. 6: Characterization of catalyst before and after reaction

Description	BET (m^2/g)	External (m^2/g)	Pore volume (cm^3/g)	Micropore volume (cm^3/g)
Fresh H-beta (formulated)	516.9	289.9	0.239	0.054
After deactivation	34.2	30	0.085	0.002
Fresh H-beta (unformulated)	638.6	341.7	0.151	0.061
After deactivation	143.4	68.8	0.075	0.022

The deactivated zeolite catalyst was washed with acetone and the washing was analyzed by GC, GC/MS, and GC-IR, results showed 4-nitrobenzoic acid, a major product, benzaldehyde, dinitrotoluene, and toluene as minor products and anthraquinone in trace quantities.

3. 4. 4 Molecular modeling studies

3. 4. 4. 1 Diffusion Characteristics of the Molecules in MFI:

The molecular graphics (MG) picture shows (Fig. 3. 10) the fitting of **3**, **4** and **5** (CPK model) inside the MFI pores (cross section of the 10-MR). The diffusion of **5** through MFI is possible, but diffusion of **3** and **4** is not possible (Table. 3.7). The diffusion of the molecules along the 'b' direction in a 10-M straight channel was carried out. The molecule passes through several energy maxima and minima, while

diffusing through a unit-cell. It is observed that **5** has a diffusion energy barrier of 9.3 kcal/mol. Similar calculations for diffusion of molecules **3**, **4** and **6** were also made. The results of these calculations are given in Table 3.6. The diffusion energy barrier for the three isomers of nitrotoluene and dinitrotoluene increase in the order **5** < **3** < **4** < **6**, the calculated diffusivity being in the order **5** > **3** ≅ **4**. The mean energies of interaction of the isomers of nitrotoluene are also in the order **6** > **4** ≅ **3** > **5**. Thus our calculations indicate that the diffusivity of **5** in MFI is distinctly more than those of **3** and **4**. This is in conformity with the results of an earlier calculation [20]. Our calculations based on adsorption and diffusion energy barriers inside MFI, indicate that the reactant molecules **1** to **2** are more mobile (Table 3.7). However, the diffusion energy barrier of **2** inside, MFI is larger than that for **1**, and **5**, because of the preferred orientation of these molecules inside the zeolite pores [24b]. The phenyl ring of **5** lies parallel to the diffusion plane (elliptical plane of b axis) while diffusing through MFI channel [24b]. The diffusion of the **5** shows two minima across the unit-cell. This happens when the phenyl ring is at the locations where the straight channels and sinusoidal channels intersect. These intersections occur twice in a unit-cell of MFI [42] and the diffusion energy profile pattern observed is in correspondence with this symmetry (not shown). Whenever the phenyl group of the molecule passes through the wall of the zeolite framework, the phenyl ring is found to be parallel to elliptical plane. Roel Prins et al. [43] reported the change of coordination of aluminum from tetrahedral to octahedral would further reduce the pore diameter by ~1Å and this will hinder the diffusivity of para isomer, affecting the shape selectivity; these are corroborated by experimental results.

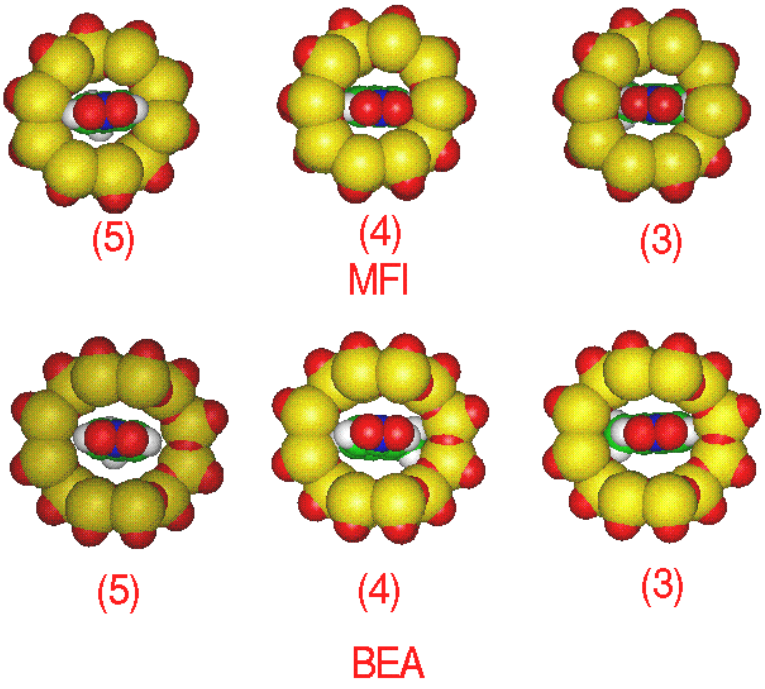

Fig. 3.10: The MG picture shows the fitting of **3**–**5** (CPK model) inside beta zeolite and MFI pores (cross-section of the 12- and 10-MR). Hydrogen atoms are whitish gray, carbon atoms are green, nitrogen atoms are dark blue, oxygen atoms are red and silicon atoms are yellow. Molecules **3**–**5** vary tightly fits in the pore of MFI (10-MR). In case of beta zeolite molecule **5** fits freely, whereas **4** and **3** fit more tightly in the pores even though it is 12-MR ring.

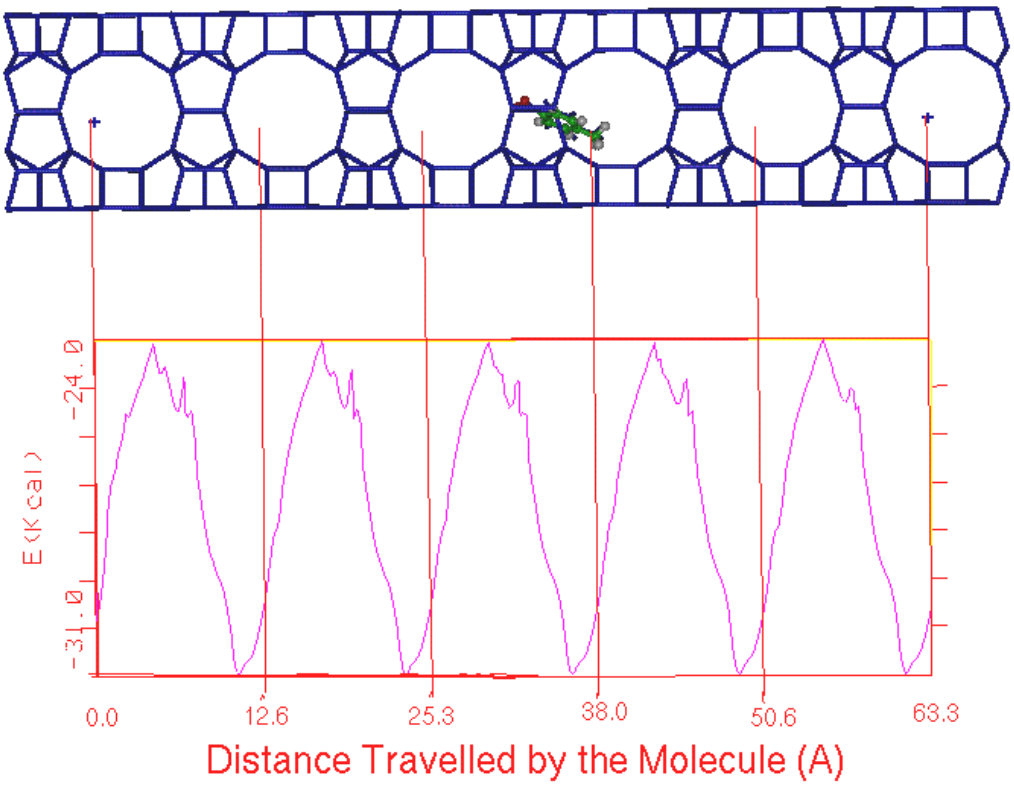

Fig. 3.11: Variation of the interaction energy of **5** and the beta framework as the molecule diffuses through the 12-M channel. The cross-section of the 12-M windows in the perpendicular direction in shown. A typical minimum energy configuration of the molecule during the diffusion is also included.

3. 4. 4. 2 Diffusion Characteristics of the Molecules in BETA:

The molecular graphics picture shows (Fig. 3.10) the fitting of **3**, **4** and **5** (CPK model) inside the beta pores (cross section of the 12-MR). From the molecular fittings, it appears that the diffusion of **5** is possible through the beta zeolite pores, whereas diffusion of **3** and **4** seems to be difficult even though the pore size is larger than the size of **3** and **4**; the difficulty may arise from molecular interaction with the zeolite wall. The structure of beta can be represented as an inter-growth of two well-defined polymorph structures, both of them having 3d-pore architecture. The diffusion of the reactant and the three possible product molecules for the nitration reaction was carried out along the 'a' direction in the 12-MR channel. The diffusion was studied for 5-unit cell shown in Fig. 3.11. Figure 3.11 shows a molecular graphics picture of the minimum energy configuration of **5** inside beta. The variation in the interaction energy between **5** and beta is also included in the form of a graph. Similar calculations for diffusion of molecules **3**, **4** and **6** were also made. The salient information derived from these diffusion studies is summarized in Table 3.7. All of the molecules have one maxima when they diffuse through one unit cell of beta; this maxima occurs when the molecule moves from one 12-M intersection to the other 12-M intersection. The mean energy is closer to the minimum energy values, which indicates that the molecule will diffuse selectively. Mean energy values and the diffusivity is given in Table 3.7. Results indicate that the diffusivity decreases in the order of **5** > **3** > **4**. The diffusion energy barrier is more for **4** as compared to the barriers for **5** and **3**. These results indicate that there will be high selectivity for the diffusion of **5** in the case of beta zeolite.

We have also analyzed the orientation of **5** when it diffuses inside the 12-MR straight channel of beta, to understand the following features: a) the favorable and

unfavorable orientations of **5** inside beta and b) the residence time of **5** at various locations inside the straight channel of beta. In the diffusion of **5**, the phenyl ring lies parallel to the diffusion plane (elliptical plane of b axis) [24b]. The diffusion of the **5** shows minima across the unit-cell when the phenyl ring is at the locations where the straight channels and perpendicular channels intersect. Whenever the phenyl group of the molecule passes through the wall of the zeolite framework, the phenyl ring is found to be parallel to diffusion plane. Our results, are consistent with the hypothesis that upon adsorption of the reactant on a rigid surface such as the zeolite framework, steric hindrance would direct the orientation of the aromatic in the adsorbed state in a way that the substituent on the aromatic ring points towards the zeolite cavity where the least repulsion would be expected. During the toluene nitration, aluminum is changing its coordination from tetrahedral to octahedral [43], reducing the pore size by ~1Å. Beta has three-dimensional interconnected channel system with 12-M elliptical channels having a diameter 7.6 x 6.4 Å. This will further reduce the pore size by ~ 1Å and will impart the para selectivity in toluene nitration due the diffusional constraints. These results agree with experimental observations.

That the para selectivity during the toluene nitration remains more or less constant even after deactivation may be due to the partial blockage of the zeolite pores (active sites) and the remaining open pores will lead to the formation of para isomer selectively.

Table 3.7: The deepest minima, peak maxima, the diffusion energy barriers, mean energy and diffusivity for organic molecules in zeolites

Zeolite	Molecule #	Deep Minima (kcal/mol)	Peak Maxima (kcal/mol)	Energy Barrier (kcal/mol)	Mean Energy (kcal/mol)	Mean/Min (Diffusi-vity)
MFI	**1**	-10.671	-9.183	1.488	-9.893	0.927
	2	-29.363	-6.550	22.813	-21.474	0.731
	3	-33.175	7.698	41.402	-10.227	0.303
	4	-34.448	19.287	53.735	-11.897	0.345
	5	-34.560	-25.247	9.313	-29.734	0.860
	6	-40.444	96.119	136.563	0.550	0.014
Beta	**1**	-8.819	-6.844	1.981	-07.766	0.881
	2	-19.321	-14.887	4.437	-17.010	0.880
	3	-27.948	-17.572	10.176	-23.225	0.831
	4	-28.383	-14.672	14.672	-26.613	0.838
	5	-30.975	-24.023	6.924	-27.204	0.878
	6	-28.626	-27.827	18.443	-31.530	0.807

Code as in Table 3.2,

3. 5 CONCLUSION

Sulphated catalysts such as sulphated zirconia, sulphated silica, sulphated yttria/zirconia and sulphated zirconia/silica showed lower conversion (10.6 %) as well as low selectivity in liquid phase nitration of toluene. The catalyst were deactivated with time on stream may be due to the leaching, and deactivation. However the H-beta and $Fe/Mo/SiO_2$ showed higher catalytic activity in liquid phase nitration of toluene.

Among these catalysts the H-beta was the good catalyst for nitration of toluene at 70°C, which showed conversion 49.1 % with *p/o* ratio 2.2 indicating the shape selectivity of beta zeolite.

Para nitrotoluene is selectively formed by the vapor phase nitration of toluene using dilute nitric acid over beta zeolite at 120 °C in high yield with longer catalyst life. The catalyst deactivated faster when the concentration of acid and the temperature of reaction and WHSV was increased. The catalyst is deactivated due to the deposition of oxidation products partially blocking the pores and fouling the catalyst surface. Even though the catalyst is deactivated; the selectivity for *para* nitrotoluene is maintained because of shape selectivity and favorable orientation of toluene molecule. The physicochemical characterization of the deactivated catalyst showed structural the stability of zeolite beta under the reaction conditions, but the *para*-nitrotoluene, and other oxidation products 4-nitrobenzoic acid, benzaldehyde, benzoic acid and anthraquinone were found deposited on the catalyst surface. Even then, the selectivity for *para* nitrotoluene remains nearly constant. The molecular modeling study revealed that *para*-nitrotoluene encounters the least resistance for diffusion in the zeolite beta. One of the major advantages of this process is the use of dilute nitric acid as a nitrating agent, leading to high selectivity towards *para* nitrotoluene and longer catalyst life. This method is superior to those using acetic anhydride or acyl nitrate as reported earlier. There is no usage of sulfuric acid, which is essential in the conventional process, thus avoiding hazardous waste disposal, which makes the process environmentally friendly. The molecular modeling study indicates that para selectivity is due to faster diffusion of *para* isomer in the pores of the catalyst. These observations indicate that the shape selective nitration of toluene takes place inside the zeolite pores. The catalyst with alumina binder was found to be more active than the catalyst

without binder because of higher acidity. The deactivated catalyst can almost be regenerated by washing the catalyst with organic solvents.

Table 3.2: Crystal characteristics and the dimensions of the simulation boxes for different zeolites

Zeolite	Symmetry	Unit-cell composition	A (Å)	B (Å)	C (Å)	Average Pore diameter (Å)	No of unit-cells in the simulation box
MFI	Orthorhombic	$(SiO_2)_{96}$	20.022	19.899	13.383	5.1 x 5.6	2 x 3 x 2
BETA	Tetragonal	$(SiO_2)_{64}$	12.660	12.660	26.406	7.6 x 6.4	6 x 2 x 1

3. 6 REFERENCES

1. K.Winnacker, L. Kuchler, in *Chemische Technologie*, Band 6, Organische Technologie II (4th edition), Edited by H. Harnisch, R. Steiner, K. Winnacker 169 (1982).
2. V. P. Glusshko, (ed.) *Thermodynamic properties of individual substances*, **1(1)**, (1978).
3. M. McKee, R.H. Wilhelm, *Ind. Eng. Chem*. **28**, 662 (1936).
4. *Ullmann's Encyclopedia of Industrial Chemistry*, VCH, Weinheim, **A17,** 411 (1991).
5. S. Suzuki, K. Tahmori, Y. Ono, Y., *Chem. Lett*, 747 (1986).
6. G. A. Olah, V.V. Krishnamurthy, S. C. Narang, *J. Org. Chem*. **47**, 596 (1982).
7. A. Cornelis, Gerstmans, P. Laszlo, *Chem. Lett*. 1839 (1988).
8. A. German, T. Akouz, F. Figueras, *Appl. Catal. A: General*, **136**, 57 (1996) and *J. Catal.* **147**, 163 (1994).
9. D. Akolekar, G. Lemay, A. Sayari, S. Kaliaguine, *Res. Chem. Interm*. **21**, 7 (1995).
10. S. H. Nagi, E. A. Zubkoz, V. G. Shubin, *Izv. Aka. Nauk SSSR, Ser. Khim*. 1650 (1990).
11. E. Suzuki, K. Tohmori, and Y. Ono, *Chem. Lett*. 2273 (1987).
12. J. M. Riego, Z. Sedin, J. M. Zaldivar, N. C. Marziano, C. Toratato, *Tetrahedron Lett*. **37**, 513 (1996).
13. Wilhelm, R. H., *US Patent* 2 109873 (1938).
14. B. M. Choudary, M. Sateesh, M. Lakshmi Kantan, K. Koteswara Rao, K. V. Ram Prasad, K. V. Raghavan, J. A. R. P. Sharma, *Chem. Commun*. **1**, 25-26 (2000).
15. D. Vassena, D. Malossa, A. Kogelbauer, R. Prins, *Proceedings of 12th Inter. Zeol. Conf.* (Eds: M. M. J. Treacy, B. K. Markus, M. E. Bisher and J. B. Higgins, Materials Research Society Warrendale, Pennsylvania, USA) 1909 (1999).
16. Jeffrey M. Smith, Haiyang Liu, Daniel E. Resasco, *Stud. Surf. Sci. Catal*., **111,**

199-206 (1997).

17. Dan Farcasiu, Jing Qi Li, *Applied Catalysis A: General;* **128**, 97-105 (1995).
18. A Keshavaraja, V. R. Hegde, B. Pandey, A.V Ramaswamy, Pradeep Kumar, T. Ravindranathan; *Angew.Chem.Int. Ed. Engl*, **34**, No: 19 (1995).
19. Andreas Kogelbauer, Diego Vassena, Roel Prins, John N. Armor, *Catalysis Today*; **55**, 151- 160 (2000).
20. Thomas J. Kwok, Keerthi Jayasuriya, *J. Org. Chem*. **59**, 4939-4942 (1994).
21. W.M. Meier, D.H. Olson, Ch. Baerlocher, "*Atlas of Zeolite Structure Types*", Elsevier, (1996), p. 1 (*Zeolites*, vol. **17**).
22. A.T. Hagler, S. Lifson, P. Dauber, *J. Am. Chem. Soc*. **101**, 5122 (1979).
23. P. Dauber-Osguthorpe, V.A. Roberts, D.J. Osguthorpe, J. Wolff, M. Genest, A.T. Hagler, *Proteins: Structure, Function and Genet*. **4**, 31 (1988).
24. a) R.C. Deka, R. Vetrivel, *J. Catal*. **174**, 88 (1998). b) S. B. Waghmode, P. Bharathi, S. Sivasanker, R. Vetrivel, *Microporous Mesoporous Mater*. **38**, 433 (2000).
25. A. Chatterjee, R. Vetrivel, *J. Chem. Soc. Faraday Trans*. **91**, 4313 (1995).
26. H. Van Koningsveld, H.Van Bekkum, J.C. Jansen, *Acta Crystallogr*. **B 43**, 127 (1987).
27. J.M. Newsam, M.M.J. Treacy, W.T. Koetsier, C.B. De Gruyter, *Proc. R. Soc. London*, ser. **A 420**, 375 (1988).
28. R. Vetrivel, C. R. A. Catlow, E. A. Colbourn, *Stud. Surf. Sci. Catal*. **49**, 231(1989).
29. Y. Nakazaki, N. Goto, T. Inui, *J. Catal*. **136**, 141 (1992).
30. J.A. Horsley, J.D. Fellmann, E.G. Derouane, C.M. Freeman, *J. Catal*. **147**, 231 (1994).
31. R. Millini, S. Rossini, *Stud. Surf. Sci. Catal*. **105**, 1389 (1996).
32. R.C. Deka, R. Vetrivel, *Chem. Commun*. 2397 (1996).
33. R.C. Deka, R. Vetrivel, A. Miyamoto, *Topics in Catal*. **9**, 225 (1999).
34. R.C. Deka and R. Vetrivel, *J. Mol. Graphics Mod*., **16**, 157 (1998).
35. a) P. Bharathi, S.B. Waghmode, S. Sivasanker, R. Vetrivel, *Bull. Chem. Soc. Jpn*., **72**, 2161 (1999). b) P. Bharathi, R.C. Deka, S. Sivasanker, R. Vetrivel, *Catal. Lett*. **55**, 113 (1998).

36. P. Tomlinson-Tschaufeser, C.M. Freeman, *Catal. Lett*. **60**, 77 (1999).

37. G. Seo, H.S. Jeong, J.M. Lee, B.J. Ahn, *Stud. Surf. Sci. Catal*., **105B**, 1431 (1997).

38. Bao-Lian Su, Valerie Norberg, *Zeolite*, **19 (1)**, 65-74 (1997).

39. Chunjuan Jia, P. Massiani, D. Barthomeuf, *J. Chem. Soc., Faraday Trans*., **89(19)**, 3659-65 (1993).

40. B.C. Lippens and J.H. de Boer, *J. Catal*. **4**, 319 (1965).

41 L. V. Malysheva. E.A. Paukshtis, K.G. Ione, *Catal. Rev. Sci. Eng*., **37**, 179 (1995).

42. H. Van Koningsveld, J.C. Jansen, H. van Bekkum, *Zeolites*, **10**, 235 (1990).

43. M. Haouas, A. Kogelbauer, R. Prins, *Catal. Today*, **70**, 61-65 (2000).

CHAPTER IV

NITRATION OF PHENOL

4. 1 INTRODUCTION

Nitrophenols are important intermediates for the manufacture of drugs and pharmaceuticals. Catalytic hydrogenation of 2-nitrophenol gives 2-aminophenol, which is used as a photographic developer and as a versatile intermediate for dyes and fine chemicals. Para-nitrophenol is an important starting material used in multiple step synthesis of valuable compounds [1].

Among the aromatic compounds phenol is very active and is nitrated with nitric acid to various nitro derivatives, which makes it difficult to isolate [2]. Nitration of phenol using mixture of nitric acid and sulfuric acid gives 2-nitrophenol and 4-nitrophenol in a ratio of 1.42 [3]. Nitration of phenol as a special case has been studied by several researchers using various nitrating agents under different conditions [4]. Recently Zolfigol et al. [5] reported a use of *solid inorganic acid salts* ($NaHSO_4.H_2O$, $Mg(HSO_4)_2$) with sodium nitrate, which gave *in situ* generation of HNO_3 and nitrophenols in high yields.

Phenols are easily mononitrated at room temperature by $NaNO_3$ in a two phase system (water-ether) in presence of HCl and a catalytic amount of La $(NO_3)_3$ with *o/p* ratio 2:1 [6]. Lazslo demonstrated that phenol can be nitrated in a system called claycop (trihydrated cupric nitrate supported on montmorillonite/acetic anhydride/CCl_4) in 92 % yield with an *o/p* ratio 13.3 [7]. Very high regioselective nitration of phenol was achieved with a surfactant suspended in acetonitrile treated with nitronium tetrafluoroborate, which gave an *o/p* ratio of 19.0 [8].

Nitration of phenol has been performed by $AcONO_2$ /HNO_3/ and aromatic solvents [9], N-nitropyrazole/$BF_3.Et_2O/CH_2Cl_2$ [10], via nitroso compounds and their subsequent oxidation to nitrocompounds with HNO_3 [11], metal nitrates [12], clay

supported nitrates [13], impregnated alumina and silica with N_2O_4 [14], $AcONO_2$ [15] and $TfONO_2$ [16]. Gaude et al. reported the nitration of phenol in a two-phase media and suggested a diffusion-controlled mode of operation to control the rate of reaction [17]. Kulkarni et al. reported a two-phase nitration of phenol in which benzene-aqueous nitric acid microemulsion (termed as a aqueous phase) with phenol in benzene (termed as a organic phase) has been employed in the reaction and the microemulsion droplet can be considered as a microreactor where chemical reactions takes place. It indicates that the process rate can be selectively regulated, also selective to desired product and the oxidation can be largely avoided by incorporating dilute nitric acid in microemulsion solution [18].

Some of these methods use less stable acetyl nitrate requires *in situ* generation of nitric acid using metal nitrates and organic acid which requires tedious work up procedures. On the basis of the above facts, it is clear that there is a need for more regioselective control of nitration of phenol using nitric acid as a nitrating agent to obtain higher conversion and selectivity. To our understanding very little study has been done on the regioselective nitration of phenol using nitric acid as a nitrating agent over solid acid catalyst.

The nitration of phenol selectively to para-nitrophenol in high yields has been recently achieved by Thomas Milczak et al. [19] over metal oxide solid acid catalysts and the selectivity for para-nitrophenol varied with the nature of the catalysts and the reaction conditions. However the micrporous zeolites, well known for their shape selective behavior have not been studied as solid acid catalysts for phenol nitration.

4. 2 EXPERIMENTAL

4. 2. 1 Materials and Catalysts

Phenol crystals and nitric acid were obtained from the S. D. Fine Ltd. India. Commercially available zeolite H-beta, H-Y, H-ZSM-5 in the powder form were procured from United Catalyst India Ltd. La-H-Beta was prepared by impregnation of lanthanum nitrate on H-beta. MoO_3/SiO_2 (MoO_3 : 20 mol %), $Fe_2O_3/MoO_3/SiO_2$ (Fe_2O_3 : 0.7, MoO_3 : 20 mol %) catalyst were prepared as per the procedure given in chapter II.

4. 2. 2 Reaction Procedure

Nitration of phenol was carried out with equimolar ratio of phenol to nitric acid using zeolite H-beta as a catalyst. Reaction was performed in a batch reactor. 2 g phenol was taken in a flask containing 3 ml solvent to which 1g of catalyst and 4 ml. of dilute nitric acid (30 %) were added. The reaction mixture was stirred at room temperature for varying period of time to study the progress of the reaction. The reaction product was extracted with diethyl ether, which was analyzed off-line by gas chromatography GC (HP6890, column : HP-1, 30m length, 0.25mm ID), GC/MS (SHIMADZU, column, DB-I). The catalyst was characterized before and after the reaction for its physical and chemical properties using various techniques such as XRD (Regaku, Miniflex), EDX (KEVEX 7000 system), and AAS (Perkin Elmer).

4. 3 RESULTS AND DISCUSSION

Nitration of phenol (1) using dilute nitric acid over solid acid catalysts gives o-nitrophenol (2) and p-nitrophenol (3) and benzoquinone in trace. The reaction scheme is shown below:

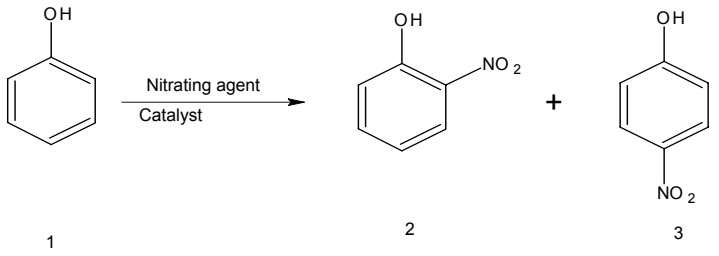

4. 3. 1 Influence of various catalysts

The results of regioselective nitration of phenol using nitric acid over solid acid catalysts are given in Table 3.1. Among the catalysts studied, zeolite H-Beta (Si/Al = 30) showed highest conversion (96 %) and selectivity (87 %) for *o*-nitrophenol. The conversion as well as selectivity for *o*-nitrophenol was low for other catalyst under study showing the influence of acidity as well as porosity of the catalyst. As the acidity of the catalyst decreased from H-Beta to H-ZSM-5 and $Fe_2O_3/MoO_3/SiO_2$, the conversion was found be decreased from 95 % to 60 %. Similarly the selectivity for *o*-nitrophenol also decreased from 87 % in case of H-beta to 60 % in the case of Y-zeolite. $Fe/Mo/SiO_2$ being dense solids having mesopores and micropores, *ONP /PNP* ratio was about 1:1 showing the selective nitration of phenol over zeolite catalysts. The highest conversion (96 %) and selectivity (87 %) in case of zeolite H-Beta may be because of preferred orientation of phenol inside the zeolite pores increasing the accessibility of ortho position to nitronium ion leading to selective formation of *o*-nitrophenol (Scheme). Lanthanum impregnated zeolite beta (La-H-Beta) showed lower

conversion (90 %) and selectivity (80 %) may be because of pore blockage, reducing pore size affecting the selectivity. When the reaction was carried out using concentrated nitric acid (70 %), formation of dinitrophenol (4-5 %) was observed. With the use of dilute nitric acid (30 %), there was no formation of dinitrophenol, which is an added advantage apart from its cheaper cost and ease in handling compared to concentrated nitric acid.

When the reaction was carried out without catalyst the conversion was low (49 %) with nearly equal *ortho*- and *para*- isomers, suggesting the influence of solid acid catalyst on the conversion and selectivity.

The selectivity for ortho-nitrophenol is lower (*o/p* ratio 10) using zeolite catalyst as compared to reported method for nitration of phenol using acetyl nitrate preadsorbed on silica gel (*o/p* ratio of 13.3) described by Rodrigues et al [9]. The acetyl nitrate used has drawbacks such as less stability of acyl nitrates and tedious workup procedures. The results of nitration of phenol over MoO_3/SiO_2 and $Fe/Mo/SiO_2$ are comparable to that of Thomas Milczak et al. over metal oxide solid acid catalysts using 100 % nitric acid [19]. When the reaction was carried out using concentrated nitric acid (70 %) over MoO_3/SiO_2 the ortho selectivity was decreased from 70 % to 51 % suggesting the influence of water on the selectivity of phenol nitration.

The zeolite beta showed the structural stability that was verified by XRD analysis after the reaction and catalyst could be used for five cycles without any appreciable reduction in the conversion and selectivity.

Table 4.1: Effect of various solid acid catalysts on nitration of phenol

Catalyst	% Conv. of Phenol	%, Selectivity			Total yield %	*o/p* ratio
		ONP	PNP	Benzq.		
Mo/SiO_2	48	70	17	13	41.76	4.11
$Fe/Mo/SiO_2$	60	48	42	10	54.0	1.14
H-ZSM-5	60	55	37	8	55.2	1.48
H-Y	60	60	30	10	54.0	2.0
H-Beta	96	87	10	3	91.9	10.0
La-H-Beta	89	61	32	7	82.77	1.9

Reaction conditions: Phenol/HNO_3 =1; Catalyst = 50% w/w; Temp. = RT; HNO_3 = 30% , solvent = CCl_4; Reaction Time = 2h; ONP = o-nitrophenol; PNP = p- nitrophenol; Benzq. = Benzoquinone; Total yield = yield of ONP + yield of PNP

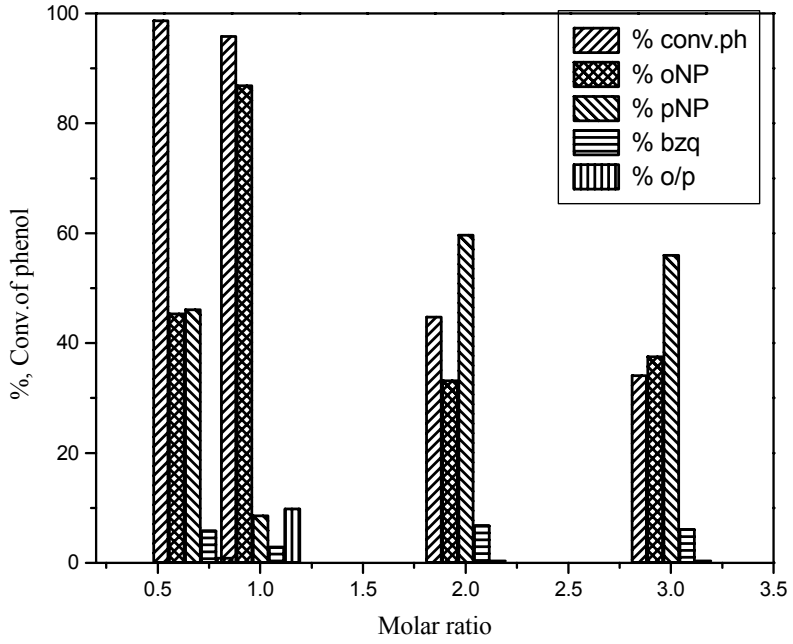

Fig. 4.2: Influence of phenol/HNO_3 molar ratio on conversion of phenol

Phenol being very active molecule and varying the ratio of phenol to nitric acid did not affect the conversion but the selectivity was affected (Fig. 4.2). As the HNO_3 content in the reactants decreased the p-nitrophenol formation was increased.

4. 3. 2 Influence of solvents

The nitration of phenol at room temperature was carried out using various common solvents such as acetone, CCl_4, MeOH, Et_2O, H_2O and hexane over H-beta zeolite and the results are given in Table 2. The highest conversion of 96 % and selectivity for o-nitrophenol of 87 % was obtained with CCl_4 indicating the influence of the solvents on the reaction. This method provides nitrated phenols directly, in short reaction times and good yields.

Table 4.2: Effect of various solvents on Nitration of Phenol over zeolite H-beta

Solvents	% Conv. of Phenol	%, Selectivity			Total yield	*o/p* ratio
		ONP	PNP	Benzq.		
CCl_4	96	87	10	3	91.9	10.0
MeOH	11.5	39.67	-	60.24	45.60	-
Et_2O	88.7	49.24	47.83	2.92	86.10	1.03
2-butanone	75.2	67.78	24.73	7.42	69.56	2.74
H_2O	63.9	58	27.36	14.63	54.5	2.12
Hexane	81.4	57.88	34.15	7.96	74.9	1.69

Reaction conditions: Phenol/HNO_3 =1; Catalyst = 50% w/w; Temperature = RT; HNO_3 = 30%
Reaction Time = 2h; ONP = o-nitrophenol; PNP = p- nitrophenol; Benzq. = Benzoquinone
Total yield = yield of ONP + yield of PNP

4. 3. 5 Influence of dilution

The influence of dilution of nitric acid on phenol nitration over beta zeolite is shown in Fig.4.3. It is seen that, as the concentration of nitric acid was increased from 10 to 70 %, the conversion of phenol to mononitrophenol was increased but upto 30 % concentration of nitric acid and again it decreased from 30 % onwards, suggesting the influence of dilution of nitric acid on conversion. When 70% HNO_3 was used for phenol nitration and then dinitrophenol was also formed alonwith mononitroproducts. When the nitric acid is diluted with water up to 30%, the reaction medium is a three-phase system i.e. solid catalyst, organic solvent and aqueous phase and as reported earlier [20]. This triphasic system may be more active in phenol nitration. At higher dilution (10 to 20%) the activity of HNO_3 was low leading to lower conversion suggesting 30% HNO_3 was suitable dilution for phenol nitration.

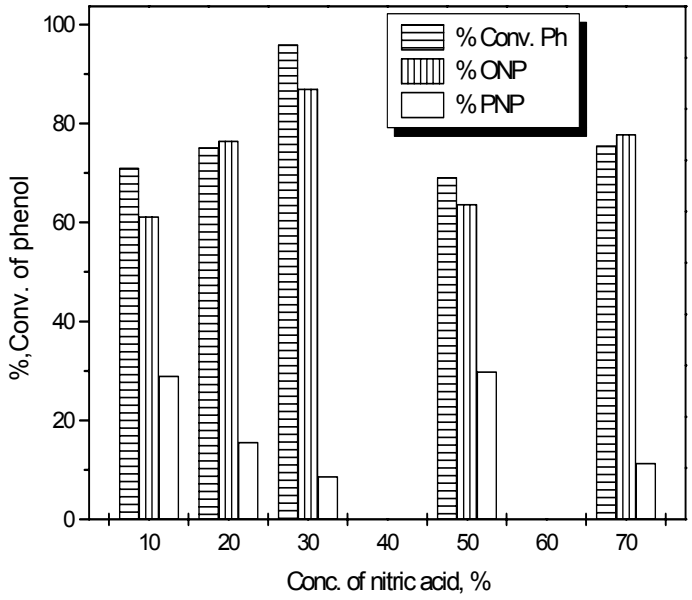

Fig. 4.3: Effect of concentration of nitric acid on conversion and o/p ratio.

4. 4 CONCLUSION

Phenol is selectively nitrated to ortho-nitrophenol in high yields with dilute nitric acid in carbon tetrachloride solvent over zeolite H-beta catalyst. The zeolite catalysts could be easily separated from the reaction mixture by filtration for recycle and the work up procedure for isolation reaction products is simpler as compared to the conventional process. The regioselective nitration of phenol using dilute nitric acid over solid acid catalyst without any use of acetic anhydride / acyl nitrate, metal nitrates or sulfuric acid is comparatively clean process. Compared to the conventional process, phenol nitration over solid acid catalyst is a clean and environment friendly process with a simpler work up procedure for quantitative isolation of the products.

4. 5 REFERENCES

1. *Ullmann's Encyclopedia of Industrial Chemistry*, VCH, Weinheim, **Vol.A17** 411(1991).

2. P. J. Zeegers, *J. Chem. Ed*., **70**, 1036 (1993).

3. A. Vogel. *A Text – Book of Practical Organic Chemistry*, 4th ed, Longman, London, (1978).

4. a) C. K. Hancock, and A. D. Clagve, *J. Am. Chem. Soc*., 86, 4942 (1964). & b) B. Gigante, A. O. Prazeres, and M. J. Marcelo-Curto, *J. Org. Chem*. **60**, 3445 (1995).

5. a) M. A. Zolfigol, N. Iranpoor, and H. Firouzabadi, *Orient. J. Chem*. **14**, 369 (1998);

   b) H. Firouzabadi, N. Iranpoor, and M. A. Zolfigol, *Synth. Commun*. **27**,3301(1997);

   c) N. Iranpoor, H. Firouzabadi, and A. M. Zolfigol, *Synth. Commun*. **28**, 2773 (1998).

6. M.Ouertani, P. Giraro and H.B. Kagan, *Tetrahedron Letters* **23 (42)**, 4315-4318 (1982).

7. B. Gigante; A. O. Prazeres; M. J. Marcelo-Curto; A. Cornelis; P. Laszlo, *J.Org. Chem*. **60**, 3445 (1995).

8. H. Pervez; S. O. Onyisiuka; J. R. Rooney; C. J. Sukling, *Tetrahedron,* **44**, 4555 (1988).

9. J.A.R. Rodrigues, Paulo J. S. Moran and Rogerio Custodio, *Tetrahedron*, **55**, 6733-6738 (1999).

10. a) M. J.Thompson; P. J. Zeegers, *Tetrahedron*, **47**, 8787 (1991).

    b) A. Germain, *J. Chem. Soc. Chem Commun*. 1697 (1990).

11. E. Santaniello; M. Ravasi, *J. Org. Chem*. **48**, 739 (1983).

12. R. J. Maleski; M. Klunge; D. Sicker, *Synth. Commun*. **25**, 2327 (1995).

13. S. C. Bisarya; S. K. Joshi; A. G. Holkar, *Synth. Commun*. **23**,1125 (1993).

14. A. Cornelis; P. P. Laszlo, *Synlett*, 155 (1994).

15. S. M. Nagy; E. A. Zubkov; V. G. Shubin; E. A. Paukshtis; N. L. Razdobarova, Acta *Chim. Hung*. **129**, 576 (1992).

16. S. M. Nagy; K. A. Yarovoy; M. M. Shakirov; V. G.Shubin; L. A. Vostrikova; K. G. Ione, *J. Mol. Catal*. **64**, L 31 (1991).

17. D. Gaude, R. Le Goaller, and J. L. Pierre, *Synth. Commun*. **16 (1)** (1986).

18. A. S. Chhatre, R. A. Joshi, B. D. Kulkarni, *J. Colloid Interface Sci*. **158(1)**, 183-7 (1993).

19 M. Tomasz; J. Jaroslaw; Z. Janusz; S. Wincenty, *Synth. Commun*. **31(2)**, 173-187 (2001).

CHAPTER V

NITRATION OF XYLENES

(*O*-& -*M*-XYLENE)

5. 1 INTRODUCTION

Nitration of organic compounds has long been a very active area of research and the subject of large body of literature. Extensive reviews have been published by Ingold [1], Olah [2-4], Schofield [5-6], Ione [7] and others. Nitration of aromatic substrates is a widely studied reaction.

The nitration of xylenes to nitroxylenes is industrially important process because the nitroxylenes are readily reduced to corresponding aminoxylenes (xylidines). These xylidines are used as starting materials for the production of riboflavin and agrochemicals respectively [8]. It is of great industrial significance as many nitroaromatics are extensively utilized as vital intermediates for dyes, pharmaceuticals, perfumes and pesticides [9]. By conventional methods nitration is carried out by the use of potent mixtures concentrated nitric acid or fuming nitric acid with sulfuric acid which has well known drawbacks like generation of large amounts of wastes that are costly to dispose off and also cause environmental problems [10]. Overnitration, oxidation to form by-products, poor selectivity for desired product and formation of alkylnitroproducts, are other associated problems.

Therefore, considerable interest is growing to develop cleaner technologies using heterogeneous catalysis. Zeolites with their well-defined cages and channels, find extensive applications [11-12] in the organic reactions because of selectivity, chemical stability, and regenrability.

Conventionally nitration of *o*- and *m*- xylenes prepared by method using a mixture of nitric acid and sulfuric acid as nitrating mixture gives the mixture of 4-nitro-*o*-xylene (31-55 %) and 3-nitro-*o*-xylene (45-69 %), and 2-nitro-*m*-xylene (25-16 %) and 4-nitro-*m*-xylene (75-84 %) respectively [8]. Isomer ratios can be changed

significantly by varing the reaction conditions. Tomasz et al. [13] studied nitration of *o*-xylene in liquid phase using 100 % nitric acid as a nitrating agent and obtained high yield over silica supported solid catalysts.

Landau et al. [14] reported the nitration of *o*-xylene in vapor phase over zeolite catalysts using nitrogen dioxide as a nitrating agent and they found high selectivity over zeolite catalyst compared to nitric acid. Nitration of xylenes and other aromatic hydrocarbons are described in liquid phase using fuming nitric acid at reflux temperature and azeotropic removal of water by Dean- Stark apparatus over modified clay catalysts reported by Choudary et al [15].

Chen, Hukui [16] et al. reported the nitration of m-xylene over the nitrating acid mixture in solvent $ClCH_2CH_2Cl$. The yield of the mixture of 2- and 4-nitro-*m*-xylene was 96 %. Due to use of conventional mixed acids, the reaction was having the same difficulty such as generation of large amounts of waste sulphuric acid that are costly to dispose off and also cause environmental problems

In the course of studies of nitration, Olah and co-workers reported the nitration of aromatic compounds with nitric acid over a solid superacidic perfluorinated resin sulfonic acid (Nafion-H) catalyst [17]. In continuation of study they reported nitration of xylenes with mercury (II)-impregnated Nafion-H superacidic catalyst under conditions of azeotropic removal of water, which gave the high selectivity and yield.

In the last few years, supported reagents have been increasingly used in organic synthesis, mainly because the reactions are carried out under mild conditions and the products are easily separated [18].

Recent advances in superacid catalysts have brought considerable research importance in the reaction. Attempts are being made to reduce the spent acid generated

during the reaction and increase in conversion and selectivity by properly selecting the type of catalyst with proper solvents.

Arata et al reported the superacid catalysts with an acid strength of up to Ho<-16.04 by exposing hydroxides or oxides of Fe, Ti, Zr, Hf, Al, Sn, and Si, to sulfate ions after calcinations in air [19]. The synthesized superacids showed common properties as follows; the acid strength of solid superacids is higher than that of oxo-acids used for the treatment, specific surface area of the treated oxides is much larger, and the degree of crystallization is lower.

Some mixed oxides are solid superacids according to measurement by the indicator method. B_2O_3/ZrO_2 calcined at 773K shows an acid strength of H_0 = -13 and is active for the acid catalyzed reactions such as nitration of aromatic compounds in liquid phase [20].

We report here the nitration of *o*- and *m*-xylene in liquid phase and vapor phase by using nitric acid over solid acid catalysts.

5. 2 EXPERIMENTAL

5. 2. 1 Materials and Catalysts

5. 2. 1. 1 Catalysts Preparation:

- **Zeolites:**

Commercially available H-beta zeolite (Si/Al=30), H-ZSM-5 (Si/Al=40), H-Mordenite (Si/Al=40) were procured from United Catalyst India Ltd.

❖ **MoO_3/SiO_2:**

MoO_3/SiO_2 (MoO_3 : 20 wt %) was prepared by using ammonium molybdate and ethyl silicate-40 (CAS registry No. 18954-71-7) as a silica source. The preparation procedure is given in Chapter II.

❖ **B_2O_3/ZrO_2 (30 mol%):**

40.46 g of zirconyl nitrate [$ZrO(NO_3)_2$, 2 H_2O] was dissolved in 110 ml distilled water and aqueous ammonia (25 %) was added to it drop wise with constant stirring till the solution become alkaline (pH=10). The resultant solution was filtered and washed with distilled water till free from ammonium nitrate. The residue was dried overnight at 85 ^oC in an oven and then impregnation of boric acid. 9.15 g boric acid (H_3BO_3) was dissolved in 200 ml distilled water. The zirconium hydroxide obtained above was added to the boric acid solution with stirring to obtain slurry. It was air-dried, heated in an oven at 110°C for 5h and calcined overnight at 550°C.

The catalyst was characterized before and after reaction for its physical and chemical properties using various techniques such as XRD (Rigaku, Miniflex), TG/DTA/DTG (METTLER TA 4000 System), EDX (KEVEX 7000 system), TPD (Micrometrics, Autochem-2910), SEM (Model JEOL JSM 5200), and Surface area (Omnisorb 100 CX).

5. 2. 2 Reaction Procedure

All catalytic liquid phase nitration reactions were carried out in a batch reactor, under atmospheric pressure as follows: Solution of 10 mmol xylenes in 10ml solvent, 10 mmol nitric acid (70 %) and freshly activated catalyst 20 wt % (based on Xylenes) were taken in the 50ml two neck round bottom flask and the mixture was continuously stirred at various temperatures under nitrogen atmosphere. The temperature of the

reaction was maintained by using oil bath. The samples were periodically collected, neutralized by sodium hydrogen carbonate and analyzed by Gas Chromatography (Perkin Elmer autosystem XL, PE-1, 30m, 0.25mm ID, 1 μm film thickness). Products were also confirmed by GC/MS (SHIMADZU, DB-I column) and GC/IR (Perkin Elmer Spectrum 2001, DB-1, 25m, 0.32mm ID).

Vapor phase nitration experiments were performed in a fixed-bed continuous down flow glass reactor at atmospheric pressure. 10g of the zeolite beta catalyst in extrudate form was loaded in a tubular glass reactor of 15 mm diameter and 25 mm length. The upper part of the reactor was packed with inert ceramic beads as the preheating zone. Before the reaction, the catalyst sample was activated at 450 °C for 4h in a 10 ml /min flow of air. The reactions were carried out by passing dilute nitric acid and o-xylene using syringe pumps (Sage feed pump), in the temperature range of 120 °C to 180 °C with nitrogen as carrier gas at the rate of 10 cc/min. The weight hourly space velocity (WHSV) was varied from 0.085 to 0.34 h^{-1}. The reaction products were collected in a receiver maintained at 5 °C. The mixture of products was extracted with diethyl ether and neutralized by sodium bicarbonate analyzed by GC as above.

5. 3 CATALYSTS CHARACTERIZATION

5. 3. 1 H-Beta catalyst

Temperature-programmed desorption (TPD) of ammonia is a common method to determine both the strength and the number of acid sites present on the surface of a solid acid catalysts [21]. H-ZSM-5 and B_2O_3/ZrO_2 showed low acidity compared to H-beta. Mo/SiO_2 has higher acidity than H-beta. But in case of H-Beta, which is desorbed

at higher temperature, indicating that it is having stronger acid sites than Mo/SiO_2. TPD of ammonia for these catalysts is shown in Fig. 5.1.

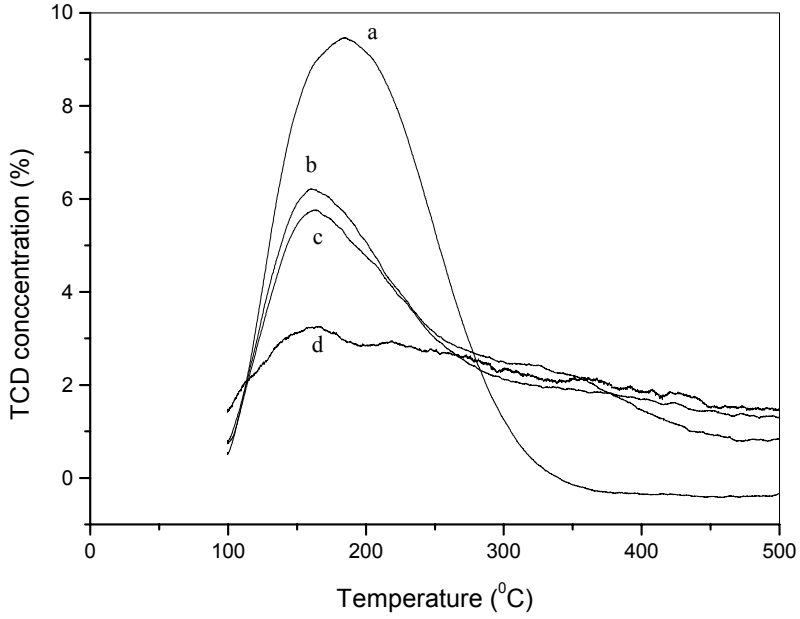

Fig. 5.1: TPD of ammonia of catalysts; a- Mo/SiO_2;
b - H-beta; c- H-ZSM-5; d- B_2O_3/ZrO_2

5. 3. 2 B_2O_3/ZrO_2

The XRD pattern of 30 mol % B_2O_3/ZrO_2 calcined at 500°C showed the amorphous nature of the solid catalyst and it also compared with XRD of pure zirconia (Fig. 5.2). Fig. 5.2, which matches with the cubic phase of zirconia and no boron oxide peaks were seen in XRD suggesting high dispersion of B_2O_3 on zirconia. The XRD pattern of pure zirconia is also given in Fig. 5.2 for comparison, which shows formation of a stable monoclinic phase while B_2O_3/ZrO_2 showed cubic structure showing stabilization of zirconia in to cubic phase. In the catalyst large amount of

BO_3^{3-} ion was impregnated but it could not show any peak containing boron. The surface area of the catalyst was found to be 114 m^2/g.

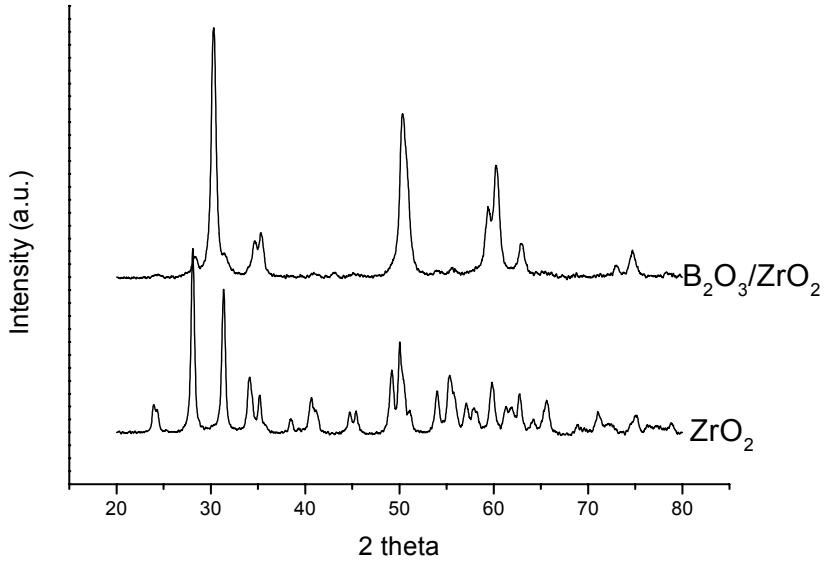

Fig. 5.2: XRD of B_2O_3/ZrO_2 and pure ZrO_2

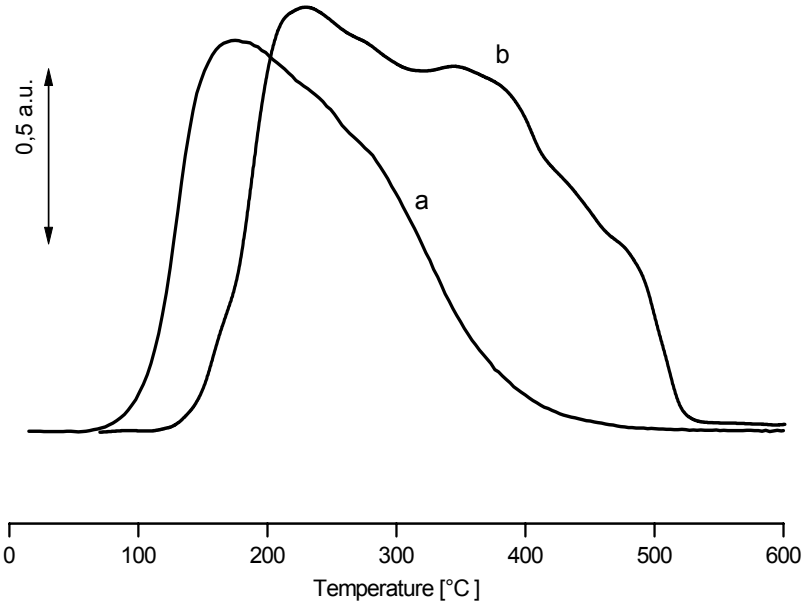

Fig. 5.3 TPD of ammonia on (a) Borated zirconia, (b) Sulphated zirconia.

TPD results on B_2O_3/ZrO_2 and sulphated zirconia are shown in Fig. 5.3. The ammonia was desorbed below 400 ^oC in case of B_2O_3/ZrO_2 whereas in case of sulphated zirconia it (Ho = -14) desorbed at much higher temperature at about 540 ^oC indicating the lower acidity of B_2O_3/ZrO_2 compared to sulphated zirconia. The acid site density in case of B_2O_3/ZrO_2 was found to be 0.398 mmol/g, which is considerably high for its use in acid catalyzed reactions.

SEM of borated zirconia is shown in Fig 5.4. It showed that the particle size is in the range of 1 to 2 μm with agglomerates and distribution of the particles is not uniform.

Fig. 5.4: Scanning electron micrograph (SEM) of B_2O_3/ZrO_2 catalyst.

TG/DTA/DTG analysis of borated zirconia was shown in Fig.5.5. It shows the initial loss of 3.12 % below 150 °C, which may be due to the loss of adsorbed water on the catalyst surface. There is no further weight loss in TG. DTA of borated zirconia showed sharp exotherm peak at 750 ^{o}C. It indicates that it may be the delayed crystallization of zirconia to the stable monoclinic phase due to the impregnation of borate ion [21]. In case of pure zirconia DTA analysis shows a sharp exotherm peak around 450 ^{o}C. This is attributed to the phase change from the amorphous phase to crystallized monoclinic phase [22] showed in Fig. 5.6.

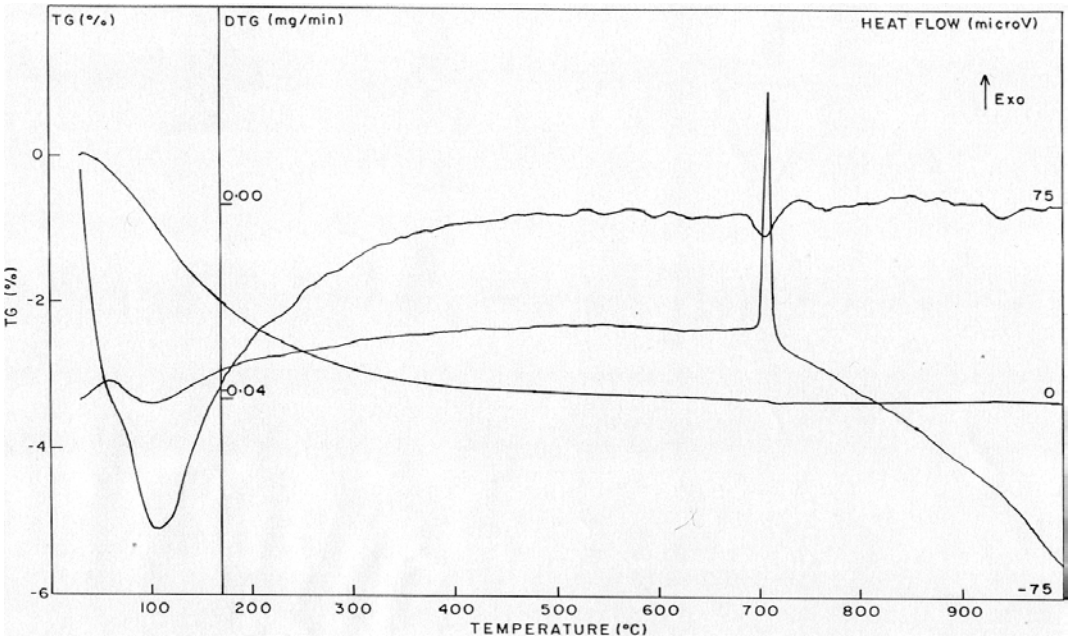

Fig. 5.5: Thermal analysis of B_2O_3/ZrO_2 catalyst.

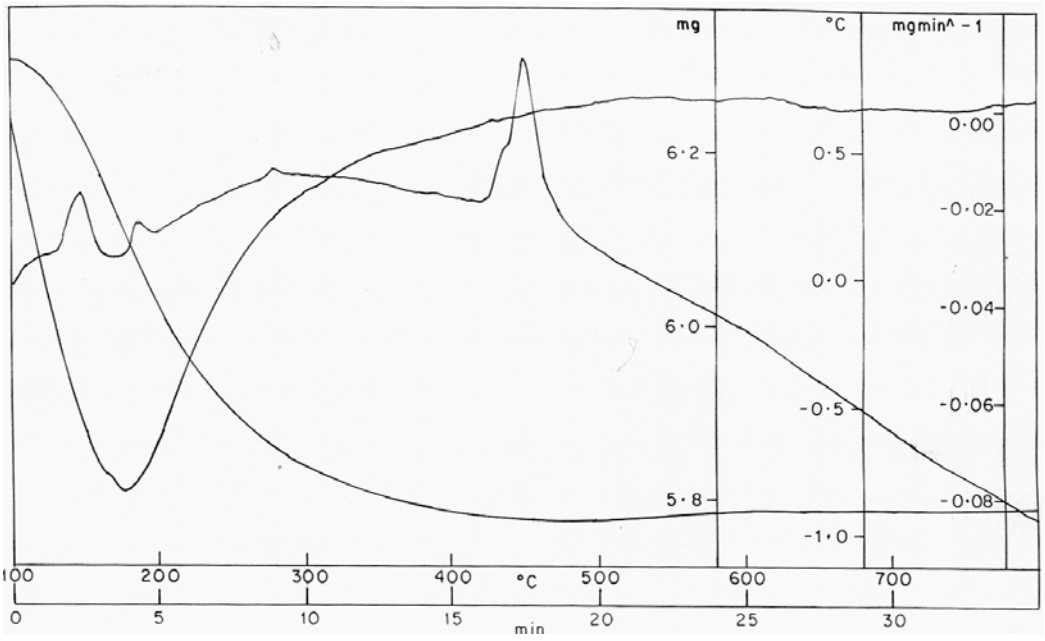

Fig. 5.6: Thermal analysis of pure zirconia.

5. 4 RESULTS AND DISCUSSION

5. 4. 1 Liquid phase nitration of o-Xylene

Nitration of o-xylene over solid acid catalysts gives the product distribution as follows:

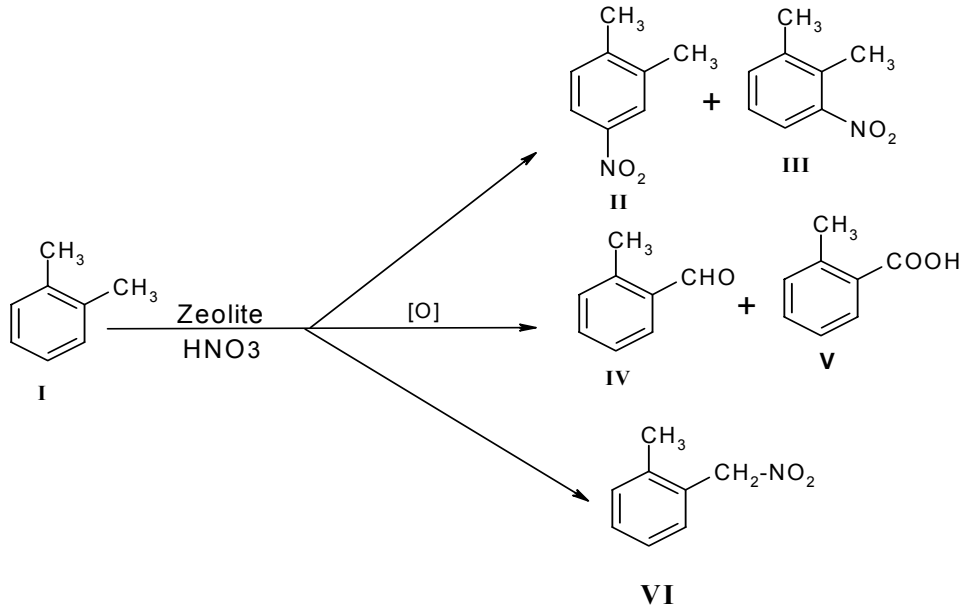

The results of nitration of o-xylene in liquid phase using 70 % nitric acid over solid acid catalysts such as H-Beta, H-ZSM-5, B_2O_3/ZrO_2 and Mo/SiO_2 in carbon tetrachloride as a solvent at 75°C are given in Table 5.1. Among the catalysts studied, H-Beta zeolite showed better activity (13.25 mmol $g^{-1}h^{-1}$) with conversion of o-xylene 28 % with 63 % selectivity for 4-NOX (4-nitro-o-xylene) and 35 % for 3-NOX (3-nitro-o-xylene) with very less amount of oxidation products and α-MPNM (α-methyl phenyl nitromethane). As the time progresses the conversion is marginally increased form 28.1 % to 33.3 % where as the selectivity for NOX decreases due to the formation of oxidation products and methyl group nitration. This shows that the ring nitration of o-xylene reaches a maximum value in liquid phase in one hour and after

words the nitration of methyl group predominates because of kinetically controlled reaction.

When the reaction was carried out without catalyst, the conversion was low (18 %) but the formation of oxidized products (27 %) was more and selectivity for 4-NOX was very low (4 %) suggesting that solid acid catalyst H-beta affect the conversion and selectivity.

The liquid phase nitration of o-xylene was also carried out with 70 % nitric acid without any solvent, the conversion (71.3 %) and selectivity (36 %) observed was lower. The use of dilute nitric acid (30 %) for liquid phase nitration showed very low conversion. B_2O_3/ZrO_2 catalyst showed low conversion with high selectivity and formation of oxidation products were high. The conversion shown by H-beta and MoO_3/SiO_2 are comparable but the selectivity for NOX products was higher in case of H-beta zeolite catalysts, which may be due to the acidity and shape selectivity of the catalyst H-beta. Therefore the catalyst H-Beta was used for the vapor phase reactions.

Table 5.1: Nitration of o-xylene in liquid phase over different catalysts

Catalysts	Reaction Time (h)	*o*-Xylene Conv (%)	Product Selectivity, (%)				4-/3-ratio	Activity mmol $g^{-1}h^{-1}$
			4-NOX	3-NOX	OP	MPNM		
H-Beta	1	28.1	63.3	35.1	-	1.6	1.8	13.3
	4	33.3	46.6	25.8	7.3	20.3	1.8	
H-ZSM-5	1	20.9	38.7	22.8	8.7	30.7	1.7	9.8
	4	26.3	29.5	17.4	9.1	44.0	1.7	
Mo/SiO_2	1	20.2	57.6	33.8	-	8.6	1.7	9.5
	4	37.0	49.9	29.7	8.1	12.3	1.7	
B_2O_3/ZrO_2	1	22.5	35.3	17.7	36.2	10.2	2.0	10.4

Reaction conditions: o-Xylene/HNO_3 mole ratio = 1; HNO_3 (Wt %) = 70 %; Catalyst =20 wt%; Temp = 75°C; Solvent = CCl_4; NOX = Nitro o-xylene, Oxidation products = tolualdhyde & Toluic acid; α-MPNM = α-methyl phenyl nitromethane;
mmoles of o-xylene converted at 1h / gm of catalyst.

5. 4. 2 Vapor phase nitration of o-Xylene

5. 4. 2. 1 Influence of temperature:

Vapor phase nitration of *o*-xylene was carried out over zeolite beta with *o*-xylene /HNO_3 ratio of 1.5 using 30 % nitric acid at various temperature and the results are shown in Fig. 5.6.

The maximum conversion of *o*-xylene (65 %) was observed at 150°C with low formation of oxidation products and better selectivity for the 4-NOX (79 %). At the lower temperature, the selectivity for NOX products was good (85 %) but the conversion of *o*- xylene was very low (23 %). At higher temperature (180°C) the conversion (40 %) as well as the selectivity for NOX decreases (50 %) as oxidation products and methyl nitration products were formed. The 4-/3- isomer ratio was not affected by temperature and it remained constant at ~ 3.

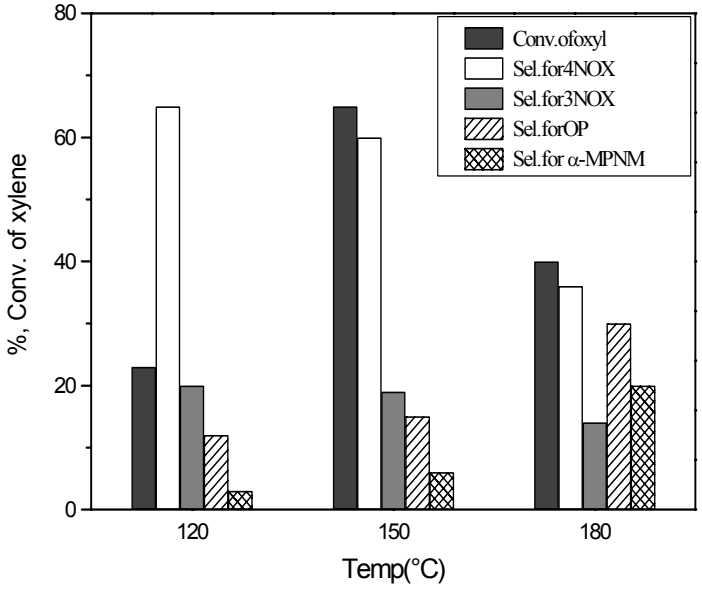

Fig. 5.6: Influence of temperature on conversion.

The nitration of *o*-xylene is an exothermic reaction, and the use of dilute nitric acid provides water vapors, which dissipates the heat of reaction so that the formation of oxidation products was minimized. The dilute nitric acid is cheaper than concentrated nitric acid, is an added advantage for the commercialization of the process.

5. 4. 2. 2 Influence of WHSV:

Influence of the WHSV on the conversion and selectivity was examined in the range $0.085h^{-1}$ -$0.34h^{-1}$. Higher conversion of *o*- xylene and selectivity for 4- NOX was observed at WHSV of 0.17 h^{-1}. Fig. 5.7 represents the effect of WHSV on the nitration. The WHSV of 0.17 was found the most suitable for this reaction, the conversion of 65 % and selectivity 79 % was observed. While for the WHSV of 0.085

and 0.34, the conversion was 80 % and 50 % and selectivity was 58 % and 84 % respectively.

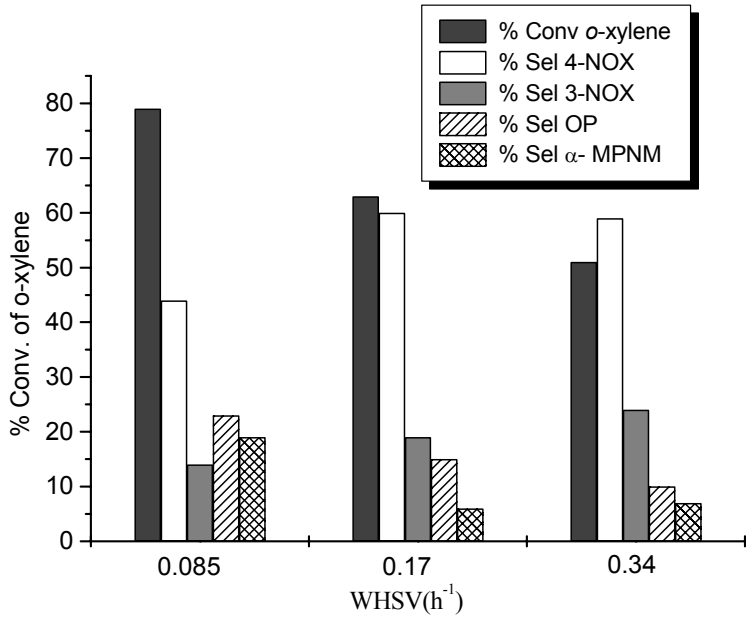

Fig. 5.7: Influence of WHSV on nitration of o-xylene.

Slight deactivation of the catalyst is observed after 78 h and deactivated H-beta catalyst washed with acetone. The washing was analyzed by gas chromatography, 4-NOX, *o*-toluic acid, o-tolualdehyde and α-MPNM was found deposited on the surface of the catalyst.

Characterization of deactivated catalyst:

A comparison of XRD patterns of H-beta sample before and after nitration showed no loss in crystallinity showing its structural stability in the acid environment of the reaction.

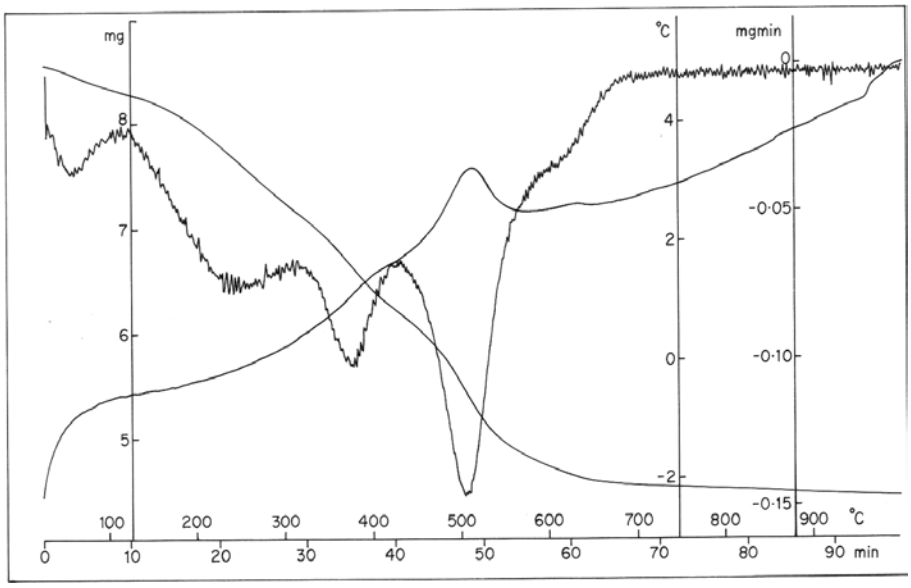

Fig. 5.3: TG/DTG/DTA analysis of deactivated catalyst H-beta.

Thermal analysis of deactivated beta zeolite in flowing air is shown in Fig.5.3. TG/DTG/DTA thermogram of H-beta after reaction was divided into three steps. First is upto 200°C, second is from 200-400°C and third step started from >550°C. It indicates that up to 200°C there is an endothermic weight loss 6.4% is due to the adsorbed water / xylene from the catalyst. Above 200-400°C the weight loss of 18.1% is due to evaporation of oxidation products deposited on the catalyst. Final exothermic weight loss of 15% above 550°C shows that it is due to the formation of high boiler coke precursors. This shows that the adsorption of high boiler on the catalyst was responsible for the deactivation.

5. 4. 3 Liquid phase nitration of *m*-xylene

5. 4. 3. 1 Reaction study:

The nitration of *m*- xylene with nitric acid (70 %) over B_2O_3/ZrO_2 can be written as:

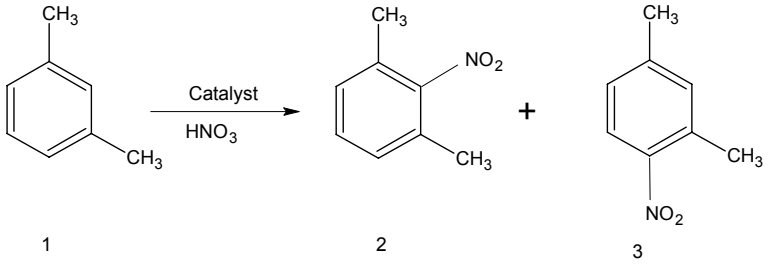

1 2 3

Nitration of *m*-xylene was carried out using nitric acid (70 %) over solid acid catalysts such as B_2O_3/ZrO_2 and zeolite H-beta and products obtained 4-NMX (4-nitro-*m*-xylene), 2-NMX (2-nitro-*m*-xylene), were formed in major amount and oxidized products in minor. Nitration of *m*-xylene over H-beta catalyst showed low conversion compared to B_2O_3/ZrO_2 catalyst. Therefore nitration of m-xylene was carried out over B_2O_3/ZrO_2 catalyst using nitric acid as a nitrating agent. Recycling of the catalyst indicates that the catalyst activity remains same in the nitration. The yields of nitro compounds vary substantially due to the reaction conditions and solvent used in the reaction. The influence of various parameters on conversion of xylene and product distribution are presented in the following sections.

5. 4. 3. 2 Influence of Temperature:

Liquid phase nitration of m-xylene was carried out over borated zirconia with m-xylene /HNO_3 ratio of 1:1.5 using 70 % nitric acid at different temperatures and the results are shown in Table 5.2. It showed that at 90°C it gives the higher conversion (64.6 %) as well as selectivity (82.4 %) towards 4-nitro-*m*-xylene with low oxidation

products (4.3 %). At lower temperature it gives the low conversion (18.1 %) and higher oxidation products (10.4 %). When the nitration of *m*-xylene was carried out at room temperature no nitro products were formed in the reaction indicating the influence of temperature on the reaction. The increased selectivity towards the formation of para-substituted product may be due to the less steric hindrance at para position. When the reaction was carried out without the catalyst the conversion was very low (~5%) indicating the influence of the catalyst.

Table 5. 2: Influence of temperature on nitration

Temp	Reaction	%, Conv	%, Selectivity				4/2
(°C)	Time (h)	of xylene	4-NMX	2-NMX	MBZH	Others	ratio
60	2	16.5	73.3	10.6	6.9	1.2	6.9
	8	18.1	72.4	9.7	4.6	5.8	7.5
90	2	51.3	88.1	9.95	0	1.5	8.9
	8	64.6	82.4	13.3	1.5	2.8	6.2

Conditions: Xylene: HNO3= 1:1.5; HNO_3= 70%; B_2O_3/ZrO_2= 0.5g; Solvent = $CHCl_3$
NMX= m-nitroxylene; MBZH= Tolualdehyde; BZOH= toulic acid

5. 4. 3. 3 Influence of Xylene to Nitric acid Molar ratio:

The influence of xylene to nitric acid molar ratio was examined over borated zirconia catalyst and results shown in Fig. 5.8. When the xylene to nitric acid molar ratio was increased from 1:1 to 2:1, the conversion was decreased from 50 % to 24 %. In case of molar ratio of xylene to nitric acid 1:1.5, the conversion was increased from 50 % to 64.6% indicating the requirement of excess amount of nitric acid than

stoichiometric amount for complete conversion of m-xylene to nitro products. This may be due to the decomposition of HNO3 under the reaction temperature of 90 °C.

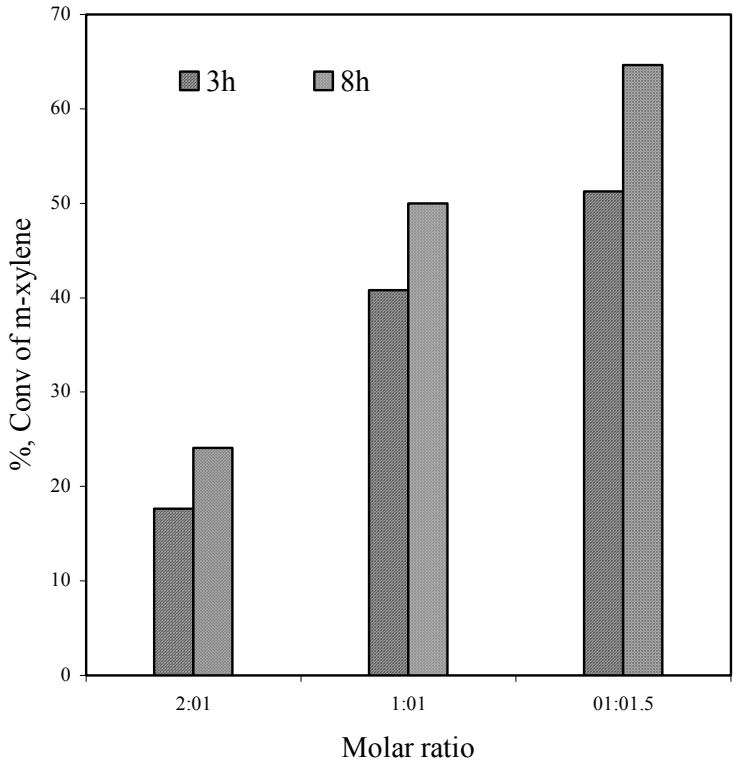

Fig. 5. 2: Influence of xylene to nitric acid molar ratio.

5. 4. 3. 4 Influence of Dilution of Nitric acid:

Liquid phase nitration of m-xylene carried out over catalyst borated zirconia with xylene to nitric acid molar ratio 1: 1.5 at 90°C using various of dilutions of nitric acid and its results showed in Table 5.3. It indicates that when the nitric acid was diluted to 50 % the conversion as well as selectivity decreases. By increasing the concentration from 50 % to 70 % the conversion as well as selectivity increases from 60 % -75 %. It showed that the amount of water in the reaction affects the reaction. In case of 50 % nitric acid the water content was more so it might be deactivate the

catalyst. Nitration of m-xylene with 30 % nitric acid gave very low conversion (of about 1% after 8h of reaction time).

Table 5. 3: Effect of dilution of nitric acid on nitration of m-xylene

HNO_3	Reaction	%, conv of	%, Selectivity				
Conc. (%)	Time (h)	*m*-xylene	4-NMX	2-NMX	MBZH	MBZOH	OP
50	2	1.13	64.60	14.16	5.31	0.00	15.93
	8	4.99	65.13	7.21	17.03	0.80	9.82
70	2	51.25	88.09	9.95	0	0	1.46
	8	64.64	82.36	13.31	1.51	0	2.8

Conditions: Xylene:HNO_3 = 1:1.5; B_2O_3/ZrO_2= 0.5g; Temp. (°C)= 90; Solvent = $CHCl_3$; NMX= m-nitroxylene; MBZH= Tolualdehyde; BZOH= toulic acid

5. 5 CONCLUSION

Thus 4-NOX has been regioselectively formed in continuous process by vapor phase nitration of *o*-xylene using dilute nitric acid over beta zeolite at 150°C in high yield. Low conversion, formation of alkyl nitro product, poor selectivity for 4-nitro *o*-xylene, use of chlorinated solvents and concentrated nitric acid are major drawbacks in liquid phase nitration which has been overcome significantly in vapor phase nitration. The maximum conversion of 65 % with selectivity of 60 % for 4-nitro-*o*-xylene and 19 % for 3-nitro-*o*-xylene was observed. The 4-/3- isomer ratio found was >3. Oxidation products (OP) like *o*-tolualdehyde and o-toluic acid formed by oxidation of methyl group, α-methyl phenyl nitromethane (α-MPNM) formed by alkyl nitration are the byproducts in small quantity. The use of dilute nitric acid and selective formation of 4-NOX are the main advantages of this process.

Liquid phase nitration of m-xylene was carried out over B_2O_3/O_2 (30 mol %) catalyst using nitric acid at 90 °C and *p/o* ratio obtained was 8.9 with higher conversion of xylene (64.6 %). Incase of m-xylene the 4-NMX was the selectively formed product. Use of superacidic catalyst B_2O_3/ZrO_2 showed good activity and acidity in nitration of m-xylene. After nitration the stability of catalyst was also good.

5. 6 REFERENCES

1. C. K. Ingold, '*Structure and mechanism in Organic Chemistry'* 2nd ed., Cornell University Press, Ithaca, New York, (1969).
2. G. A. Olah, S. J. Kuhn, '*Friedel –Crafts and Related reactions*,' Olah G.A. ed., Wiley Interscience, New York, Vol. **2** (1964).
3. G. A. Olah, *ACS Symp*. Series, Vol **22**, [Albright, F., ed., Washington DC.], p.1 (1976).
4. G. A. Olah, R. Malhotra, S. C. Narang, ' *Nitration: Methods and Mechanisms*' Feuer, H., ed., VCH Publishers, New York, (1989).
5. J. G. Hogget, K. Schofield, '*Nitration and aromatic reactivity'*, Cambridge University Press, London, (1971).
6. K. Schofield, '*Aromatic Nitration'*, Cambridge University Press, London, (1980)
7. L. V. Malysheva, K. G. Ione, *Catal. Rev – Sci. Eng*., **37**,179 (1985).
8. *Ulmann's Encyclopedia of Industrial Chemistry*, VCH, Weinheim, **Vol.17**, (1995).
9. "*Kirk-Othmer Encyclopedia of Chemical Technology*," 2nd. Interscience, N.Y., (1967).
10. J. H. Clark, D. J. Macquarrie, *Org. process res. dev*., **1**, 149 (1997).
11. Holdrich W.F., H. Van Beckkum, *Stud. Surf. Sci. Catal*. **58**, 631 (1991).
12. A. Corma, Garcia H., *Catal. Today* **38**, 257 (1997).
13. M. Tomaz, J. Jaroslav, *Synn. Comm*. **31(2)**, 173 (2001).
14. M. V. Landau, S. B. Kogan, *Catal. Today* **36**, 497 (1997).

15. B. M. Choudhari et. al. U.S. Pat. No. 6,376,726
16. Chen, Hukui; Jin, Jianpin, *Ranliao Gongye*, **37(2)**, 19-20 (Chinese) (2000).
17. Olah, G. A.; Malhotra, R.; Narang, S.C. *J. Org. Chem*., **43**, 4628 (1978).
18. A. Mckillop and D.W. Young, Synthesis, 401, (1979).
19. K. Arata, *Appl. Catal. A: General* **146**, 3-32 (1996).
20. H. Matsuhashi, K. Kato, K. Arata, *Stud. Surf. Sci. Catal*., **90**, 251-6 (1994).
21. K. Parida, V. Quaschning, E. Lieske and E. Kemnitz, *J. Mater. Chem*., **11**, 1903-1911 (2001)
22. T. Yamaguchi, *Catal. Today*, **20**, 199-218 (1994).

CHAPTER VI

SUMMARY AND CONCLUSIONS

6. 1 SUMMARY:

The thesis includes the study of nitration of benzene, toluene, phenol and xylenes (o-& m- xylene) over solid acid catalysts using dilute nitric acid as a nitrating agent. The solid acid catalysts investigated were mixed oxide catalysts and zeolites such as H_2SO_4/SiO_2, H_2SO_4/ZrO_2, $H_2SO_4/Y_2O_3/ZrO_2$, $Fe/Mo/SiO_2$, Mo/SiO_2, Fe/SiO_2, B_2O_3/ZrO_2, H-beta, H-Y, H-ZSM-5 and H-mordenite catalysts.

The various mixed oxide catalysts are prepared by sol-gel technique. Using this method we were able to prepare metal oxides with good homogeneity, high surface area required for catalytic reactions. In case of zeolites, commercially available catalysts were used for the nitration reactions.

The metal oxides and zeolite catalysts were characterized by XRD for structural purity and homogeneity. Other methods like EDX, Thermal analysis, surface area FT-IR spectra of adsorbed pyridine and temperature programmed desorption of ammonia were also used for characterization.

The summary and conclusions of the studies of nitration reactions using these catalysts are given below:

1) Nitration of Benzene

The XRD pattern of $Fe/Mo/SiO_2$ matched well with the reported MoO_3 pattern without any reflections of silica species indicating the dispersion of MoO_3 on amorphous silica with high surface area of about 490.7 m^2/g. Comparison of acidity of H-beta (0.78mmol g^{-1}), Mo/SiO_2 (1.10 mmol g^{-1}) and $Fe/Mo/SiO_2$ (1.22 mmol g^{-1}) showed that the $Fe/Mo/SiO_2$ is having more acidity compared to others.

Vapor-phase nitration of benzene to nitrobenzene over solid acid catalysts is a clean process without sulfuric acid waste. A number of zeolites and metal oxide

catalysts have been used such as H-beta (Si/Al=30), Mo/SiO_2 (Mo= 20 mol%), MoO_3, and various compositions of $Fe/Mo/SiO_2$ (Fe/Mo = 12/8 mol %, 10/10 mol %) and $Fe/Mo/SiO_2$ (Fe/Mo=0.72/20 mol %) for nitration of benzene. Among these catalysts investigated, the mixed oxide catalyst comprising $Fe/Mo/SiO_2$ (Fe/Mo=0.72/20 mol %) showed high conversion (87 %) with high selectivity (100 %) of nitrobenzene with negligible deactivation for 300h. H-beta catalyst also showed good activity showing almost 100 % selectivity with conversion of 46.8 % and showed steady conversion upto 72 hours. Afterwards conversion was slowly decreased due to deactivation of the catalyst.

The nitration of benzene was carried out in vapor phase also over $Fe/Mo/SiO_2$ (I) catalyst using dilute nitric acid as a nitrating agent. Very high yield was obtained in this continuous nitration process without any waste byproduct formation. One of the major advantage of this nitration was the use of dilute nitric acid as a nitrating agent, leading to high selectivity and longer catalyst life. The results are correlated with structure and acidity of the catalysts. There is no usage of sulfuric acid, unlike in the conventional process**,** thus avoiding hazardous waste disposal, which makes the nitration environmentally friendly.

2) Nitration of Toluene

Liquid phase nitration of toluene was carried out over sulphated catalysts such as sulphated zirconia, sulphated silica, sulphated yttria/zirconia and sulphated zirconia/silica. Sulphated yttria/zirconia showed the maximum conversion (20.5 %) but the selectivity for para isomer was less (*p/o*= 0.5). So the nitration was tried with H-beta and $Fe/Mo/SiO_2$. Among these catalysts the H-beta was better catalyst for nitration of toluene at 70°C, showing higher selectivity for para isomer.

Nitration of toluene was carried out in vapor phase also over zeolite H-beta catalyst using dilute nitric acid. The molecular modeling study was also done. The major products were *o*-nitrotoluene and *p*-nitrotoluene. Minor oxidized products were also obtained which include benzaldehyde, benzoic acid, nitro benzoic acid, and dinitro products. The maximum conversion of 55 % (toluene to HNO_3 ratio, 1.7: 1), selectivity to *para*-nitrotoluene of 70 %, and catalyst life of 75 hours (WHSV=0.2) were obtained using 20 % nitric acid at temperature of 120 ^oC. The catalyst deactivated faster when the concentration of nitric acid, temperature of reaction and WHSV was increased. The physicochemical characterization of the deactivated catalyst showed the structural stability of zeolite beta under the reaction conditions, but the *para*-nitrotoluene, and other oxidation products 4-nitrobenzoic acid, benzaldehyde, benzoic acid and anthraquinone were found deposited on the catalyst surface. Even then, the selectivity for *para*-nitrotoluene remains nearly constant. The molecular modeling study revealed that *para*-nitrotoluene encounters the least resistance for diffusion in the zeolite beta. These observations indicate that the shape selective nitration of toluene takes place inside the zeolite pores. The catalyst with alumina binder was found to be more active than the catalyst without binder because of higher acidity. The deactivated catalyst can almost be regenerated by washing the catalyst with organic solvents.

3) Nitration of Phenol

Phenol was selectively nitrated in liquid phase to *ortho*-nitrophenol in high yield using dilute nitric acid over solid acid catalysts such as Mo/SiO_2, $Fe/Mo/SiO_2$, H-ZSM-5 and H-Y and H-beta. Among the catalysts studied, zeolite H-Beta (Si/Al = 30) showed highest conversion (96 %) and selectivity (87 %) for *o*-nitrophenol. Zeolite H-

beta was found to be a very active catalyst for nitration of phenol to *ortho*-nitrophenol at room temperature in carbon tetrachloride as a solvent. Compared to the conventional process, phenol nitration over solid acid catalyst is a clean and environment friendly process with a simpler work up procedure of the products.

Other catalysts such as Mo/SiO_2, $Fe/Mo/SiO_2$, H-ZSM-5 and H-Y showed low conversion as well as selectivity for *o*-nitrophenol showing the influence of acidity as well as porosity of the catalyst. As the acidity of the catalyst decreased from H-Beta to H-ZSM-5 and $Fe/Mo/SiO_2$, the conversion was found to be decreased from 95 % to 60%.

The highest conversion (96 %) and selectivity (87 %) in case of zeolite H-Beta may be because of preferred orientation of phenol inside the zeolite pores increasing the accessibility of *ortho* position to nitronium ion leading to selective formation of *o*-nitrophenol

With the use of dilute nitric acid (30 %), there was no formation of dinitrophenol, which is an added advantage apart from its cheaper cost and ease in handling compared to concentrated nitric acid.

4) Nitration of Xylene

Regioselective nitration of *o*-xylene to 4-nitro-*o*-xylene has been studied in liquid phase and vapor phase over various solid acid catalysts such as H-beta, H-Y, H-ZSM-5, H-Mordenite, B_2O_3/ZrO_2 and Mo/SiO_2. In case of liquid phase nitration, among the catalysts studied, H-beta zeolite showed better activity (13.25 mmol $g^{-1}h^{-1}$) with conversion of *o*-xylene 28 % with 63 % selectivity for 4-nitro-*o*-xylene and 35 % for 3-nitro-*o*-xylene with very less amount of oxidation products and α-methyl phenyl

nitromethane. Low conversion, formation of alkyl nitro product, poor selectivity for 4-nitro-*o*-xylene, use of chlorinated solvents and concentrated nitric acid are major drawbacks in liquid phase nitration which has been overcome significantly in vapor phase nitration. The maximum conversion of 65 % (*o*-xylene: HNO_3 ratio=1.5:1) with selectivity for 4-nitro-*o*-xylene of 60 % was obtained in the vapor phase nitration of *o*-xylene over H-beta zeolite using 30 % nitric acid at 150 °C. The 4-/3- isomer ratio was found to be <1.8 and >3 in liquid phase and vapor phase reaction respectively. The TPD of ammonia for H-Beta, showed desorption at higher temperature, indicating that it is having stronger acid sites than other catalysts. Oxidation products (OP) like *o*-tolualdehyde and *o*-toluic acid formed by oxidation of methyl group, α-methyl phenyl nitro methane formed by alkyl nitration are the major byproducts. A comparison of XRD patterns of H-beta catalyst before and after nitration showed no loss in crystallinity showing its structural stability. Thermal analysis of deactivated beta showed maximum weight loss upto temperature 550 °C indicating adsorption of high boiler on the catalyst was responsible for the deactivation. The use of dilute nitric acid and selective formation of 4-nitro-*o*-xylene were the main advantages of this nitration.

In case of *m*-xylene, the liquid phase nitration was carried out over B_2O_3/ZrO_2 (30 mol%) catalyst using nitric acid at 90°C and p/o ratio obtained was 8.9 with higher conversion of xylene (64.6%). 4-nitro-*m*-xylene and 2-nitro-*m*-xylene were the major products formed, α-methyl phenyl nitromethane as a minor product and oxidized products were m-tolualdehyde and m-toluic acid in minor quantities. Use of superacidic catalyst B_2O_3/SiO_2 showed good activity (10.4 $mmolg^{-1}h^{-1}$) and acidity in nitration of m-xylene. The XRD pattern of 30mol % B_2O_3/ZrO_2 shows amorphous nature of the solid catalyst. After nitration the stability of catalyst was also good.

The nitration of aromatics using solid acid catalysts showed the potential for further study for developing process as an attractive alternative to the conventional process from environmental as well as technological point of view. The activity and selectivity of catalyst depends upon the acid strength and pore structure of the catalyst.

In conclusion, the solid acid catalysts developed in this study have potential applications as “green catalysts” for industrially important nitration reactions of aromatic compounds.